

Some Remarks on Eigenvalue Approximation by Finite Elements

Daniele Boffi, Francesca Gardini, and Lucia Gastaldi

Abstract The aim of this paper is to supplement the results of Boffi (Acta Numer. 19:1–120, 2010) with some additional remarks. In particular we deal with three distinct topics: we review some tutorial examples in one dimension and provide numerical codes for them; we analyze the case of multiple eigenvalues and show some numerical; we review a posteriori error analysis for eigenvalue problems.

1 Introduction

A recent survey [21] reports on the state of the art of the approximation of symmetric and compact eigenvalue problem by the finite element method. The aim of this paper is to supplement it with some additional theoretical results, application examples, and numerical codes.

This paper deals with three different topics. The first topic is considered in Sects. 2, 3, and 4 where some preliminary examples reported in [21, Part 1] are revisited in more detail. With a didactic purpose, particular emphasis is put on basic one dimensional examples in the standard and in the mixed Galerkin setting. Each example is completed by appropriate Matlab codes.

The second topic, discussed in Sect. 5, deals with the approximation of multiple eigenvalues. It is a common practice to restrict the analysis of eigenvalue/eigenfunction convergence to the case of simple modes and to only state the results in the case

D. Boffi (✉) · F. Gardini

Dipartimento di Matematica, Università degli Studi di Pavia, via Ferrata 1, I-27100 Pavia, Italy
e-mail: daniele.boffi@unipv.it; francesca.gardini@unipv.it; <http://www-dimat.unipv.it/boffi>;
<http://www-dimat.unipv.it/gardini>

L. Gastaldi

Dipartimento di Matematica, Università di Brescia, via Valotti 9, I-25133 Brescia, Italy
e-mail: lucia.gastaldi@ing.unibs.it; <http://www.ing.unibs.it/~gastaldi>

of multiplicities higher than one. Here we want to make it precise how the analysis goes in the case of multiple eigensolutions and, in particular, to focus on the case when an eigenspace can contain eigenfunctions of variable smoothness. The typical example of this situation is given by a double eigenvalue with one singular and one smooth eigenfunction. We will recall the theoretical estimates for this particular situation and we will confirm them with appropriate numerical experiments.

Finally, Sect. 6 is devoted to a fundamental topic which could not be covered in [21]: a posteriori error control for eigenvalue approximations. We will review the main ideas behind adaptive mesh refinement for the approximation of eigenvalue problems in the case of standard elliptic and mixed formulations.

2 Variationally Posed Eigenvalue Problems

In this paper we deal with the finite element approximation of *symmetric* and *compact* eigenvalue problem arising from partial differential equations. We introduce in this section our setting and recall some basic results.

The convergence analysis for eigenvalue problems usually consists of two parts: in the first step one shows that all continuous eigensolutions are approximated by the correct number of discrete eigenmodes (counted according to their multiplicities) and that no spurious eigenvalue is present; in the second step error estimates are looked for, which provide the order of convergence for eigenvalues and eigenfunctions. In this section we focus on the first step. The question of the rate of convergence will be detailed in Sect. 5

Let V and H be real Hilbert spaces. We suppose $V \subset H$ with dense and continuous embedding. Let $a : V \times V \rightarrow \mathbb{R}$ and $b : H \times H \rightarrow \mathbb{R}$ be symmetric and continuous bilinear forms, and consider the problem: find $\lambda \in \mathbb{R}$ and $u \in V$, with $u \neq 0$, such that

$$a(u, v) = \lambda b(u, v) \quad \forall v \in V. \quad (1)$$

The Galerkin discretization of problem (1) is based on a finite dimensional space $V_h \subset V$ and reads: find $\lambda_h \in \mathbb{R}$ and $u_h \in V_h$, with $u_h \neq 0$, such that

$$a(u_h, v) = \lambda_h b(u_h, v) \quad \forall v \in V_h. \quad (2)$$

The convergence analysis of the eigensolutions of (2) to those of (1) is usually performed with the introduction of suitable solution operators. We assume that for any $f \in H$ there exists a unique $Tf \in V$ and a unique $T_h f \in V_h$ such that

$$a(Tf, v) = b(f, v) \quad \forall v \in V \quad (3)$$

and

$$a(T_h f, v) = b(f, v) \quad \forall v \in V_h. \quad (4)$$

This is the case, for instance, when a is V -elliptic and b is equivalent to a scalar product in H . Unless otherwise expressly written, we will assume that we are in this setting. We are then given two self-adjoint operators from H into itself and we assume that

$$T : H \rightarrow H \text{ is compact.} \quad (5)$$

It is clear that, being a finite rank operator, T_h is compact as well.

Our main question about the convergence of the eigenvalue and the absence of spurious modes is indeed equivalent to the convergence in norm of T_h to T (see [21] for more details and for a formal definition of convergence): we will then discuss sufficient and necessary conditions for obtaining

$$\|T - T_h\|_{\mathcal{L}(H)} \rightarrow 0 \quad \text{when } h \rightarrow 0. \quad (6)$$

It can be seen that the eigenvalue convergence is also ensured by a convergence in the norm of V

$$\|T - T_h\|_{\mathcal{L}(V)} \rightarrow 0 \quad \text{when } h \rightarrow 0, \quad (7)$$

which can of course hold true only under the additional hypothesis that T is compact in $\mathcal{L}(V)$.

The most elegant theorem that proves (6) has been stated in this framework by Kolata in [58], although results in this direction were known and used before by many authors (see [8], for instance). The starting point is the standard Galerkin orthogonality which reads

$$T_h = P_h T, \quad (8)$$

where $P_h : V \rightarrow V_h$ is the elliptic projection associated to the bilinear form a . The next theorem (see [58] and [21, Theorem 7.6]) is often referred to by saying that compactness turns *pointwise* into *uniform* convergence.

Theorem 1. *If T is compact from H to V and P_h converges strongly (i.e., pointwise) to the identity operator from V to H , then T_h converges to T (uniformly) in the norm of $\mathcal{L}(H)$ (see (6)).*

Remark 1. It should be noted that the compactness hypothesis of Theorem 1 is stronger than (5). This is however needed when using the representation $T_h = P_h T$, since P_h is naturally defined in V and not in H . There is another option which consists of assuming T to be compact in $\mathcal{L}(V)$ and P_h converging strongly to I in $\mathcal{L}(V)$: this implies the convergence in norm (7).

Remark 2. The convergence in norm (6) can often be obtained by examining directly the error estimates linking (4) and (3). In many applications it is possible to get estimates of the form

$$\|Tf - T_h f\|_V \leq Ch^k \|f\|_H.$$

3 One Dimensional Examples

In this section we consider some one dimensional examples. We start with the standard Laplace eigenvalue problem which fits pretty well the theory presented in Sect. 2. Then we consider eigenvalue problems in mixed form and show how the theory of Sect. 2 should be changed in order to deal with this setting. In particular, an analogue of Theorem 1 cannot be proved in the case of the Laplace eigenvalue problem in mixed form due to a lack of compactness.

The examples are discussed in detail and particular emphasis is given to the numerical results (including the source code for Matlab computations).

3.1 Standard Laplace Eigenvalue Problem

Given the interval $\Omega =]0, \pi[$ we look for eigenvalues λ and eigenfunctions u with $u \neq 0$ such that

$$\begin{cases} -u''(x) = \lambda u(x) & \text{in } \Omega \\ u(0) = u(\pi) = 0. \end{cases} \quad (9)$$

The exact eigenvalues are given by $\lambda = 1, 4, 9, 16, \dots$ and the eigenspaces are generated by $\sin(kx)$ for $k = 1, 2, 3, 4, \dots$

This problem fits the setting of Sect. 2 with the following choices:

$$\begin{aligned} V &= H_0^1(\Omega) \\ H &= L^2(\Omega) \\ a(u, v) &= \int_0^\pi u'(x)v'(x)dx \\ b(u, v) &= \int_0^\pi u(x)v(x)dx. \end{aligned}$$

Let us consider the conforming approximation of (9) by *continuous piecewise linear* finite elements. It is well-known that the matrix form of the discrete problem is given by

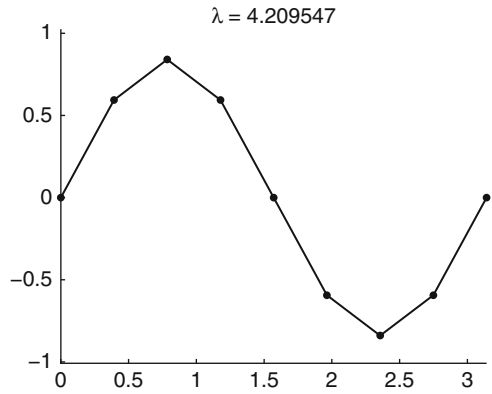
$$A\mathbf{x} = \lambda M\mathbf{x}$$

where the stiffness matrix A is

$$a_{ij} = \frac{1}{h} \cdot \begin{cases} 2 & \text{for } i = j \\ -1 & \text{for } |i - j| = 1 \\ 0 & \text{otherwise,} \end{cases}$$

Table 1 Eigenvalues computed using the code in Listing 1.1 for different values of n

Exact	Computed (rate)				
	$n = 8$	$n = 16$	$n = 32$	$n = 64$	$n = 128$
1	1.0129	1.0032 (2.0)	1.0008 (2.0)	1.0002 (2.0)	1.0001 (2.0)
4	4.2095	4.0517 (2.0)	4.0129 (2.0)	4.0032 (2.0)	4.0008 (2.0)
9	10.0803	9.2631 (2.0)	9.0652 (2.0)	9.0163 (2.0)	9.0041 (2.0)
16	19.4537	16.8382 (2.0)	16.2067 (2.0)	16.0515 (2.0)	16.0129 (2.0)
25	33.2628	27.0649 (2.0)	25.5059 (2.0)	25.1257 (2.0)	25.0314 (2.0)
36	51.3724	40.3212 (1.8)	37.0525 (2.0)	36.2610 (2.0)	36.0651 (2.0)
49	69.5582	57.0672 (1.3)	50.9572 (2.0)	49.4840 (2.0)	49.1206 (2.0)
64		77.8147	67.3528 (2.0)	64.8266 (2.0)	64.2059 (2.0)
81		103.0473	86.3943 (2.0)	82.3258 (2.0)	81.3299 (2.0)
100		133.0513	108.2597 (2.0)	102.0237 (2.0)	100.5030 (2.0)
DOF	7	15	31	63	127

Fig. 1 The second eigenfunction computed and plotted using the code in Listing 1.1 ($n = 8$ and $k = 2$)

and the mass matrix M is

$$m_{ij} = h \cdot \begin{cases} 2/3 & \text{for } i = j \\ 1/6 & \text{for } |i - j| = 1 \\ 0 & \text{otherwise,} \end{cases}$$

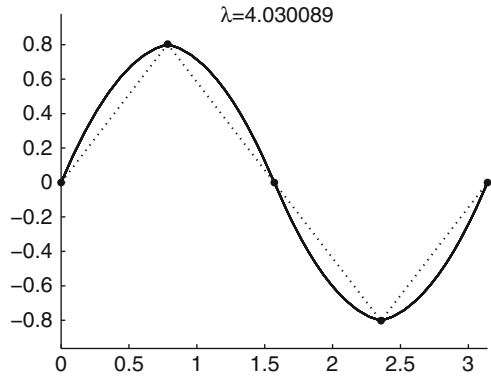
with $i, j = 1, \dots, n-1$, where n is the number of subdivisions of the interval $[0, \pi]$ (the dimensions of A and M equal the number of internal nodes).

In Listing 1.1 we report a simple Matlab code that solves our problem, which displays the first ten eigenvalues, and plots a specific eigenfunction. The result of the computations for successively refined meshes is included in Table 1. Second order convergence can be clearly appreciated (this is compatible with the error estimates which will be made precise in Sect. 5.1). Figure 1 shows the second eigenfunction for $n = 16$ (this is the plot which is generated with the parameters reported in Listing 1.1).

Table 2 Eigenvalues computed using the code in Listing 1.2 for different values of n

Exact	Computed (rate)				
	$n = 8$	$n = 16$	$n = 32$	$n = 64$	$n = 128$
1	1.0000	1.0000 (4.0)	1.0000 (4.0)	1.0000 (4.0)	1.0000 (4.0)
4	4.0020	4.0001 (4.0)	4.0000 (4.0)	4.0000 (4.0)	4.0000 (4.0)
9	9.0225	9.0015 (3.9)	9.0001 (4.0)	9.0000 (4.0)	9.0000 (4.0)
16	16.1204	16.0082 (3.9)	16.0005 (4.0)	16.0000 (4.0)	16.0000 (4.0)
25	25.4327	25.0307 (3.8)	25.0020 (3.9)	25.0001 (4.0)	25.0000 (4.0)
36	37.1989	36.0899 (3.7)	36.0059 (3.9)	36.0004 (4.0)	36.0000 (4.0)
49	51.6607	49.2217 (3.6)	49.0148 (3.9)	49.0009 (4.0)	49.0001 (4.0)
64	64.8456	64.4814 (0.8)	64.0328 (3.9)	64.0021 (4.0)	64.0001 (4.0)
81	95.7798	81.9488 (4.0)	81.0659 (3.8)	81.0042 (4.0)	81.0003 (4.0)
100	124.9301	101.7308 (3.8)	100.1229 (3.8)	100.0080 (3.9)	100.0005 (4.0)
DOF	15	31	63	127	255

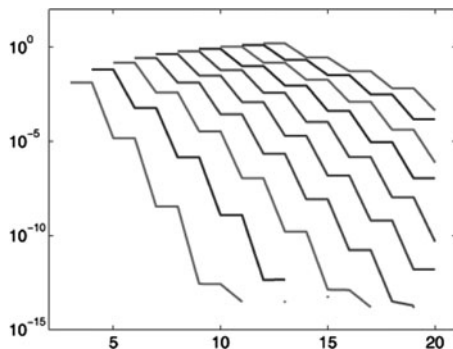
Fig. 2 The second eigenfunction computed and plotted using the code in Listing 1.2 ($n = 4$ and $k = 2$). The dashed line represents the linear part of the solution



As an additional example, in Listing 1.2 we report a code that solves the same problem using continuous piecewise quadratic finite elements. The matrix construction has been made using a hierarchical approach: in the interval $[x_i, x_{i+1}]$ a quadratic function is seen as the sum of its affine part with matching values at the endpoints and a quadratic bubble. It turns out that the stiffness matrix A is a 2×2 block matrix of size $2n - 1$ (n being the number of subintervals) in which only the two blocks on the main diagonal are different from zero: the block A_{11} of size $n - 1$ is equal to the stiffness matrix of the previous case and the block A_{22} of size n is given by the contribution of the bubbles. The mass matrix M has a block structure too, but now the off-diagonal terms are non zero since there are contributions coming from the interaction between affine functions and bubbles.

The results in Table 2 show that the eigenvalues are approximated with fourth order accuracy. A direct comparison with Table 1 confirms that quadratic elements provide much more accurate results even with less degrees of freedom. Figure 2 shows the second eigenfunctions computed with the code reported in Listing 1.2: the linear part is drawn with a dashed line and the sum of the linear part and the

Fig. 3 Exponential convergence of eigenvalues computed with the code reported in Listing 1.3



bubble (i.e., the full solution) is represented by the solid line. This plot compares to Fig. 1, where the same eigenfunctions was computed with piecewise linear elements. It is apparent that (even on such coarse meshes) quadratic elements provide a more accurate result using the same number of degrees of freedom (7).

The results shown so far concern the approximation of problem (9) using the h version of the finite element method. This means that a better approximation is obtained by successive refinements of the mesh and error estimates are given in terms of the meshsize h , which is supposed to tend to zero. We conclude the discussion of this example with a remark on the p version of the finite element methods, that is the mesh is kept fixed and a better approximation is obtained by raising the order of the polynomials. The code reported in Listing 1.3 computes the eigenvalues of problem (9) using p -th order polynomials on a mesh which is composed of a single element (i.e., using a plain spectral method).

The stiffness and mass matrix are evaluated using the arguments presented in [30, Sect. 3.8]. It is interesting to analyze the results of some computations. Since we are expecting exponential convergence, we plot the errors using a semilog scale in Fig. 3. The x axis represents the polynomial order (ranging from 3 to 20) and the y axis reports the logarithm of the error. The errors in the approximation of the eigenvalues are reported from the left to the right (this means, in particular, that the most left line corresponds to the error in the approximation of the first eigenvalue $\lambda = 1$). It can be observed a typical behavior of spectral approximations: the convergence is exponential and is dependent on the parity of the polynomial order. Table 3, for instance, shows the computed values of the fifth discrete eigenvalue approximating $\lambda = 25$. The polynomial order varies from 7 to 20 (the fifth eigenvalue shows up only when the order is at least 7 and the dimension of the system is 5). It is apparent that the approximation improves only every other step (when the order is raised from even to odd in this case, but the situation is the opposite if an even eigenvalue is considered, see Fig. 3). It is also clear that the accuracy of the discrete values is not very good when the order is 7 or 8 but, after the convergence has started, it is very fast (more than 10 digits with 17 degrees of freedom, while we needed over 100 degrees of freedom to get only 3 digits with quadratic elements, see Table 2).

Table 3 Fifth eigenvalue computed with the code in Listing 1.3 for different values of p

p	DOF	Computed
7	5	35.5593555378041
8	6	35.5593555378041
9	7	25.7779168651921
10	8	25.7779168651921
11	9	25.0306605127133
12	10	25.0306605127132
13	11	25.0004945052929
14	12	25.0004945052929
15	13	25.0000037734250
16	14	25.0000037734250
17	15	25.0000000156754
18	16	25.0000000156756
19	17	25.0000000000389
20	18	25.0000000000389

Listing 1.1 Matlab code for the 1D Laplace eigenvalue problem: piecewise linear elements

```

clear all
close all
k=2; % eigenfunction to be plotted
n=8; % number of subdivisions
kev=4; % number of eigenvalues to compute
a=0; b=pi; % interval endpoints
h=(b-a)/n; % mesh size
x=linspace(a,b,n+1); % mesh nodes
%
% stiffness matrix A
%
e=ones(n-1,1);
A=spdiags([-e 2*e -e]/h,-1:1,n-1,n-1);
%
% mass matrix M
%
M=spdiags([1/6*e 2/3*e 1/6*e]*h,-1:1,n-1,n-1);
%
% compute solution and sort eigenmodes
%
[v,d]=eigs(A,M,min(kev,length(M)), 'SM');
[ev,I]=sort(diag(d));
ef=v(:,I);
%
% display first 10 eigenvalues
%
ev(1:min(length(ev),10))

```



```

%
% plot selected eigenfunction
%
vector=[0;ef(:,k);0];
c=min(vector); d=max(vector);
c=c-(d-c)*.1; d=d+(d-c)*.1;
set(0,'defaultaxesfontsize',15)
set(0,'defaulttextfontsize',15)
figure
hold on
plot(x,vector,'-k')
plot(x,vector,'.k')
axis([a b c d])
set(findobj('type','line'),'linewidth',2,...
    'markersize',20)
lambda=sprintf('%0.7g',ev(k));
title(['\lambda=' lambda])

```

Listing 1.2 Matlab code for the 1D Laplace eigenvalue problem: piecewise quadratic elements

```

clear all
close all
k=2; % eigenfunction to be plotted
n=4; % number of subdivisions
kev=4; % number of eigenvalues to compute
a=0; b=pi; % interval endpoints
h=(b-a)/n; % mesh size
x=linspace(a,b,n+1); % mesh nodes
%
% stiffness matrix A (contributions coming from P1)
%
e=ones(n,1);
A11=spdiags([-e 2*e -e]/h,-1:1,n-1,n-1);
%
% stiff. matrix A (contributions coming from bubbles)
%
A22=spdiags(16/3*e/h,0,n,n);
%
% stiff. matrix A: assembly
%
A=[A11,zeros(n-1,n);zeros(n,n-1),A22];
%
% mass matrix M (contributions coming from P1)
%

```

```

M11=spdiags([1/6*e 2/3*e 1/6*e]*h,-1:1,n-1,n-1);
%
% mass matrix M (contributions coming from bubbles)
%
M22=spdiags(8/15*e*h,0,n,n);
%
% mass matrix M (interactions P1/bubbles)
%
M12=spdiags([e e]/3*h,[0 1],n-1,n);
%
% mass matrix M: assembly
%
M=[M11,M12;M12',M22];
%
% compute solution and sort eigenmodes
%
[v,d]=eigs(A,M,min(kev,length(M)), 'SM');
[ev,I]=sort(diag(d));
ef=v(:,I);
%
% display first 10 eigenvalues
%
ev(1:min(length(ev),10))
%
% plot selected eigenfunction
%
% P1 component
%
vector=[0;ef(1:n-1,k);0];
%
% bubble component
%
bubble=ef(n:end,k);
%
c=min(vector); d=max(vector);
c=c-(d-c)*.1; d=d+(d-c)*.1;
figure
hold on
set(0,'defaultaxesfontsize',15)
set(0,'defaulttextfontsize',15)
%
kk=10; % number of points for bubble reconstructions
for i=1:n
    for j=1:kk

```

```

    xx=linspace(0,h,kk);
    plot([x(i)+xx],[bubble(i)*4/h^2*xx.*(h-xx)+...
        (vector(i)+(vector(i+1)-vector(i))/h*xx)],...
        '-k')
    end
end
%
plot(x,vector,'-k')
plot(x,vector,'.k')
axis([a b c d])
set(findobj('type','line'),'linewidth',2,...
    'markersize',20)
lambda=sprintf('%0.7g',ev(k));
title(['\lambda=' lambda])

```

Listing 1.3 Matlab code for the 1D Laplace eigenvalue problem: spectral method

```

clear all;
p=10; % order of the polynomial
a=0; b=pi; % interval endpoints
%
% stiffness matrix A (modal basis in [-1 1])
%
A=eye(p+1);
A(1:2,1:2)=[1/2 -1/2;-1/2 1/2];
%
% mass matrix M (modal basis in [-1 1])
%
diagonal=zeros(p,1);
for k=2:p
    diagonal(k+1)=2/(2*k-3)/(2*k+1);
end
M=diag(diagonal);
%
diagonal2=zeros(p,1);
for k=2:p-2
    diagonal2(k+2)=-1/(2*k+1)/sqrt((2*k-1)*(2*k+3));
end
M=M+diag(diagonal2(2:p),-2)+diag(diagonal2(2:p),2);
%
M(1:2,1:4)=[2/3 1/3 1/sqrt(6) -1/3/sqrt(10);...
    1/3 2/3 1/sqrt(6) 1/3/sqrt(10)];
M(3:4,1:2)=[1/sqrt(6) 1/sqrt(6);...
    -1/3/sqrt(10) 1/3/sqrt(10)];

```

```

%
% solve for Dirichlet boundary conditions
% and rescale interval
%
ev=sort(eig(A(3:p,3:p),M(3:p,3:p)))*4/(b-a)/(b-a);
ev(1:min(10,p-2))

```

3.2 Laplace Eigenvalue Problem in Mixed Form

The standard mixed formulation of problem (9) is: given $\Sigma = H^1(\Omega)$ and $U = L^2(\Omega)$, find $\lambda \in \mathbb{R}$ and $u \in U$, with $u \neq 0$, such that for some $s \in \Sigma$

$$\begin{cases} \int_0^\pi s(x)t(x)dx + \int_0^\pi u(x)t'(x)dx = 0 & \forall t \in \Sigma \\ \int_0^\pi s'(x)v(x)dx = -\lambda \int_0^\pi u(x)v(x)dx & \forall v \in U. \end{cases} \quad (10)$$

Its Galerkin discretization is based on discrete subspaces $\Sigma_h \subset \Sigma$ and $U_h \subset U$ and reads: find $\lambda_h \in \mathbb{R}$ and $u_h \in U_h$ with $u_h \neq 0$, such that for some $s_h \in \Sigma_h$ it holds

$$\begin{cases} \int_0^\pi s_h(x)t(x)dx + \int_0^\pi u_h(x)t'(x)dx = 0 & \forall t \in \Sigma_h \\ \int_0^\pi s_h'(x)v(x)dx = -\lambda_h \int_0^\pi u_h(x)v(x)dx & \forall v \in U_h. \end{cases}$$

The matrix form of the problem is

$$\begin{pmatrix} A & B^T \\ B & 0 \end{pmatrix} \begin{pmatrix} \mathbf{x} \\ \mathbf{y} \end{pmatrix} = -\lambda \begin{pmatrix} 0 & 0 \\ 0 & M \end{pmatrix} \begin{pmatrix} \mathbf{x} \\ \mathbf{y} \end{pmatrix},$$

where A is the mass matrix in Σ_h , M is the mass matrix in U_h , and B is the matrix defined as follows:

$$b_{jk} = \int_0^\pi \varphi_k'(x)\psi_j(x)dx,$$

where $\{\varphi_k\}$ and $\{\psi_j\}$ are bases in Σ_h and U_h , respectively.

Example 1 (P1-P1 element). We start with the simplest choice of finite element spaces: continuous piecewise linears for both Σ_h and U_h . The corresponding Matlab code is reported in Listing 1.4. It should be noted that the homogeneous Dirichlet boundary conditions are enforced in a natural way through the formulation (10), so that the matrices A , B , and M do not include boundary conditions.

Table 4 Eigenvalues computed using the code in Listing 1.4 for different values of n

Exact	Computed (rate)				
	$n = 8$	$n = 16$	$n = 32$	$n = 64$	$n = 128$
	0.0000	−0.0000	0.0000	0.0000	−0.0000
1	1.0001	1.0000 (4.1)	1.0000 (4.0)	1.0000 (4.0)	1.0000 (4.0)
4	3.9660	3.9981 (4.2)	3.9999 (4.0)	4.0000 (4.0)	4.0000 (4.0)
	7.4257	8.5541	8.8854	8.9711	8.9928
9	8.7603	8.9873 (4.2)	8.9992 (4.1)	9.0000 (4.0)	9.0000 (4.0)
16	14.8408	15.9501 (4.5)	15.9971 (4.1)	15.9998 (4.0)	16.0000 (4.0)
25	16.7900	24.5524 (4.2)	24.9780 (4.3)	24.9987 (4.1)	24.9999 (4.0)
	38.7154	29.7390	34.2165	35.5415	35.8846
36	39.0906	35.0393 (1.7)	35.9492 (4.2)	35.9970 (4.1)	35.9998 (4.0)
49		46.7793	48.8925 (4.4)	48.9937 (4.1)	48.9996 (4.0)

In [21, Table 4.1] it has already been observed that this method does not provide reliable results. Table 4 shows that the correct eigenvalues are approximated with fourth order accuracy, while several other *spurious* modes are present. Figure 4 shows the first two spurious modes, corresponding to the value $\lambda = 0$ and to a discrete value which seems to converge to $\lambda = 9$ (i.e., this mode is spurious in the sense of a wrong multiplicity). The eigenfunction u is plotted in the left part of the figure, while the corresponding component s is on the right. An example of correct eigenfunction is shown in Fig. 5: this is the eigenfunction obtained exactly with the parameters of Listing 1.4 and should be compared with Figs. 1 and 2. For the sake of completeness, we report in Fig. 6 the eigenfunction corresponding to the discrete eigenvalue approximating the *correct* continuous eigenvalue $\lambda = 9$ (i.e., the fifth discrete mode).

Example 2 (P1-P0 element). We now describe a *convergent* mixed scheme for which no spurious mode is present. Since the space U is $L^2(\Omega)$, there is no need to consider a finite element approximation U_h made of continuous functions. For reasons which are clear from the abstract theory, it is natural to consider the following choice: continuous piecewise linear elements for the approximation of Σ and discontinuous piecewise constants for the approximation of U . The corresponding Matlab code is reported in Listing 1.5.

As already observed in [21, Sect. 4.2], the numerical results are pretty much related to the ones of the standard Galerkin approximation of the Laplace eigenvalue problem: the eigenvalues are reported in Table 5 where second order of convergence is clearly detected. As far as the number of degrees of freedom is concerned, Table 5 shows the dimension of the space U_h , since in the solution procedure the variable s can be eliminated (see Listing 1.5).

Figure 7 shows the second eigenfunction computed using the code in Listing 1.5 and should be compared with Fig. 1.

Example 3 (P2-P0 element). We conclude this section about one-dimensional examples with the discussion of the P2-P0 scheme for the approximation of the

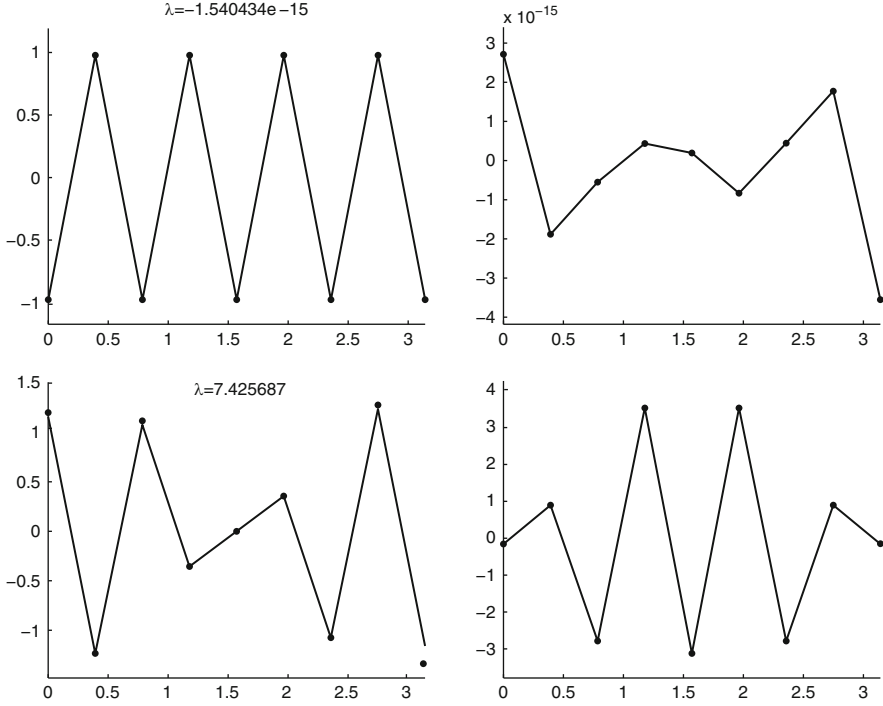


Fig. 4 Some spurious modes computed with the code in Listing 1.4: the first (top) and fourth (bottom) eigenfunction. The left subplots correspond to the component u and the right ones to s . Notice that the function in the top right subplot is zero up to machine precision

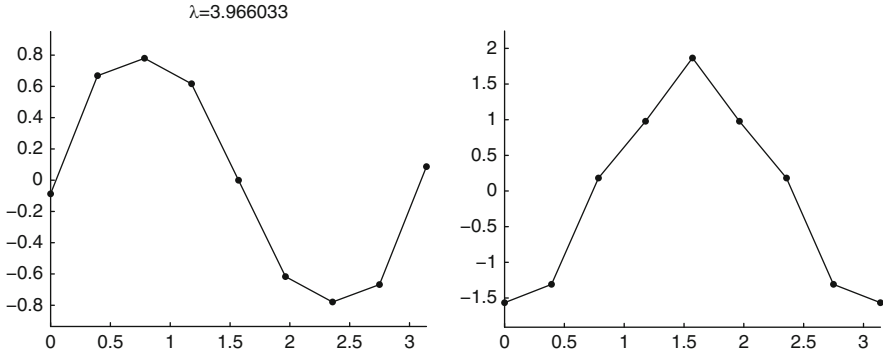


Fig. 5 An approximation of the second eigenfunction of problem (10) (the component u on the left side and the component s on the right) computed with the code in Listing 1.4 for $n = 8$ and $k = 3$

mixed problem (10). We started from the P1-P1 element (see Example 1) which is affected by spurious modes and moved to the P1-P0 element (see Example 2) which is nicely convergent. In this last example, we shall demonstrate the bad behavior of the P2-P0 element where we use continuous piecewise quadratic elements for

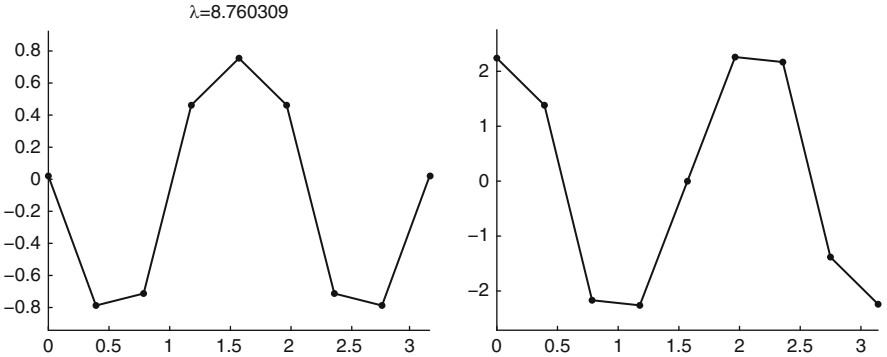


Fig. 6 An approximation of the third eigenfunction of problem (10) (the component u on the left side and the component s on the right) computed with the code in Listing 1.4 for $n = 8$ and $k = 5$

Table 5 Eigenvalues computed using the code in Listing 1.5 for different values of n

Exact	Computed (rate)				
	$n = 8$	$n = 16$	$n = 32$	$n = 64$	$n = 128$
1	1.0129	1.0032 (2.0)	1.0008 (2.0)	1.0002 (2.0)	1.0001 (2.0)
4	4.2095	4.0517 (2.0)	4.0129 (2.0)	4.0032 (2.0)	4.0008 (2.0)
9	10.0803	9.2631 (2.0)	9.0652 (2.0)	9.0163 (2.0)	9.0041 (2.0)
16	19.4537	16.8382 (2.0)	16.2067 (2.0)	16.0515 (2.0)	16.0129 (2.0)
25	33.2628	27.0649 (2.0)	25.5059 (2.0)	25.1257 (2.0)	25.0314 (2.0)
36	51.3724	40.3212 (1.8)	37.0525 (2.0)	36.2610 (2.0)	36.0651 (2.0)
49	69.5582	57.0672 (1.3)	50.9572 (2.0)	49.4840 (2.0)	49.1206 (2.0)
64	77.8147	77.8147 (0.0)	67.3528 (2.0)	64.8266 (2.0)	64.2059 (2.0)
81		103.0473	86.3943 (2.0)	82.3258 (2.0)	81.3299 (2.0)
100		133.0513	108.2597 (2.0)	102.0237 (2.0)	100.5030 (2.0)
DOF	8	16	32	64	128

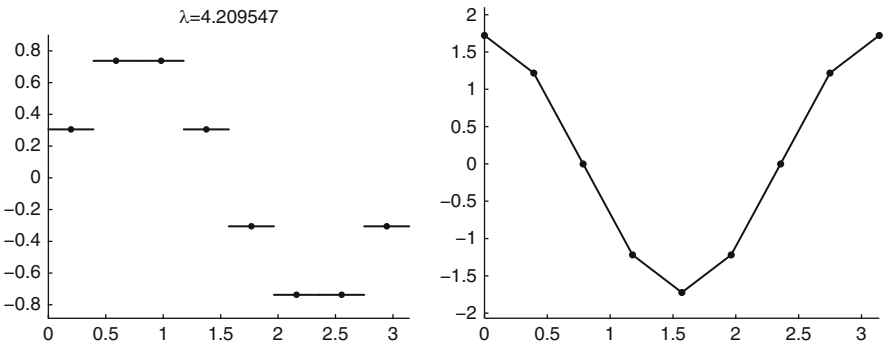
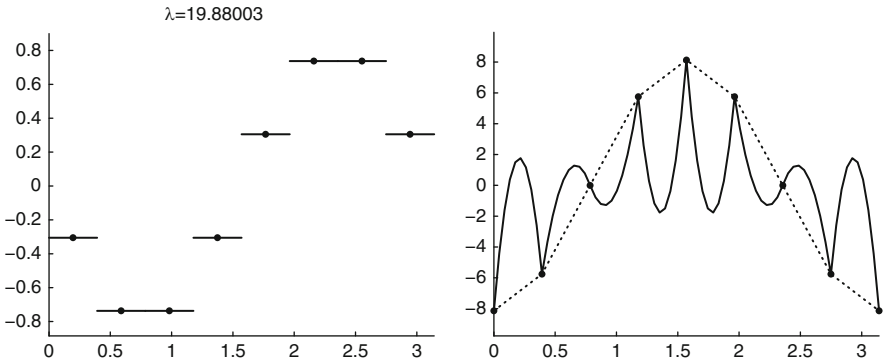


Fig. 7 The second eigenfunction computed and plotted using the code in Listing 1.5 ($n = 8$ and $k = 2$). The component u is on the left side and the component s on the right

Table 6 Eigenvalues computed using the code in Listing 1.6 for different values of n

Exact	Computed (rate with respect to 6λ)				
	$n = 8$	$n = 16$	$n = 32$	$n = 64$	$n = 128$
1	5.7061	5.9238 (1.9)	5.9808 (2.0)	5.9952 (2.0)	5.9988 (2.0)
4	19.8800	22.8245 (1.8)	23.6953 (1.9)	23.9231 (2.0)	23.9807 (2.0)
9	36.7065	48.3798 (1.6)	52.4809 (1.9)	53.6123 (2.0)	53.9026 (2.0)
16	51.8764	79.5201 (1.4)	91.2978 (1.8)	94.7814 (1.9)	95.6925 (2.0)
25	63.6140	113.1819 (1.2)	138.8165 (1.7)	147.0451 (1.9)	149.2506 (2.0)
36	71.6666	146.8261 (1.1)	193.5192 (1.6)	209.9235 (1.9)	214.4494 (2.0)
49	76.3051	178.6404 (0.9)	253.8044 (1.5)	282.8515 (1.9)	291.1344 (2.0)
64	77.8147	207.5058 (0.8)	318.0804 (1.4)	365.1912 (1.8)	379.1255 (1.9)
81		232.8461	384.8425 (1.3)	456.2445 (1.8)	478.2172 (1.9)
100		254.4561	452.7277 (1.2)	555.2659 (1.7)	588.1806 (1.9)
DOF	8	16	32	64	128

**Fig. 8** The second eigenfunction computed and plotted using the code in Listing 1.6 ($n = 8$ and $k = 2$). The component u is on the left side and the component s on the right

the approximation of Σ and discontinuous piecewise constants for U . The final message will be that, as expected, when dealing with mixed schemes the choice of the discrete spaces has to be made very carefully in order to meet suitable assumptions. For a discussion on this issues the reader is referred to Sect. 4.

A Matlab code for this element is presented in Listing 1.6. As in Listing 1.2 we use a hierarchical approach in order to implement the P2 element, that is the space of quadratic elements is presented as the sum of continuous piecewise linears and local bubbles.

In [21, Sect. 4.4] it has been shown that this scheme does not converge. More precisely, the discrete eigenvalues computed with the code in Listing 1.6 converge up to second order to wrong values which correspond to six times the correct eigenvalues. Table 6 shows this behavior.

Moreover, it can be shown that the eigenspaces are good approximations of the correct ones as far as the component u is concerned, while the component s is badly

approximated. Figure 8, for instance, shows the eigenfunctions corresponding to the second eigenvalue (which converges to six times $\lambda = 4$). It can be observed that u_h is a good approximation of the space generated by $\sin(2x)$; on the other hand, the *linear* part of s_h is a good approximation of the space generated by $2\cos(2x)$, while the *bubble* part of s provides a *spurious* component of the solution. This fact is a consequence of the lack in the ellipticity in the kernel property (see Sect. 4).

Listing 1.4 Matlab code for the 1D Laplace eigenvalue problem in mixed form: P1-P1 element

```

clear all
close all
k=3; % eigenfunction to be plotted
n=8; % number of subdivisions
kev=5; % number of eigenvalues to compute
a=0; b=pi; % interval endpoints
h=(b-a)/n; % mesh size
x=linspace(a,b,n+1); % mesh nodes
%
% mass matrix A (no boundary conditions)
%
e=ones(n+1,1);
A=spdiags([1/6*e 2/3*e 1/6*e]*h,-1:1,n+1,n+1);
A(1,1)=1/3*h; A(n+1,n+1)=1/3*h;
%
% the matrix B (no boundary conditions)
%
B=spdiags([e/2 -e/2],[-1 1],n+1,n+1);
B(1,1)=1/2; B(n+1,n+1)=-1/2;
%
% mass matrix M is equal to A
%
%
% compute solution and sort eigenmodes
%
Schur=A\B';
[v,d]=eigs(B*Schur,A,min(kev,length(A)),.1);
[ev,I]=sort(diag(d));
ef=v(:,I);
%
% display first 10 eigenvalues
%
ev(1:min(10,length(ev)))
%
% plot selected eigenfunction
%
```

```

set(0,'defaultaxesfontsize',15)
set(0,'defaulttextfontsize',15)
%
% the component "u"
%
figure(1)
clf
hold on
vector=ef(:,k);
c=min(vector); d=max(vector);
c=c-(d-c)*.1; d=d+(d-c)*.1;
plot(x,vector,'-k')
plot(x,vector,'.k')
set(findobj('type','line'),'linewidth',2,...
    'markersize',20)
axis([a b c d])
lambda=sprintf(' %0.7g',ev(k));
title(['\lambda=' lambda])
%
% the component "s"
%
figure(2)
clf
hold on
vector=-Schur*ef(:,k);
c=min(vector); d=max(vector);
c=c-(d-c)*.1; d=d+(d-c)*.1;
plot(x,vector,'-k')
plot(x,vector,'.k')
set(findobj('type','line'),'linewidth',2,...
    'markersize',20)
axis([a b c d])

```

Listing 1.5 Matlab code for the 1D Laplace eigenvalue problem in mixed form: P1-P0 element

```

clear all
close all
k=2; % eigenfunction to be plotted
n=8; % number of subdivisions
kev=4; % number of eigenvalues to compute
a=0; b=pi; % interval endpoints
h=(b-a)/n; % mesh size
x=linspace(a,b,n+1); % mesh nodes
%

```

```

% mass matrix A
%
e=ones(n+1,1);
A=spdiags([1/6*e 2/3*e 1/6*e]*h,-1:1,n+1,n+1);
A(1,1)=1/3*h; A(n+1,n+1)=1/3*h;
%
% the matrix B
%
B=spdiags([-e e],[0 1],n,n+1);
%
% mass matrix M
%
M=spdiags(e*h,0,n,n);
%
% compute solution and sort eigenmodes
%
Schur=A\B';
[v,d]=eigs(B*Schur,M,min(kev,length(M)),'SM');
[ev,I]=sort(diag(d));
ef=v(:,I);
%
% display first 10 eigenvalues
%
ev(1:min(10,length(ev)))
%
% plot selected eigenfunction
%
set(0,'defaultaxesfontsize',15)
set(0,'defaulttextfontsize',15)
%
% the component "u"
%
figure(1)
clf
hold on
c=min(ef(:,k)); d=max(ef(:,k));
c=c-(d-c)*.1; d=d+(d-c)*.1;
for j=1:n
    value=ef(j,k);
    plot([x(j) x(j+1)],[value,value'],'-k')
    plot((x(j)+x(j+1))/2,value','k')
end
set(findobj('type','line'),'linewidth',2,...
    'markersize',20)

```

```

axis ([ a b c d])
lambda=sprintf( '%0.7g',ev(k));
title ([ '\lambda=' lambda])
%
% the component "s"
%
figure (2)
clf
hold on
vector=-Schur*ef(:,k);
c=min(vector); d=max(vector);
c=c-(d-c)*.1; d=d+(d-c)*.1;
plot(x,vector, '-k')
plot(x,vector, '.k')
set(findobj('type','line'),'linewidth',2,...
    'markersize',20)
axis ([ a b c d])

```

Listing 1.6 Matlab code for the 1D Laplace eigenvalue problem in mixed form: P2-P0 element

```

clear all
close all
k=2; % eigenfunction to be plotted
n=8; % number of subdivisions
kev=4; % number of eigenvalues to compute
a=0; b=pi; % interval endpoints
h=(b-a)/n; % mesh size
x=linspace(a,b,n+1); % mesh nodes
%
% mass matrix A (contributions coming from P1)
%
e=ones(n+1,1);
A11=spdiags([1/6*e 2/3*e 1/6*e]*h,-1:1,n+1,n+1);
A11(1,1)=1/3*h; A11(n+1,n+1)=1/3*h;
%
% mass matrix A (contributions coming from bubbles)
%
A22=spdiags(8/15*e*h,0,n,n);
%
% mass matrix A (interactions P1/bubbles)
%
A12=spdiags([e e]/3*h,[-1 0],n+1,n);
A=[A11,A12;A12',A22];
%

```

```

% the matrix B
%
B=spdiags([-e e],[0 1],n,n+n+1);
%
% mass matrix M
%
M=spdiags(e*h,0,n,n);
%
% compute solution and sort eigenmodes
%
Schur=A\B';
[v,d]=eigs(B*Schur,M,min(kev,length(M)),'SM');
[ev,I]=sort(diag(d));
ef=v(:,I);
%
% display first 10 eigenvalues
%
ev(1:min(length(ev),10))
%
% plot selected eigenfunction
%
set(0,'defaultaxesfontsize',15)
set(0,'defaulttextfontsize',15)
%
% the component "u"
%
figure(1)
clf
hold on
for j=1:n
    value=ef(j,k);
    plot([x(j) x(j+1)],[value,value'],'-k')
    plot((x(j)+x(j+1))/2,value','k')
end
set(findobj('type','line'),'linewidth',2,...
    'markersize',20)
c=min(ef(:,k)); d=max(ef(:,k));
c=c-(d-c)*.1; d=d+(d-c)*.1;
axis([a b c d])
lambda=sprintf('%0.7g',ev(k));
title(['\lambda=' lambda])
%
% the component "s"
%
```

```

figure (2)
clf
hold on
vector=Schur*ef(:,k);
%
% P1 component
%
linear=vector(1:n+1);
c=min(linear); d=max(linear);
c=c-(d-c)*.1; d=d+(d-c)*.1;
%
% bubble component
%
bubble=vector(n+2:end);
%
kk=10; % number of points for bubble reconstructions
%
for i=1:n
    for j=1:kk
        xx=linspace(0,h,kk);
        plot([x(i)+xx],[bubble(i)*4/h^2*xx.*(h-xx)+...
            (linear(i)+(linear(i+1)-linear(i))/h*xx)],...
            '-k')
    end
end
%
plot(x,linear,'-k')
plot(x,bubble,'-k')
axis([a b c d])
set(findobj('type','line'),'linewidth',2,...
    'markersize',20)

```

4 Eigenvalue Problems in Mixed Form

The examples presented in Sect. 3 confirm that Galerkin discretizations of eigenvalue problems in mixed form present a different behavior from standard Galerkin approximations of variationally posed eigenvalue problems. In particular, Sect. 3.1 shows that standard Galerkin approximations of the Laplace eigenvalue problem are optimally convergent as soon as we choose a reasonable approximating space. This is the important consequence of Theorem 1. Let us define $T : L^2 \rightarrow L^2$ using the source problem associated to (9): given $f \in L^2$ let $Tf \in H^1$ be the solution of the

problem

$$\int_0^\pi (Tf)'(x)v'(x)dx = \int_0^\pi f(x)v(x)dx.$$

The discrete operator $T_h : L^2 \rightarrow L^2$ can be defined analogously using the discrete source problem. It turns out that the operator T is compact from L^2 into H^1 and that the elliptic projection onto standard finite element spaces converges pointwise to the identity operator from H^1 to L^2 . Hence, we can apply Theorem 1 with the choice $H = L^2$ and $V = H^1$ in order to conclude that T_h converges to T in the space $\mathcal{L}(L^2)$.

On the other hand, Examples 1, 2 and 3 show that in the case of mixed approximation we need to impose suitable compatibility assumptions between the two approximating finite element spaces. This fact is not surprising since we are used to the classical inf-sup conditions [29] for mixed finite elements, but we shall see that for eigenvalue problems the situation is different from that of the source problem.

4.1 Inf-Sup Conditions

We now discuss Examples 1, 2, and 3 in respect to the classical inf-sup conditions.

It is well-known that for the well-posedness of the *source* problem associated with (10) the following two conditions are sufficient and, in a suitable sense, necessary: the ellipticity in the discrete kernel

$$\|t_h\|_{L^2}^2 \geq \alpha \|t_h\|_{H^1}^2 \quad \forall t_h \in \mathbb{K}_h, \quad (11)$$

where $\mathbb{K}_h = \{t_h \in \Sigma_h : \int_0^\pi v(x)t_h'(x)dx = 0 \ \forall v \in U_h\}$, and the inf-sup condition

$$\inf_{v_h \in U_h} \sup_{t_h \in \Sigma_h} \frac{\int_0^\pi v_h(x)t_h'(x)dx}{\|v_h\|_{L^2} \|t_h\|_{H^1}} \geq \beta. \quad (12)$$

Remark 3. Conditions (11) and (12) should be changed to use the divergence operator instead of the first derivative and $H(\text{div})$ instead of H^1 in the multidimensional case.

We start by showing that the P1-P0 element discussed in Example 2 satisfies both conditions (11) and (12).

The ellipticity in the discrete kernel is a trivial consequence of the fact that the derivative of a function in P1 is an object of P0, hence functions in \mathbb{K}_h have vanishing derivative (take $v = t'$ in the definition of \mathbb{K}_h).

The inf-sup condition can be proved by constructing a Fortin operator (see [29, Prop. II.2.8]). We need to find $\Pi_h : H^1 \rightarrow \Sigma_h$ such that

$$\int_0^\pi (s'(x) - (\Pi_h s)'(x))v(x)dx = 0 \quad \forall v \in U_h$$

and $\|\Pi_h s\|_{H^1} \leq C\|s\|_{H^1}$. It can be easily observed that the standard *nodal* interpolation operator $s \mapsto s_I$ satisfies the required properties; indeed, for each element $[x_i, x_{i+1}]$ we have

$$\int_{x_i}^{x_{i+1}} s'_I(x)dx = s_I(x_{i+1}) - s_I(x_i) = s(x_{i+1}) - s(x_i) = \int_{x_i}^{x_{i+1}} s'(x)dx.$$

Remark 4. The P1-P0 element is the one dimensional counterpart of the well-known Raviart–Thomas element

Moving to the P1-P1 element discussed in Example 1, it has been observed several times in the literature that it does not satisfies the inf-sup condition (see, for instance, [11]). What is surprising about the bad behavior reported in Table 4 is that the P1-P1 element is convergent for the corresponding *source* problem when the solution is smooth and the eigenfunctions of the Laplace problem are analytic. It turns out that the approximation of eigenvalue problems does not follow the same lines as the approximation of the corresponding source problem: there are several spurious modes even if the regularity of the eigenfunctions is not an issue. To be more precise, the zero frequency reported in Table 4 was expected and is a consequence of the lack of the inf-sup condition: there is a function $u_h \in U_h$ with $u_h \neq 0$ such that $\int_0^\pi u_h(x)t'(x)dx = 0$ for all $t \in \Sigma_h$; such a function is the eigenfunction shown in Fig. 4 (top left); on the other hand, the other spurious modes cannot be predicted from the standard theory of mixed finite elements.

Let us conclude this section with the analysis of the P2-P0 element presented in Example 3 which can be seen as a modification of the P1-P0 element with an enrichment of the space Σ_h . The hierarchical construction of the matrices in Listing 1.6 shows explicitly the nature of the enrichment which consists of a single quadratic bubble in each element. Since the P1-P0 element satisfies the inf-sup condition (12), the P2-P0 satisfies the inf-sup condition as well (the supremum is taken over a larger space). On the other hand the enrichment of the space Σ_h implies a modification of the discrete kernel \mathbb{K}_h for the definition of the ellipticity condition (11). In particular, all the element bubbles are elements of \mathbb{K}_h (they vanish at the endpoints of the interval, hence their first derivatives have zero mean value) and, moreover, are functions for which the uniform ellipticity (11) does not hold as it can be easily observed by a standard scaling argument or by explicit computation. Figure 8 confirms that the bad behavior of the method is due to the presence of the bubbles which pollute the discrete solution. For similar consideration related to the corresponding source problem the reader is referred to [26].

4.2 Convergence of Eigenvalue Problems in Mixed Forms

From the discussion of Sect. 4.1 it might seem that the two main conditions for the stability of the mixed source problem, namely the ellipticity in the discrete kernel (11) and the inf-sup condition (12), are sufficient for the convergence of the mixed eigenvalue problem as well. On the other hand, the analysis of the P1-P1 element should warn the reader: in that case the approximation of the source problem is convergent when the solution is smooth enough, while the approximation of the eigenvalue problem presents spurious modes (even though all exact eigenfunctions are smooth).

The fundamental results contained in [22, 23] state that the natural conditions for the good approximation and the absence of spurious modes in the approximation of eigenvalue problems in mixed form *are not* the classical inf-sup conditions. We recall in this setting the conditions introduced in [22] (see also [21, Part 3]).

In order to convince the reader that the eigenvalue problem has a substantially different nature from the source problem, we try to repeat the argument of Theorem 1 in the framework of mixed approximations: we will show that the situation is now more complicated. Roughly speaking, Theorem 1 says that a suitable compactness assumption turns pointwise convergence into uniform convergence. In order to use a similar argument in this framework, we need to introduce a suitable solution operator T and to show a suitable compactness property. Since the solution of the source problem corresponding to (10) has two components s and u , we firstly have to choose how to define the solution operator. A first (and, as we shall see, wrong) possibility is to define $T_{\Sigma U} : L^2 \times L^2 \rightarrow L^2 \times L^2$ as follows:

$$(f, g) \xrightarrow{\text{cutoff}} (0, g) \xrightarrow{T_2} (s, u),$$

where the operator $T_2 : L^2 \times L^2 \rightarrow L^2 \times L^2$ corresponds to $T_2(f, g) = (s, t) \in H^1 \times L^2$ solution of the following source problem

$$\begin{cases} \int_0^\pi s(x)t(x)dx + \int_0^\pi u(x)t'(x)dx = \int_0^\pi f(x)t(x)dx & \forall t \in H^1 \\ \int_0^\pi s'(x)v(x)dx = - \int_0^\pi g(x)v(x)dx & \forall v \in L^2. \end{cases} \quad (13)$$

The discrete operator $T_{\Sigma U, h}$ can be defined analogously using the same cutoff function and the discrete source problem. In order to fit the framework of Theorem 1 one needs to introduce a suitable projection operator. This can be done by using the source mixed problem: let $Q_h : H^1 \times L^2 \rightarrow \Sigma_h$ and $R_h : H^1 \times L^2 \rightarrow U_h$ be defined starting from $(s, u) \in H^1 \times L^2$ in order to satisfy the following equations

$$\begin{aligned}
& \int_0^\pi Q_h(s, u)(x)t(x)dx + \int_0^\pi R_h(s, u)(x)t'(x)dx \\
&= \int_0^\pi s(x)t(x)dx + \int_0^\pi u(x)t'(x)dx \quad \forall t \in H^1 \\
& \int_0^\pi (Q_h(s, u))'(x)v(x)dx = \int_0^\pi s'(x)v(x)dx \quad \forall v \in L^2.
\end{aligned}$$

Taking $P_h = (Q_h, R_h)$, it is clear that we have $T_{\Sigma U, h} = P_h T_{\Sigma U}$, so that we might think of adapting Theorem 1 to this situation.

Unfortunately, the compactness assumption on $T_{\Sigma U}$ *does not* hold. Indeed, taking $H = L^2 \times L^2$ and $V = H^1 \times L^2$, we would need $T_{\Sigma U}$ compact from $L^2 \times L^2$ in $H^1 \times L^2$ which is in conflict with the fact that in (13) the derivative of s is equal to $-g$. As a possible workaround, we can try to use the second comment contained in Remark 1. Unfortunately, for the same reason as before $T_{\Sigma U}$ is not compact from $H^1 \times L^2$ in $H^1 \times L^2$ either.

The correct approach for the definition of the solution operator has been introduced in [22]. Being interested in an eigenvalue problem which involves the eigenfunction u , the natural choice is to define $T : L^2 \rightarrow L^2$ as follows: given $g \in L^2$ find $s \in H^1$ and $Tg \in U_h$ such that

$$\begin{cases} \int_0^\pi s(x)t(x)dx + \int_0^\pi Tg(x)t'(x)dx = 0 & \forall t \in H^1 \\ \int_0^\pi s'(x)v(x)dx = - \int_0^\pi g(x)v(x)dx & \forall v \in L^2. \end{cases} \quad (14)$$

The discrete operator T_h can be defined analogously using the discrete source problem. In [22] sufficient (and, in a suitable sense, necessary) conditions for the convergence of T_h to T have been introduced. These conditions, which in particular imply the good approximation of Problem (10), are:

the *weak approximability* of H^2 , that is

$$\int_0^\pi v(x)t_h'(x)dx \leq \rho(h)\|t_h\|_{L^2}\|v\|_{H^2} \quad \forall v \in H^2 \quad \forall t_h \in \mathbb{K}_h, \quad (15)$$

where here and in the next two properties $\rho(h)$ denotes a quantity that tends to zero as h goes to zero;

the *strong approximability* of H^2 , that is for all $v \in H^2$ there exists $v_I \in \mathbb{K}_h$ such that

$$\|v - v_I\|_{H^1} \leq \rho(h)\|v\|_{H^2}; \quad (16)$$

the *Fortin* condition, that is there exists a bounded Fortin operator $\Pi_h : H^1 \rightarrow \Sigma_h$ converging in norm to the identity

$$\|t - \Pi_h t\|_{L^2} \leq \rho(h)\|t\|_{H^1} \quad \forall t \in H^1. \quad (17)$$

For the sake of completeness, we recall that a bounded Fortin operator satisfies

$$\int_0^\pi (s'(x) - (\Pi_h s)'(x))v(x)dx = 0 \quad \forall s \in H^1 \quad \forall v \in U_h$$

and $\|\Pi_h s\|_{H^1} \leq C \|s\|_{H^1}$.

Coming back to the three mixed methods discussed in Examples 1, 2, and 3, it can be seen that all of them satisfy the strong approximability property, while only the P1-P0 element satisfies the remaining two properties. Indeed, we have already shown in Sect. 4.1 that it satisfies the ellipticity in the kernel property (which implies the weak approximability property) and we proved that the interpolation operator is a Fortin operator (which easily implies the Fortin property). On the other hand, the P1-P1 element does not satisfy the Fortin property (it is known not to meet the inf-sup condition) and the P2-P0 element does not satisfy the weak approximability condition.

5 Error Estimates for Multiple Eigenvalues

This part of the paper is devoted to a priori error estimates for the eigenvalue problem in variational formulation. After a brief review of the fundamental results on spectral approximation mainly based on the theory of Babuška and Osborn [12], in the second section, we focus on the problem of error estimates for multiple eigenvalues. The main result of this section, due to Knyazev and Osborn [57], shows that the eigenvalue errors depend mainly on the approximability of the corresponding eigenspace. We end this section with some numerical results.

5.1 Fundamental Results on Spectral Approximation

In this section, we recall the error estimates, collected in [21], which show how the eigenvalues and eigenfunctions of T are approximated by those of T_h and then how they apply to the case of variationally posed eigenproblems. Throughout this section we assume that X is a Hilbert space with inner product (u, v) and that $T : X \rightarrow X$ is a compact self-adjoint positive linear operator. Let $T_h : X \rightarrow X$ be a family of compact self-adjoint positive linear operators of finite rank. We assume that T_h converges uniformly to T , that is

$$\|T - T_h\|_{\mathcal{L}(X)} \rightarrow 0 \quad \text{as } h \rightarrow 0. \quad (18)$$

Let μ be an eigenvalue of T of algebraic multiplicity m . Since T is self-adjoint and X is a Hilbert space, then the ascent of μ is 1. Let $\mu_{i,h}$ for $i = 1, \dots, m$ be the eigenvalues, repeated according to their multiplicity, of T_h converging to μ . We

denote by $E \subseteq X$ the eigenspace associated to μ and by E_h the direct sum of all the eigenspaces associated to the eigenvalues $\mu_{i,h}$. Then it holds

$$\hat{\delta}(E, E_h) \leq C \|(T - T_h)|_E\|_{\mathcal{L}(X)}, \quad (19)$$

where $\hat{\delta}(E, F)$ represents the gap between Hilbert subspaces and is defined by

$$\delta(E, F) = \sup_{\substack{u \in E \\ \|u\|_X=1}} \inf_{v \in F} \|u - v\|_X, \quad \hat{\delta}(E, F) = \max(\delta(E, F), \delta(F, E)). \quad (20)$$

Let us introduce some notation and observations which will be useful later on. For nonzero functions u and v , if $E = \text{span}\{u\}$, we write $\delta(u, F)$ instead of $\delta(E, F)$ and if $E = \text{span}\{u\}$ and $F = \text{span}\{v\}$, we write $\delta(u, v)$ for $\delta(E, F)$. We have $0 \leq \delta(E, F) \leq 1$ and $\delta(E, F) = 0$ if and only if $E \subseteq F$. If $\dim E = \dim F < \infty$ then $\delta(E, F) = \delta(F, E)$.

In the remainder of the section we shall have $\dim E \leq \dim F$, then the following Lemma holds true, see [28, Lemma 3.4].

Lemma 1. *Let $\{\phi_i, i = 1, \dots, \dim E\}$ form an orthogonal basis for the subspace E . Then*

$$\delta^2(E, F) \leq \sum_i \delta^2(\phi_i, F).$$

If P and Q are the orthogonal projections onto E and F , respectively, then $\delta(E, F)$ equals the largest singular value of the operator $(I - Q)P$ and

$$\delta(E, F) = \|(I - Q)P\|_X. \quad (21)$$

Let us now go back to the approximation of eigenvalues and eigenfunctions. We have the following error estimate for the eigenvalues.

Theorem 2. *Let $\{\phi_1, \dots, \phi_m\}$ be a basis of the eigenspace E associated to the eigenvalue μ . Then, for $i = 1, \dots, m$*

$$|\mu - \mu_{i,h}| \leq C \left(\sum_{j,k=1}^m |((T - T_h)\phi_j, \phi_k)| + \|(T - T_h)|_E\|_{\mathcal{L}(X)}^2 \right). \quad (22)$$

Moreover, we have the following estimate for the eigenfunctions.

Theorem 3. *Let $\{\mu_h\}$ be a sequence of discrete eigenvalues of T_h converging to a non-zero eigenvalue μ of T . Consider a sequence $\{u_h\}$ of unit vectors in the eigenspace E_h associated to μ_h . Then there exists an eigenfunction $u(h)$ associated to the eigenvalue μ of T such that*

$$\|u(h) - u_h\|_X \leq C \|(T - T_h)|_E\|_{\mathcal{L}(X)}.$$

We first observe that Theorems 2 and 3 also hold in the case of operators which are not self-adjoint. In such a case, one has to take into account the concept of ascent multiplicity of $\mu - T$.

As a corollary of the above theorems we obtain the error estimates for eigenvalues and eigenfunctions of problem (1). In order to embed the operator T defined in Sect. 2 (see (3)) into the abstract setting of this section, we assume that $T : V \rightarrow V$ is compact, hence we can apply the results of Theorems 2 and 3 with $X = V$ and $\lambda = 1/\mu$. This is the case, for instance, if $V \subset H$ is compact; the convergence (18) is a consequence of Theorem 1 (see Remark 1).

Corollary 1. *Let λ be an eigenvalue of problem (1) and let $\lambda_{i,h}$, for $i = 1, \dots, m$ be the eigenvalues of problem (2) converging to λ . Then we have for $i = 1, \dots, m$:*

$$|\lambda - \lambda_{i,h}| \leq C \sup_{\substack{u \in E \\ \|u\|=1}} \inf_{v \in V_h} \|u - v\|_V^2. \quad (23)$$

Corollary 2. *Let $\{\lambda_h\}$ be a sequence of discrete eigenvalues of (2) converging to an eigenvalue λ of (1). Consider a sequence $\{u_h\}$ of unit vectors in the eigenspace E_h associated to λ_h . Then there exists an eigenfunction $u(h)$ associated to the eigenvalue λ of (1) such that*

$$\|u(h) - u_h\|_V \leq C \sup_{\substack{u \in E \\ \|u\|=1}} \inf_{v \in V_h} \|u - v\|_V.$$

We notice here that one can deduce analogous results using the less strong assumption (6). We refer to [21, Sect. 10], for instance, for a discussion on the error estimates for the Laplace eigenproblem.

From the last theorems, we infer that the rate of convergence of multiple eigenvalues depends on the rate of approximability of the corresponding eigenspace, hence on the approximation rate of the least regular eigenfunction. On the other hand, the numerical experiments reported in [12, Sect. 10] show different rates of convergence for the approximate eigenvalues in the presence of eigenfunctions having different approximabilities. In the next section this point will be addressed following the ideas of Knyazev and Osborn [57] in the case of variationally posed eigenproblems.

5.2 Error Estimates for Ritz-Galerkin Approximation of Multiple Eigenvalues

This section is devoted to sharp error estimates in the case of multiple eigenvalues which take into account the possibility that a multiple eigenvalue might be associated to eigenfunctions with different regularities. In particular, we shall see that in this case it is possible to identify discrete eigenvalues converging to the multiple eigenvalue with different rates of convergence which take into account

the regularities of the corresponding eigenfunctions. More precisely, the rate of convergence towards an eigenvalue λ of multiplicity m associated to eigenfunctions with different regularities depends on the regularity of the eigenspace which is approximated by the sequence of the discrete eigenvectors associated to the m eigenvalues $\lambda_{i,h}$ for $1 \leq i \leq m$ which converge to λ .

The results we are going to report here are based on the theory developed in [57].

Let us go back to the setting of Sect. 2. Let V_h a finite dimensional subspace of V with $\dim V_h = N$. Let $T : V \rightarrow V$ and $T_h : V \rightarrow V$ be defined, respectively, in (3) and in (4). Then we have that T_h is the Ritz approximation of $T : V \rightarrow V$ since

$$T_h = P_h T \quad (24)$$

where $P_h : V \rightarrow V_h$ is the elliptic projection onto V_h defined as follows: for all $u \in V$, $P_h u \in V_h$ is such that

$$a(P_h u - u, v) = 0 \quad \forall v \in V_h. \quad (25)$$

We assume that the bilinear form $a : V \times V \rightarrow \mathbb{R}$ is coercive and continuous in V , that is

$$\begin{aligned} \alpha \|u\|_V^2 &\leq a(u, u) \quad \forall u \in V, \quad \text{with } \alpha > 0, \\ |a(u, v)| &\leq C \|u\|_V \|v\|_V \quad \forall u, v \in V, \quad \text{with } C > 0 \end{aligned} \quad (26)$$

Since $\sqrt{a(u, u)}$ is an equivalent norm in V , in this section we will use the following norm in V

$$\|u\|_V = \sqrt{a(u, u)}. \quad (27)$$

Notice that the elliptic projection P_h results in an orthogonal projection with respect to this norm.

Let us denote by $0 < \lambda_1 \leq \lambda_2 \leq \dots$ the eigenvalues of (1) and by $0 < \lambda_{1,h} \leq \lambda_{2,h} \leq \dots \leq \lambda_{N,h}$ those of (2), both repeated according to their algebraic multiplicity. Moreover, we denote by u_i the eigenfunction associated to the eigenvalue λ_i and by $u_{i,h}$ the discrete eigenfunction associated to $\lambda_{i,h}$, that is

$$\begin{aligned} a(u_i, v) &= \lambda_i b(u_i, v) \quad \forall v \in V \\ a(u_{i,h}, v) &= \lambda_{i,h} b(u_{i,h}, v) \quad \forall v \in V_h. \end{aligned}$$

From now on we assume that $b(u_i, u_j) = \delta_{ij}$ and $b(u_{i,h}, u_{j,h}) = \delta_{ij}$ for $i, j = 1, \dots, N$. Notice that this implies

$$\begin{aligned} a(u_i, u_i) &= \lambda_i \\ a(u_i, u_j) &= 0 \quad i \neq j \end{aligned}$$

and

$$\begin{aligned} a(u_{i,h}, u_{i,h}) &= \lambda_{i,h} \\ a(u_{i,h}, u_{j,h}) &= 0 \quad i \neq j. \end{aligned}$$

Let $E_{1,\dots,i} \subset V$ (resp. $E_{1,\dots,i,h} \subset V_h$) denote the span of the first i eigenvectors u_1, \dots, u_i (resp. $u_{1,h}, \dots, u_{i,h}$) and let $P_{1,\dots,i}$ (resp. $P_{1,\dots,i,h}$) be the elliptic projection onto $E_{1,\dots,i}$ (resp. $E_{1,\dots,i,h}$), that is

$$\begin{aligned} a(u - P_{1,\dots,i}u, v) &= 0 \quad \forall v \in E_{1,\dots,i} \\ a(u - P_{1,\dots,i,h}u, v) &= 0 \quad \forall v \in E_{1,\dots,i,h}. \end{aligned}$$

We recall here the following characterization of the eigenvalues by means of the Rayleigh quotient:

$$\begin{aligned} \lambda_1 &= \min_{\substack{v \in V \\ v \neq 0}} \frac{a(v, v)}{b(v, v)}, \lambda_i = \min_{\substack{v \in (\oplus_{j=1}^{i-1} E_j)^\perp \\ v \neq 0}} \frac{a(v, v)}{b(v, v)}, \\ \lambda_{1,h} &= \min_{\substack{v \in V_h \\ v \neq 0}} \frac{a(v, v)}{b(v, v)}, \lambda_{i,h} = \min_{\substack{v \in (\oplus_{j=1}^{i-1} E_{j,h})^\perp \\ v \neq 0}} \frac{a(v, v)}{b(v, v)}, \end{aligned} \quad (28)$$

Moreover, the i -th eigenvalue λ_i of (1) and the i -th discrete eigenvalue $\lambda_{i,h}$ of (2) satisfy:

$$\lambda_i = \min_{E \in V^{(i)}} \max_{v \in E} \frac{a(v, v)}{b(v, v)}, \quad \lambda_{i,h} = \min_{E \in V_h^{(i)}} \max_{v \in E} \frac{a(v, v)}{b(v, v)} \quad (29)$$

where $V^{(i)}$ and $V_h^{(i)}$ denote the set of all subspaces of V , respectively V_h with dimension equal to i (see, for instance, [21, Prop. 7.2]).

Notice that as a consequence of (29) we have that

$$\lambda_i \leq \lambda_{i,h} \quad \text{for } i = 1, \dots, N. \quad (30)$$

In the case of self-adjoint operators and of their Ritz approximation, one can make more precise the statement of Theorem 2 with the following result, proved in [55], which shows that the error for an eigenvalue depend on the approximability of all previous eigenvectors.

Theorem 4. *For $i = 1, \dots, N$ we have*

$$0 \leq \frac{\lambda_{i,h} - \lambda_i}{\lambda_{i,h}} \leq \delta^2(E_{1,\dots,i}, V_h) = \|(I - P_h)P_{1,\dots,i}\|_{\mathcal{L}(V)}^2. \quad (31)$$

Proof. We have $\delta(E_{1,\dots,i}, V_h) \leq 1$. If $\delta(E_{1,\dots,i}, V_h) = 1$ then (31) is obviously true. Hence, let us suppose that

$$\delta(E_{1,\dots,i}, V_h) < 1.$$

Since $\dim E_{1,\dots,i} = i \leq \dim V_h = N < +\infty$, we can apply (21) and obtain

$$\delta(E_{1,\dots,i}, V_h) = \|(I - P_h)P_{1,\dots,i}\|_{\mathcal{L}(V)},$$

from which, thanks to [53, Theorem 6.34, Cap. I], we deduce that P_h provides a one-to-one map from $E_{1,\dots,i}$ to $P_h E_{1,\dots,i}$. Therefore $\dim P_h E_{1,\dots,i} = \dim E_{1,\dots,i} = i$.

Let us take $\bar{u} \in P_h E_{1,\dots,i}$ such that $\|\bar{u}\|_V = 1$ and

$$\lambda(\bar{u}) = \max_{w \in P_h E_{1,\dots,i}, w \neq 0} \lambda(w)$$

where $\lambda(w)$ is the Rayleigh quotient defined by

$$\lambda(w) = \frac{a(w, w)}{b(w, w)}.$$

We recall that thanks to the coercivity assumption (26) and to the norm definition (27) we also have $a(\bar{u}, \bar{u}) = \|\bar{u}\|_V^2 = 1$.

We consider the following orthogonal decomposition of \bar{u} in V

$$\bar{u} = u + v \quad \text{for } u \in E_{1,\dots,i}, \quad v \in E_{1,\dots,i}^\perp. \quad (32)$$

Hence, we have $a(v, w) = 0$ for all $w \in E_{1,\dots,i}$ and consequently $a(v, Tw) = 0$, since $E_{1,\dots,i}$ is an invariant subspace of T . By the definition of T we also get that $b(v, w) = a(v, Tw) = 0$ for all $w \in E_{1,\dots,i}$.

The definition (32) of v yields

$$\begin{aligned} \|v\|_V &= \delta(\bar{u}, E_{1,\dots,i}) \leq \delta(P_h E_{1,\dots,i}, E_{1,\dots,i}) \\ &= \delta(E_{1,\dots,i}, P_h E_{1,\dots,i}) = \delta(E_{1,\dots,i}, V_h) < 1, \end{aligned} \quad (33)$$

since $P_h E_{1,\dots,i}$ and $E_{1,\dots,i}$ have the same dimension.

From (33) we obtain that $u \neq 0$ so that $\lambda(u)$ is well defined. We now show that

$$\lambda(u) \leq \lambda_i \leq \lambda_{i,h} \leq \lambda(\bar{u}). \quad (34)$$

We already know that $\lambda_i \leq \lambda_{i,h}$ (see (30)). By the definition of \bar{u} and the min-max characterization of the eigenvalues (28) the last inequality holds true. It remains to prove the first one. Since $u \in E_{1,\dots,i}$, we have $u = \sum_{j=1}^i \alpha_j u_j$ and

$$\lambda(u) = \frac{a(u, u)}{b(u, u)} = \frac{\sum_{j=1}^i \alpha_j^2 a(u_j, u_j)}{\sum_{j=1}^i \alpha_j^2 b(u_j, u_j)} = \frac{\sum_{j=1}^i \alpha_j^2 \lambda_j}{\sum_{j=1}^i \alpha_j^2} \leq \lambda_i.$$

due to the orthogonalities of the eigenfunctions.

We observe that

$$\lambda(\bar{u}) = \frac{a(u, u) + a(v, v)}{b(u, u) + b(v, v)}$$

If $v = 0$, then $\lambda(\bar{u}) = \lambda(u)$. If $v \neq 0$, a direct calculation gives

$$\frac{1}{\lambda(u)} - \frac{1}{\lambda(\bar{u})} = \left(\frac{1}{\lambda(\bar{u})} - \frac{1}{\lambda(v)} \right) \frac{a(v, v)}{a(u, u)} \leq \frac{1}{\lambda(\bar{u})} \frac{a(v, v)}{a(u, u)} \leq \frac{1}{\lambda_{i,h}} \frac{a(v, v)}{a(u, u)}.$$

It is now easy to see that

$$0 \leq \frac{1}{\lambda_i} - \frac{1}{\lambda_{i,h}} \leq \frac{1}{\lambda(u)} - \frac{1}{\lambda(\bar{u})} \leq \frac{1}{\lambda_{i,h}} \frac{a(v, v)}{a(u, u)},$$

which implies

$$\frac{\lambda_{i,h}}{\lambda_i} \leq \frac{a(v, v)}{a(u, u)} + 1 = \frac{1}{a(u, u)}$$

and

$$\frac{\lambda_{i,h} - \lambda_i}{\lambda_{i,h}} = 1 - \frac{\lambda_i}{\lambda_{i,h}} \leq 1 - a(u, u) = a(v, v) = \|v\|_V.$$

This inequality together with (33) concludes the proof of the theorem. \square

We see that the error estimate for the eigenvalue in Theorem 4 depends on the approximability properties of all previous eigenvectors, while in Corollary 1 it depends on the approximability properties of eigenspace associated to the eigenvalue of interest. On the other hand we see that the estimate (31) does not depend on any undetermined constant. Let us consider an eigenvalue λ_p with multiplicity $m > 1$, then from the above theorem it is easy to derive the following result.

Corollary 3. *Assume that*

$$\lambda_{p-1} < \lambda_p = \dots \lambda_{p+m-1} < \lambda_{p+m}, \quad (35)$$

with $p + m - 1 \leq N$. Then for any index $i = p, \dots, p + m - 1$ we have

$$\begin{aligned} 0 \leq \frac{\lambda_{i,h} - \lambda_p}{\lambda_{i,h}} &\leq \inf_{\substack{E_{1,\dots,p-1} \subset E_{1,\dots,i} \subseteq E_{1,\dots,p+m-1} \\ \dim E_{1,\dots,i} = i}} \delta^2(E_{1,\dots,i}, V_h) \\ &= \delta^2(E_{1,\dots,p+m-1}, V_h). \end{aligned} \quad (36)$$

Corollary 3 provides different estimates for every eigenvalue, but it requires approximability of all previous eigenvectors.

The following lemma suggests that the rate of convergence of the error for the multiple eigenvalue does not necessarily depend on the approximability of all the associated eigenfunctions.

Lemma 2. For $i = 1, \dots, N$, the following relation holds true

$$0 \leq \frac{\lambda_{i,h} - \lambda_i}{\lambda_{i,h}} = \frac{1}{\lambda_i} \|(I - P_{i,h})u_i\|_V^2 - \frac{\lambda_i}{\lambda_{i,h}} a((I - P_i)u_{i,h}, T(I - P_i)u_{i,h})$$

where P_i and $P_{i,h}$ are the elliptic projection onto $\text{span}\{u_i\}$ and $\text{span}\{u_{i,h}\}$, respectively.

Proof. The proof is quite simple. Using the definition of the Rayleigh quotient and the equality $b(u_i, u_i) = b(u_{i,h}, u_{i,h}) = 1$, we have $\lambda_{i,h} = a(u_{i,h}, u_{i,h})$ and $1 = b(u_{i,h}, u_{i,h}) = a(T_h u_{i,h}, u_{i,h})$, hence

$$\begin{aligned} 0 \leq \frac{\lambda_{i,h} - \lambda_i}{\lambda_i} &= \frac{\lambda_{i,h}}{\lambda_i} - 1 = \frac{1}{\lambda_i} a(u_{i,h}, u_{i,h}) - a(T_h u_{i,h}, u_{i,h}) \\ &= \frac{1}{\lambda_i} a((I - P_i)u_{i,h}, (I - P_i)u_{i,h}) + \frac{1}{\lambda_i} a(u_{i,h}, P_i u_{i,h}) - a(T u_{i,h}, u_{i,h}) \\ &= \frac{1}{\lambda_i} \|(I - P_i)u_{i,h}\|_V^2 + \frac{1}{\lambda_i} a(u_{i,h}, P_i u_{i,h}) \\ &\quad - a(T(I - P_i)u_{i,h}, u_{i,h}) - a(T P_i u_{i,h}, u_{i,h}) \\ &= \frac{1}{\lambda_i} \|(I - P_i)u_{i,h}\|_V^2 + a\left(u_{i,h}, \frac{1}{\lambda_i} P_i u_{i,h} - T P_i u_{i,h}\right) \\ &= \frac{1}{\lambda_i} \|(I - P_i)u_{i,h}\|_V^2 - a((I - P_i)u_{i,h}, T(I - P_i)u_{i,h}) \end{aligned}$$

thanks to $\left(\frac{1}{\lambda_i} I - T\right) P_i u_{i,h} = 0$ and $a(T(I - P_i)u_{i,h}, P_i u_{i,h}) = a((I - P_i)u_{i,h}, T P_i u_{i,h}) = 0$. We conclude the proof by observing that

$$\frac{1}{\lambda_{i,h}} \|(I - P_i)u_{i,h}\|_V^2 = \frac{1}{\lambda_i} \|(I - P_{i,h})u_i\|_V^2,$$

so that

$$\begin{aligned} 0 \leq \frac{\lambda_{i,h} - \lambda_i}{\lambda_{i,h}} &= \frac{\lambda_i}{\lambda_{i,h}} \frac{\lambda_{i,h} - \lambda_i}{\lambda_i} \\ &= \frac{1}{\lambda_{i,h}} \|(I - P_i)u_{i,h}\|_V^2 - \frac{\lambda_i}{\lambda_{i,h}} a((I - P_i)u_{i,h}, T(I - P_i)u_{i,h}). \end{aligned}$$

□

Since T is positive, we immediately obtain using (21)

$$0 \leq \frac{\lambda_{i,h} - \lambda_i}{\lambda_i} \leq \frac{1}{\lambda_i} \|(I - P_{i,h})u_i\|^2 \leq \frac{1}{\lambda_i} \delta^2(u_i, u_{i,h}).$$

Lemma 2 shows that the estimate on the i -th eigenvalue depends explicitly on both the continuous and the discrete associated eigenfunctions u_i and $u_{i,h}$.

The next theorem, proved in [57], provides an estimate which does not depend explicitly on the approximate eigenfunction $u_{i,h}$, but only on the approximability properties of u_i in the discrete space V_h .

Theorem 5. *Let us fix an index i with $1 \leq i \leq N$ such that*

$$\min_{j=1,\dots,i-1} |\lambda_{j,h} - \lambda_i| \neq 0, \quad (37)$$

then

$$\begin{aligned} 0 \leq \frac{\lambda_{i,h} - \lambda_i}{\lambda_{i,h}} &\leq \frac{\|(I - P_h + P_{1,\dots,i-1,h})u_i\|_V^2}{\|u_i\|_V^2} \\ &\leq \left(1 + \max_{j=1,\dots,i-1} \frac{\lambda_{j,h}^2 \lambda_j^2}{|\lambda_{j,h} - \lambda_i|^2} \|(I - P_h)TP_{1,\dots,i-1,h}\|_{\mathcal{L}(V)}^2\right) \delta^2(u_i, V_h), \end{aligned} \quad (38)$$

where $P_{1,\dots,i-1,h}$ is the elliptic projection onto $E_{1,\dots,i-1,h} = \text{span}\{u_{1,h}, \dots, u_{i-1,h}\}$ defined as follows: for $u \in V$, $P_{1,\dots,i-1,h}u \in E_{1,\dots,i-1,h}$ such that

$$a(u - P_{1,\dots,i-1,h}u, v) = 0 \quad \forall v \in E_{1,\dots,i-1,h},$$

Proof. The proof of the first inequality in (5) follows the same lines as that of Theorem 31. Let $i > 1$, since the case $i = 1$ is already covered by Theorem 4.

Let $\tilde{u}_i = u_i / \|u_i\|_V$. Since the operator $I - P_h + P_{1,\dots,i-1,h}$ is an orthogonal projection in V with respect to the norm defined in (27) and \tilde{u}_i is normalized, we have $\|(I - P_h + P_{1,\dots,i-1,h})\tilde{u}_i\|_V \leq 1$. We assume that $\|(I - P_h + P_{1,\dots,i-1,h})\tilde{u}_i\|_V < 1$, since otherwise the inequality (38) is obviously true.

Let $E_i = \text{span}\{u_i\}$, then $\dim E_i = 1$ and also $\dim(P_h - P_{1,\dots,i-1,h})E_i = 1$. Then by [53, Theorem 6.34, Cap. I] we obtain

$$\delta(E_i, (P_h - P_{1,\dots,i-1,h})E_i) = \delta(u_i, (P_h - P_{1,\dots,i-1,h})u_i) = \|(I - P_h + P_{1,\dots,i-1,h})\tilde{u}_i\|_V < 1.$$

Let us take $\bar{u} \in (P_h - P_{1,\dots,i-1,h})E_i$ such that $\|\bar{u}\|_V = 1$ and consider its orthogonal decomposition with respect to the norm of V as follows:

$$\bar{u} = u + v \quad \text{with } u \in E_{1,\dots,i}, \quad v \in (E_{1,\dots,i})^\perp,$$

so that

$$a(v, w) = a(\bar{u} - u, w) = 0 \quad \forall w \in E_{1,\dots,i}.$$

Hence

$$\begin{aligned} \|v\|_V &= \|\bar{u} - u\|_V = \inf_{w \in E_{1,\dots,i}} \|\bar{u} - w\|_V \\ &= \delta(\bar{u}, E_{1,\dots,i}) \leq \delta(\bar{u}, u_i) = \delta((P_h - P_{1,\dots,i-1,h})u_i, u_i) < 1. \end{aligned} \quad (39)$$

This implies that $u \neq 0$ and that $\lambda(u)$ is defined. As in Theorem 4, if we show that

$$\lambda(u) \leq \lambda_i \leq \lambda_{i,h} \leq \lambda(\bar{u}), \quad (40)$$

then we get

$$0 \leq \frac{\lambda_{i,h} - \lambda_i}{\lambda_{i,h}} \leq \|v\|_V,$$

and this would conclude the proof of the theorem.

We prove only the last inequality in (40), since the others are quite standard.

We observe that the operator $P_h - P_{1,\dots,i-1,h}$ is the projection onto the subspace of V_h spanned by the eigenfunctions $u_{j,h}$ with $j = i, \dots, N$. Hence, by definition, we have

$$\bar{u} \in \left(\bigoplus_{j=1}^{i-1} E_{j,h} \right)^\perp,$$

then (28) yields

$$\lambda(\bar{u}) = \frac{a(\bar{u}, \bar{u})}{b(\bar{u}, \bar{u})} \geq \min_{\substack{w \in \left(\bigoplus_{j=1}^{i-1} E_{j,h} \right)^\perp \\ w \neq 0}} \frac{a(w, w)}{b(w, w)} = \lambda_{i,h}.$$

It remains to obtain the second line of (38). We have

$$\|(I - P_h + P_{1,\dots,i-1,h})\tilde{u}_i\|_V^2 = \|(I - P_h)\tilde{u}_i\|_V^2 + \|P_{1,\dots,i-1,h}\tilde{u}_i\|_V^2.$$

In order to use [56, Theorem 3.2], we observe that $P_{1,\dots,i-1,h}TP_{1,\dots,i-1,h}|_{E_{1,\dots,i-1,h}} = T_h|_{E_{1,\dots,i-1,h}}$, hence the spectrum of $P_{1,\dots,i-1,h}TP_{1,\dots,i-1,h}|_{E_{1,\dots,i-1,h}}$ is the set of the eigenvalues $1/\lambda_{j,h}$ for $j = 1, \dots, i-1$ of T_h . Then we have

$$\|P_{1,\dots,i-1,h}\tilde{u}_i\|_V \leq \frac{\|(I - P_h)TP_{1,\dots,i-1,h}\|_{\mathcal{L}(V)}}{d_h} \|(I - P_h)\tilde{u}_i\|_V$$

where

$$d_h = \min_{j=1,\dots,i-1} \left| \frac{1}{\lambda_{j,h}} - \frac{1}{\lambda_i} \right| = \min_{j=1,\dots,i-1} \frac{|\lambda_{j,h} - \lambda_i|}{|\lambda_{j,h}\lambda_i|}.$$

□

Remark 5. Let us assume that each $\lambda_{i,h}$ converges to λ_i , then the assumption (37) reads:

$$\min_{j=1,\dots,i-1} |\lambda_{j,h} - \lambda_i| \approx \lambda_i - \lambda_{i-1}.$$

Notice that this quantity enters in the denominator of (38), hence the constant in the second line of (38) increases as $\lambda_i - \lambda_{i-1}$ becomes smaller.

In order to better explain the result presented in Theorem 5, let us consider the case of an eigenvalue λ_p with multiplicity $m = 2$ so that

$$\lambda_{p-1} < \lambda_p = \lambda_{p+1} < \lambda_{p+2}.$$

We can choose $i = p$ or $i = p + 1$. If $i = p$ then the denominator in (38) approximates $\lambda_p - \lambda_{p-1}$ hence it is strictly positive. For $i = p + 1$, instead, we have

$$\min_{j=1,\dots,p} |\lambda_{j,h} - \lambda_{p+1}| \approx |\lambda_{p,h} - \lambda_{p+1}|$$

and it tends to 0 as $h \rightarrow 0$.

We can make the result of Theorem 5 more precise in the following corollary.

Corollary 4. *Assume that the eigenvalue λ_p with $p > 1$ has multiplicity $m > 1$ so that (35) holds with $p + m - 1 \leq N$ and that (37) holds true for $i = p$. Let $E_{p,\dots,p+m-1}$ be the corresponding eigenspace, then*

$$\begin{aligned} 0 &\leq \frac{\lambda_{p,h} - \lambda_p}{\lambda_{p,h}} \leq \min_{u \in E_{p,\dots,p+m-1}, \|u\|_V=1} \|(I - P_h + P_{1,\dots,p-1,h})u\|_V^2 \\ &\leq \left(1 + \max_{j=1,\dots,p-1} \frac{\lambda_{j,h}^2 \lambda_p^2}{|\lambda_{j,h} - \lambda_p|^2} \|(I - P_h)TP_{1,\dots,p-1,h}\|_{\mathcal{L}(V)}^2 \right) \min_{\substack{u \in E_{p,\dots,p+m-1} \\ \|u\|_V=1}} \delta^2(u, V_h) \\ &= \left(1 + \max_{j=1,\dots,p-1} \frac{\lambda_{j,h}^2 \lambda_p^2}{|\lambda_{j,h} - \lambda_p|^2} \|(I - P_h)TP_{1,\dots,p-1,h}\|_{\mathcal{L}(V)}^2 \right) \delta^2(E_{p,\dots,p+m-1}, V_h). \end{aligned}$$

Notice that Corollary 4 gives an estimate containing only the gap between the eigenspace spanned by the m eigenfunctions associated to λ_p and the discrete space V_h , even if the approximability of the previous eigenfunctions still appears in the constant.

The final result of this section provides an error estimate for λ_p which can take into account the case of eigenfunctions associated to a multiple eigenvalue with different approximability properties. In addition, this estimate also covers the case of clustered eigenvalues.

Theorem 6. *Let i and q be fixed with $1 \leq i \leq N$ and $1 \leq q \leq i$. Let us denote by $E_{i-q+1,\dots,i}$ the q -dimensional invariant subspace corresponding to eigenvalues $\lambda_{i-q+1} \leq \dots \leq \lambda_i$ and by $P_{i-q+1,\dots,i}$ the elliptic projection onto $E_{i-q+1,\dots,i}$. If*

$$\min_{j=1,\dots,i-q} |\lambda_{j,h} - \lambda_i| \neq 0 \quad (41)$$

then the following error estimate holds true

$$\begin{aligned}
 0 &\leq \frac{\lambda_{i,h} - \lambda_i}{\lambda_{i,h}} \leq \|(I - P_h + P_{1,\dots,i-q,h})P_{i-q+1,\dots,i}\|_{\mathcal{L}(V)}^2 \\
 &\leq \left(1 + \max_{j=1,\dots,i-q} \frac{\lambda_{j,h}^2 \lambda_i^2}{|\lambda_{j,h} - \lambda_i|^2} \|(I - P_h)TP_{1,\dots,i-q,h}\|_{\mathcal{L}(V)}^2\right) \|(I - P_h)P_{i-q+1,\dots,i}\|_{\mathcal{L}(V)}^2
 \end{aligned} \tag{42}$$

where $P_{1,\dots,i-q,h}$ is the elliptic projection onto $E_{1,\dots,i-q,h} = \text{span}\{u_{1,h}, \dots, u_{i-q,h}\}$.

Proof. The proof is similar to that of Theorem 5. The operators $I - P_h + P_{1,\dots,i-q,h}$ and $P_{i-q+1,\dots,i}$ are orthogonal projections with respect to the norm of V , therefore $\|(I - P_h + P_{1,\dots,i-q,h})P_{i-q+1,\dots,i}\|_{\mathcal{L}(V)} \leq 1$. We consider the case

$$\|(I - P_h + P_{1,\dots,i-q,h})P_{i-q+1,\dots,i}\|_{\mathcal{L}(V)} < 1,$$

since otherwise the inequality (42) is obviously true. By [53, Theorem 3.6, Cap. I] $\dim(P_h - P_{1,\dots,i-q,h})E_{i-q+1,\dots,i} = \dim E_{i-q+1,\dots,i} = q$.

We choose $\bar{u} \in (P_h - P_{1,\dots,i-q,h})E_{i-q+1,\dots,i}$ such that $\|\bar{u}\|_V = 1$ and

$$\lambda(\bar{u}) = \max_{\substack{w \in (P_h - P_{1,\dots,i-q,h})E_{i-q+1,\dots,i} \\ w \neq 0}} \lambda(w),$$

where $\lambda(\bar{u})$ is the Rayleigh quotient. Let us consider the following V -orthogonal decomposition of \bar{u} :

$$\bar{u} = u + v, \quad \text{with } u \in E_{1,\dots,i}, \quad v \in (E_{1,\dots,i})^\perp,$$

then working as in (39) we have

$$\begin{aligned}
 \|v\|_V &= \delta(\bar{u}, E_{1,\dots,i}) \\
 &\leq \delta((P_h - P_{1,\dots,i-q,h})E_{i-q+1,\dots,i}, E_{i-q+1,\dots,i}) \\
 &= \|(I - P_h + P_{1,\dots,i-q,h})P_{i-q+1,\dots,i}\|_{\mathcal{L}(V)}.
 \end{aligned}$$

Then the required estimate

$$0 \leq \frac{\lambda_{i,h} - \lambda_i}{\lambda_{i,h}} \leq \|v\|_V$$

follows from the following chain of inequalities working as in the proof of Theorem 4

$$\lambda(u) \leq \lambda_i \leq \lambda_{i,h} \leq \lambda(\bar{u}).$$

The last estimate is a consequence of the definition of \bar{u} and of (29).

To obtain the second line of (42) it is enough to apply [56, Theorem 3.2]. \square

The first consequence of Theorem 6 concerns the case of multiple eigenvalues.

Corollary 5. *Assume that the eigenvalue λ_p with $p > 1$ has multiplicity $m > 1$ so that (35) holds with $p + m - 1 \leq N$ and*

$$\min_{j=1,\dots,p-1} |\lambda_{j,h} - \lambda_p| \neq 0.$$

Then, for $i = p, \dots, p + m - 1$ we have

$$\begin{aligned} 0 \leq \frac{\lambda_{i,h} - \lambda_p}{\lambda_{i,h}} &\leq \|(I - P_h + P_{1,\dots,p-1,h})P_{p,\dots,i}\|_{\mathcal{L}(V)}^2 \\ &\leq \left(1 + \max_{j=1,\dots,p-1} \frac{\lambda_{j,h}^2 \lambda_p^2}{|\lambda_{j,h} - \lambda_p|^2} \|(I - P_h)TP_{1,\dots,p-1,h}\|_{\mathcal{L}(V)}^2\right) \|(I - P_h)P_{p,\dots,i}\|_{\mathcal{L}(V)}^2, \end{aligned}$$

where $P_{1,\dots,p-1,h}$ is the orthogonal projection with respect to the norm of V onto $E_{1,\dots,p-1,h} = \text{span}\{u_{1,h}, \dots, u_{p-1,h}\}$ and $P_{p,\dots,i}$ is the orthogonal projection onto any $i - p + 1$ dimensional subspace of the eigenspace $E_{p,\dots,p+m-1}$ corresponding to the eigenvalue λ_p .

Remark 6. We remark that the error estimates for the eigenvalues of Theorems 5 and 6 contain multiplicative constants which approach 1, provided that assumptions (37) and (41) hold true.

Let us consider some particular cases in order to see the strength of Theorem 6 and of Corollary 5.

CASE 1: $\lambda_1 < \lambda_2 = \lambda_3 < \lambda_4$

Let us suppose that λ_2 has multiplicity 2, so we can apply Corollary 5 with $p = m = 2$. Assumption (37) gives

$$\min_{j=1,\dots,p-1} |\lambda_{j,h} - \lambda_p| = |\lambda_{1,h} - \lambda_2| \approx \lambda_2 - \lambda_1.$$

In Corollary 5 we can take $i = 2$ or $i = 3$. For $i = 2$ we obtain

$$\frac{\lambda_{2,h} - \lambda_2}{\lambda_{2,h}} \leq \left(1 + \frac{\lambda_{1,h}^2 \lambda_2^2}{|\lambda_{1,h} - \lambda_2|^2} \|(I - P_h)TP_{1,h}\|_{\mathcal{L}(V)}^2\right) \|(I - P_h)P_2\|_{\mathcal{L}(V)}^2. \quad (43)$$

For $i = 3$ we have

$$\begin{aligned} \frac{\lambda_{3,h} - \lambda_3}{\lambda_{3,h}} &= \frac{\lambda_{3,h} - \lambda_2}{\lambda_{3,h}} \\ &\leq \left(1 + \frac{\lambda_{1,h}^2 \lambda_2^2}{|\lambda_{1,h} - \lambda_2|^2} \|(I - P_h)TP_{1,h}\|_{\mathcal{L}(V)}^2\right) \|(I - P_h)P_{2,3}\|_{\mathcal{L}(V)}^2. \end{aligned} \quad (44)$$

In the first inequality the error is bounded by the best approximation error for eigenfunction u_2 , while in the second one we have the bound in terms of the best approximation error for $\text{span}\{u_2, u_3\}$. Therefore, we can separate the rate of convergence according to approximability of each eigenfunction. Notice that if u_2 is less regular than u_3 , we have from both the estimates (43) and (44) the same rate of convergence, while in the opposite case the inequality (43) could give the best rate of convergence corresponding to the most regular eigenfunction. Moreover, we also see here the improvement with respect to the result of Theorem 5, which would not give a valid estimate in this case since the denominator tends to zero.

CASE 2: $\lambda_1 < \lambda_2 \approx \lambda_3 < \lambda_4$

This case is similar to the previous one but we have clustered eigenvalues. We obtain results similar to the ones quoted for Case 1. In particular, as in the previous case Theorem 5 would not give a good estimate for $i = 3$ since $|\lambda_3 - \lambda_{2,h}| \approx 0$.

CASE 3: $\lambda_1 < \lambda_2 = \lambda_3 < \lambda_4$

We apply Theorem 6 with $i = 3$. Then we can choose $q = 1, 2, 3$ and obtain the following bounds.

For $q = 1$ we have

$$\frac{\lambda_{3,h} - \lambda_3}{\lambda_{3,h}} \leq \left(1 + \max_{j=1,2} \frac{\lambda_{j,h}^2 \lambda_3^2}{|\lambda_{j,h} - \lambda_3|^2} \|(I - P_h)TP_{1,2,h}\|_{\mathcal{L}(V)}^2 \right) \|(I - P_h)P_3\|_{\mathcal{L}(V)}^2.$$

but this estimate is not optimal since $\min_{j=1,2} |\lambda_{j,h} - \lambda_3| \approx 0$.

For $q = 2$ we have

$$\frac{\lambda_{3,h} - \lambda_3}{\lambda_{3,h}} \leq \left(1 + \frac{\lambda_{1,h}^2 \lambda_3^2}{|\lambda_{1,h} - \lambda_3|^2} \|(I - P_h)TP_{1,h}\|_{\mathcal{L}(V)}^2 \right) \|(I - P_h)P_{2,3}\|_{\mathcal{L}(V)}^2.$$

If $\lambda_3 - \lambda_1$ is large enough this inequality gives a sharp estimate in the case we have u_1 with poor approximability property.

For $q = 3$ we obtain

$$\frac{\lambda_{3,h} - \lambda_3}{\lambda_{3,h}} \leq \|(I - P_h)P_{1,2,3}\|_{\mathcal{L}(V)}^2,$$

and this estimate recovers the result of Theorem 4 so that we estimate the error in terms of the approximability of the span of all the previous eigenfunctions.

5.3 Numerical Results

In this section we report some numerical results of eigenproblems with multiple eigenvalues, whose associated eigenfunctions can have different regularities.

The first example in this direction is due to Babuška and Osborn [12]. Let us consider the following one-dimensional differential equation: find $\lambda \in \mathbb{R}$ such that there exists $u \neq 0$ with:

$$\begin{aligned} -\left(\frac{1}{\varphi'(x)}u'(x)\right)' &= \lambda\varphi'(x)u(x), \quad x \in (-\pi, \pi) \\ u(-\pi) &= u(\pi), \quad \left(\frac{1}{\varphi}u'\right)(-\pi) = \left(\frac{1}{\varphi}u'\right)(\pi), \end{aligned}$$

where

$$\varphi(x) = \pi^{-\alpha}|x|^{1+\alpha} \operatorname{sign}(x), \quad 0 < \alpha < 1.$$

It is easy to check that the continuous eigenvalues and eigenfunctions are given by

$$\begin{aligned} \lambda_0 &= 0, \quad \lambda_{2i-1} = \lambda_{2i} = i^2 \quad \text{for } i = 1, 2, \dots \\ u_0 &= 1, \quad u_{2i-1} = \cos(i\varphi(x)), \quad u_{2i} = \sin(i\varphi(x)) \quad \text{for } i = 1, 2, \dots \end{aligned}$$

Due to the definition of φ we have that $\cos(\varphi(x)) \in H^2(-\pi, \pi)$ while $\sin(\varphi(x)) \in H^{1+\alpha}(-\pi, \pi)$. Each eigenvalue has multiplicity 2 and its eigenspace contains a regular eigenfunction approximated optimally by piecewise linear finite elements and a less regular eigenfunction for which the optimal rate of convergence cannot be reached. We refer to the numerical results reported in [12, Sect. 10] showing that for each double eigenvalue the rate of convergence is either 2 or $1 + \alpha$.

The second example does not fit the theory presented so far, however the problem is an important one and the numerical experiments show that the results presented in Sect. 5.2 also hold in this case. It would also be interesting to extend the theory to this situation.

Let $\Omega \subseteq \mathbb{R}^2$ be an open polygon, denote by \mathbf{n} the outward normal vector to its boundary $\partial\Omega$ and by \mathbf{t} the counterclockwise oriented tangent vector. We consider the following eigenproblem which describes the vibration frequencies of a fluid in a cavity, hence it can be considered as the simplest problem in fluid-structure interaction (see e.g. [19, 24, 34]):

$$\begin{cases} -\nabla \operatorname{div} \mathbf{u} = \lambda \mathbf{u} & \text{in } \Omega \\ \operatorname{rot} \mathbf{u} = 0 & \text{in } \Omega \\ \mathbf{u} \cdot \mathbf{n} = 0 & \text{on } \partial\Omega. \end{cases} \quad (45)$$

By standard orthogonalities in \mathbb{R}^2 between the operators ∇ and rot , (45) can be transformed into

$$\begin{cases} -\operatorname{rot} \operatorname{rot} \mathbf{u} = \lambda \mathbf{u} & \text{in } \Omega \\ \operatorname{div} \mathbf{u} = 0 & \text{in } \Omega \\ \mathbf{u} \cdot \mathbf{t} = 0 & \text{on } \partial\Omega, \end{cases}$$

which arises in electromagnetic applications (see e.g. [20, 25, 54, 63]).

Here we focus on (45). One can observe that the constraint $\text{rot } \mathbf{u} = 0$ follows automatically from the first equation if $\lambda \neq 0$, hence one could drop the irrotationality constraint and add a zero frequency corresponding to the infinite dimensional null space of the functions which belong to $\nabla H_0^1(\Omega)$. Numerical methods based on this idea have been analyzed, for instance, in [20, 27, 54, 74] for the Maxwell's problem and in [19, 34] for the fluid-structure example. Another approach is based on a penalization strategy (see, e.g., [18, 47, 54, 73]), which we are going to consider in the present paper.

Let s be a positive real number, then the penalized formulation of (45) reads: find $\lambda \in \mathbb{R}$ and $\mathbf{u} \neq 0$ such that:

$$\begin{cases} -\nabla \text{div } \mathbf{u} + \frac{1}{s} \text{rot rot } \mathbf{u} = \lambda \mathbf{u} & \text{in } \Omega \\ \mathbf{u} \cdot \mathbf{n} = 0 & \text{on } \partial\Omega \\ \text{rot } \mathbf{u} = 0 & \text{on } \partial\Omega \end{cases} \quad (46)$$

Let us introduce the following Hilbert spaces

$$\begin{aligned} H_0^1(\Omega) &= \{v \in H^1(\Omega) : v = 0 \text{ on } \partial\Omega\} \\ \mathbf{H}_0(\text{div}; \Omega) &= \{\mathbf{v} \in L^2(\Omega)^2 : \text{div } \mathbf{v} \in L^2(\Omega), \mathbf{v} \cdot \mathbf{n} = 0\} \\ \mathbf{H}(\text{rot}; \Omega) &= \{\mathbf{v} \in L^2(\Omega)^2 : \text{rot } \mathbf{v} \in L^2(\Omega)\} \end{aligned}$$

The variational formulation of (46) reads: given $s \in \mathbb{R}$ with $s > 0$, find $\lambda \in \mathbb{R}$ and $\mathbf{u} \in \mathbf{H}_0(\text{div}; \Omega) \cap \mathbf{H}(\text{rot}; \Omega)$ with $\mathbf{u} \neq 0$ such that

$$(\text{div } \mathbf{u}, \text{div } \mathbf{v}) + \frac{1}{s} (\text{rot } \mathbf{u}, \text{rot } \mathbf{v}) = \lambda (\mathbf{u}, \mathbf{v}) \quad \forall \mathbf{v} \in \mathbf{H}_0(\text{div}; \Omega) \cap \mathbf{H}(\text{rot}; \Omega). \quad (47)$$

It is well-known that if Ω is convex the space $\mathbf{H}_0(\text{div}; \Omega) \cap \mathbf{H}(\text{rot}; \Omega)$ is equal to $H^1(\Omega)^2 \cap \mathbf{H}_0(\text{div}; \Omega)$. But this equivalence fails if Ω is a nonconvex polygon, as it has been shown in [37]. On the other hand, we observe that it is not possible to construct a piecewise polynomial function which is contained in $\mathbf{H}_0(\text{div}; \Omega) \cap \mathbf{H}(\text{rot}; \Omega)$ but not in $H^1(\Omega)^2$. For this reason we introduce a mixed formulation of (47) by setting $sp = \text{rot } \mathbf{u}$, thus we obtain the following problem: given $s > 0$, find $\lambda \in \mathbb{R}$ and $\mathbf{u} \in \mathbf{H}_0(\text{div}; \Omega)$ with $\mathbf{u} \neq 0$ such that for some $p \in H_0^1(\Omega)$

$$\begin{aligned} (\text{div } \mathbf{u}, \text{div } \mathbf{v}) + (\text{rot } p, \mathbf{v}) &= \lambda (\mathbf{u}, \mathbf{v}) \quad \forall \mathbf{v} \in \mathbf{H}_0(\text{div}; \Omega) \\ (\text{rot } q, \mathbf{u}) - s(p, q) &= 0 \quad \forall q \in H_0^1(\Omega) \end{aligned} \quad (48)$$

Notice that if we take $s = 0$ in (48), then the second equation implies that $\text{rot } \mathbf{u} = 0$, so that p is the Lagrange multiplier associated to the irrotational constraint (see [54] for the analogous situation in the case of Maxwell eigenproblem).

Given a regular family $\{\mathcal{T}_h\}$ of triangulations of the domain Ω , we consider the following finite element spaces

$$\begin{aligned}\mathbf{V}_h &= \{\mathbf{v} \in \mathbf{H}_0(\text{div}; \Omega) : \mathbf{v}|_K \in RT_0(K) \ \forall K \in \mathcal{T}_h\} \\ Q_h &= \{q \in H_0^1(\Omega) : q|_K \in P_1(K) \ \forall K \in \mathcal{T}_h\}\end{aligned}\tag{49}$$

where $P_k(K)$ is the set of polynomials of degree less than or equal to k on K and $RT_0(K) = P_0(K)^2 + P_0(K)(x, y)^t$ is the space of lowest order Raviart-Thomas elements (see [65]). Then the discrete counterpart of (48) reads: given $s > 0$, find $\lambda_h \in \mathbb{R}$ and $\mathbf{u}_h \in \mathbf{V}_h$ with $\mathbf{u}_h \neq 0$ such that for some $p_h \in Q_h$

$$\begin{aligned}(\text{div } \mathbf{u}_h, \text{div } \mathbf{v}) + (\mathbf{rot } p_h, \mathbf{v}) &= \lambda_h (\mathbf{u}_h, \mathbf{v}) \quad \forall \mathbf{v} \in \mathbf{V}_h \\ (\mathbf{rot } q, \mathbf{u}_h) - s(p_h, q) &= 0 \quad \forall q \in Q_h.\end{aligned}\tag{50}$$

Problem (48) with $s = 0$ is an eigenproblem in mixed form (see Sect. 4) and the term which is added when $s > 0$ contributes to its stability (since it has the right negative sign). We refer to [10] for the analysis in a more general framework.

Here we use this problem as an example of problems with multiple eigenvalues associated to eigenfunctions of different regularity. We observe that, thanks to the Helmholtz decomposition, the eigensolutions of problem (48) split into two families. The first one is given by the eigensolutions $(\lambda^n, \mathbf{u}^n)$ such that $\mathbf{rot } \mathbf{u}^n = 0$ and $\mathbf{u}^n = \nabla \varphi$ with (λ^n, φ) the eigensolution of the following Laplace equation with Neumann boundary conditions

$$\begin{aligned}-\Delta \varphi &= \lambda^n \varphi \quad \text{in } \Omega \\ \frac{\partial \varphi}{\partial \mathbf{n}} &= 0 \quad \text{on } \partial \Omega.\end{aligned}$$

The second family $(\lambda^d, \mathbf{u}^d)$ satisfies $\text{div } \mathbf{u}^d = 0$ so that $\mathbf{u}^d = -\mathbf{rot } \psi$ with (λ^d, ψ) the eigensolution of the following Laplace equation with Dirichlet boundary conditions

$$\begin{aligned}-\frac{1}{s} \Delta \psi &= \lambda^d \psi \quad \text{in } \Omega \\ \psi &= 0 \quad \text{on } \partial \Omega.\end{aligned}$$

As a consequence of this characterization, the Neumann eigenvalues λ^n do not depend on s , while the Dirichlet ones λ^d grow linearly with $\frac{1}{s}$.

We consider the L-shaped domain Ω reported in Fig. 9. Since Ω is not convex, there are eigenfunctions which are not in $H^2(\Omega)$. We use as reference values for the eigenvalues of the Neumann problem the solution published in [39], which are computed by a Galerkin approximation with a geometrical refined mesh near the

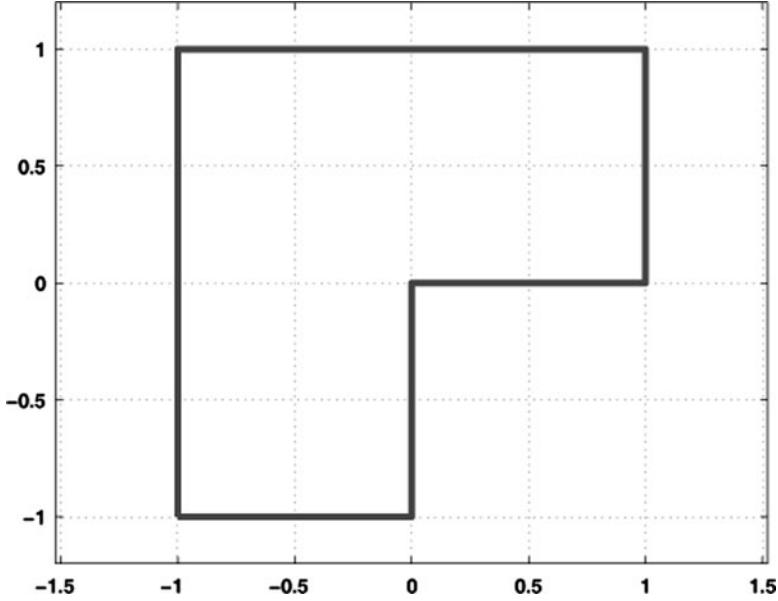


Fig. 9 The L-shaped domain

corner (10 layers and ratio 4) and polynomials of “high” degree (degree 10). The first 5 eigenvalues with 11 correct digits are:

$$\begin{aligned}
 \lambda_1^n &= 0.147562182408E + 01 \\
 \lambda_2^n &= 0.353403136678E + 01 \\
 \lambda_3^n &= 0.986960440109E + 01 \\
 \lambda_4^n &= 0.986960440109E + 01 \\
 \lambda_5^n &= 0.113894793979E + 02.
 \end{aligned} \tag{51}$$

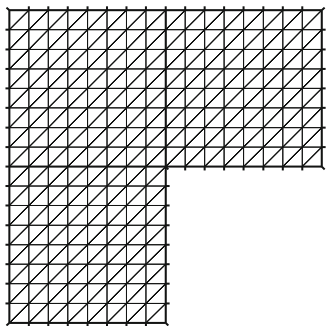
The first eigenvector has a strong singularity; notice, in particular, that $\lambda_3^n = \lambda_4^n = \pi^2$.

We computed the solution of problem (50) using the package FreeFem++ [50]: an open source software for solving partial differential problems by the finite element method. The results of this computation have been taken from [69]. In Listing 1.7 we report the FreeFem++ code which computes eigenvalues and eigenfunctions of problem (48).

In the first computation we set $s = 0$ so that we obtain the first five eigenvalues associated to the irrotational eigenfunction, that is the Neumann eigenvalues λ_i^n for $i = 1, \dots, 5$. In Table 7 we report the computed eigenvalues together with the rate of convergence estimated by using the exact values quoted in (51). The integer n represents the number of subdivision of the interval $[0, 1]$, the total number of elements is $NE = 6n^2$. Figure 10 reports the mesh corresponding to the value $n = 8$.

Table 7 Eigenvalues computed using the code listed in Listing 1.7 for $s = 0$

Exact	Computed (rate)				
	$n = 2$	$n = 4$	$n = 8$	$n = 16$	$n = 32$
1.48	1.3248	1.4176 (1.4)	1.4531 (1.4)	1.4668 (1.4)	1.4722 (1.4)
3.53	3.4976	3.5217 (1.6)	3.5305 (1.8)	3.5331 (1.9)	3.5338 (1.9)
9.87	9.0496	9.6577 (2.0)	9.8161 (2.0)	9.8562 (2.0)	9.8662 (2.0)
9.87	9.3021	9.7420 (2.0)	9.8385 (2.0)	9.8619 (2.0)	9.8677 (2.0)
11.39	10.7739	11.2193 (1.9)	11.3448 (1.9)	11.3781 (2.0)	11.3866 (2.0)
DOF	65	225	833	3201	12545
$NE = 6n^2$	24	96	384	1563	6144

Fig. 10 The mesh in the L-shaped domain Ω for $n = 8$, $NE = 384$ 

We see in this first example that the discrete eigenvalues stay below the corresponding continuous one. We remark that the technique used to prove the error estimates in Sect. 5.2 cannot be applied to the approximation of problem (48). Indeed the estimates in Theorems 4–6 are based on (30), that is the Ritz approximations of the eigenvalues bound the continuous ones by above. In general, no relation of this type can be deduced for the approximation of the eigenvalues of the problem in mixed form.

The second computation is performed using the value $s = 13.376875077383353$, so that there is a regular Dirichlet eigenvalue which equals the first Neumann eigenvalue λ_1^n that is not regular. This value for s has been computed by solving the equation $2\pi^2/s = \lambda_1^n$: since there is a Dirichlet eigenvalue $\lambda^d = 2\pi^2$ (for $s = 1$) associated to a smooth eigenfunction, it follows that this choice for s shifts this eigenvalue in such a way that its value is superimposed to λ_1^n .

Table 8 reports the first 5 computed eigenvalues together with the rate of convergence for those eigenvalues converging to λ_1^n .

We see that in this case the rate of convergence is different from one eigenvalue to the other and depends on the regularity of the associated eigenfunction as predicted by Theorem 6, even if the problem does not fit within the theory presented in Sect. 5.2. Moreover, we notice that $\lambda_{3,h}$, as $n \geq 4$, converges to λ_1^n from below, while $\lambda_{4,h}$ converges from above to the same value.

Table 8 Eigenvalues computed using the code listed in Listing 1.7 for $s = 13.376875077383353$

Exact	Computed (rate)					
	$n = 2$	$n = 4$	$n = 8$	$n = 16$	$n = 32$	$n = 64$
	0.9867	0.7905	0.7413	0.7273	0.7229	0.7214
	1.3248	1.2669	1.1688	1.1443	1.1381	1.1366
1.48	1.6462	1.4176 (1.6)	1.4531 (1.4)	1.4668 (1.4)	1.4722 (1.3)	1.4743 (1.3)
1.48	2.3922	1.7059 (1.9)	1.5327 (2.0)	1.4899 (2.0)	1.4792 (2.0)	1.4765 (2.0)
	3.4976	2.7079	2.3317	2.2381	2.2147	2.2088
DOF	65	225	833	3201	12545	49665
$NE = 6n^2$	24	96	384	1563	6144	24576

Listing 1.7 FreeFem++ code for problem (50)

```

int n=32; // numbers of subdivision of [0,1]
/*
  Construction of the mesh
  The domain is subdivided into three squares
  The mesh for each square is constructed separately
*/
mesh Th1=square(n,n);
mesh Th2=square(n,n,[x-1,y]);
mesh Th3=square(n,n,[x-1,y-1]);
verbosity=3;
plot(Th1,Th2,Th3);
int [int] r1=[4,0], r2=[2,0], r3=[1,0];
int [int] r4=[3,0], r5=[1,5], r6=[2,6];
Th1=change(Th1,label=r1);
Th2=change(Th2,label=r2);
Th2=change(Th2,label=r3);
Th3=change(Th3,label=r4);
Th3=change(Th3,label=r5);
Th3=change(Th3,label=r6);
// the three meshes are glued together
mesh Th=Th1+Th2+Th3;
plot(Th,wait=1);
//
/* s is the penalization parameter */
// real s=0;
real s=13.376875077383353;
real sigma=0; // shift parameter
// finite element spaces
fespace VQh(Th,[RT0,P1]);
VQh [u1,u2,p],[v1,v2,q];
//

```

```

/* Definition of the partial differential equation */
varf op([u1,u2,p],[v1,v2,q])=
    int2d(Th)( (dx(u1)+dy(u2)) * (dx(v1)+dy(v2))
        -dx(p)*v2 + dy(p)*v1
        +dx(q)*u2 - dy(q)*u1
        + s*p*q - sigma*u1*v1 - sigma*u2*v2)
    +on(1,2,3,4,5,6,u1=0,u2=0,p=0);
/* Construction of the matrices */
matrix OP=op(VQh,VQh,solver=sparse solver);
varf m([u1,u2,p],[v1,v2,q])=int2d(Th)( u1*v1 + u2*v2 );
matrix M=m(VQh,VQh,solver=GMRES);
/* Number of computed eigenvalues */
real nev=5;
real [int] ev(nev);
VQh[int] [eV,eW,ep](nev);
int k;
int nold=cout.precision(20);
/* computation of eigenvalues and eigenvectors */
k=EigenValue(OP,M,sym=true,nev=nev,value=ev,
    sigma=sigma,tol=1e-10,vector=eV);
/* plot of the eigenvectors */
for(int i=0;i<k;++i)
{
    cout << "Eigenvalue " << i << " = " << ev[i] << endl;
    plot([eV[i],eW[i]],ep[i], cmm="Eigenvalue " + ev[i],
        wait=1,value=true);
}

```

6 A Posteriori Error Analysis

In this section we present an introduction to the subject of a posteriori error estimation and adaptive mesh refinement for the approximation of the eigenvalue problem. The main purpose of this section is to underline the difficulties which arise in the a posteriori error analysis of eigenvalue problems. In this sense, the presentation is by no means exhaustive and focuses on error estimators of the residual type. We first recall the bibliography, which is now very extensive for eigenvalue problem as well as for source problems. Then in Sects. 6.3, 6.4 we highlight the difficulties which arise in dealing with eigenvalue problems, both in standard and mixed form, and we show why the techniques used to develop an a posteriori error analysis for the source problem cannot be trivially extended to the eigenvalue problem.

6.1 Some Introductory Remarks

In the last twenty years there has been a great deal of research work on a posteriori error estimation and adaptive refinement for the finite element approximation of PDEs that arise from physical and engineering applications. The aim is to obtain a numerical solution within a prescribed tolerance using a minimal amount of work.

The a priori error estimates provided by the standard error analysis for the finite element method yield information only on the asymptotic error behavior, and strongly depend on the regularity of the solution. In particular in the presence of local singularities, such as re-entrant corners and interior or boundary layers, the overall accuracy of the numerical solution deteriorates. A first remedy is to refine the mesh; nevertheless the uniform refinement could lead to an excessive computational effort, when actually it is enough to refine only the elements in the neighborhood of the singularities. The question then is how to detect the elements which have to be refined and how to obtain a good balance between the refined and the un-refined regions such that the overall accuracy is optimal.

Another issue is to be able to judge the quality of the numerical solution, namely to obtain reliable estimates of the accuracy of the computed solution in order to decide whether a prescribed tolerance has been achieved or not.

In this context the need of an error estimator which can be computed locally from the numerical solution and the data of the problem appears clear. The error estimator should yield reliable upper and lower bounds for the actual error. Indeed global upper bounds are sufficient to ensure that the numerical solution achieves a prescribed tolerance. Local lower bounds however are essential to guarantee that the error is not overestimated and that its local distribution is correctly resolved. Finally, the calculation of the a posteriori error estimate should be far less expensive than the computation of the numerical solution.

The bibliography on a posteriori error estimators for the finite element method is now very extensive (see, in particular the books by Verfürth [71] and Ainsworth and Oden [1], and the references therein).

For classical finite element approximations of eigenvalue problems, Babuška and Rheinboldt in [13] first introduced an a posteriori error estimator for a one dimensional problem; Verfürth in [70] derived an upper bound of suboptimal order in the approximation of the eigenvalue and only a global lower bound by considering the eigenvalue problem as a parameter-dependent nonlinear equation and using general results for the Galerkin approximation of such type of problems. Alonso *et al.* in [5] presented an error estimator of the residual type for piecewise linear finite element approximation of structure vibration problems. Then Larson in [60] obtained optimal order estimates assuming the H^2 -regularity of the eigenfunctions, which however excludes domain with re-entrant corners or discontinuous coefficients; Heuveline and Rannacher in [51] obtained results based on a general analysis for nonlinear equations without requiring the H^2 -regularity of the problem. In [41] Durán *et al.* developed a simple analysis for a residual type error estimator for the linear finite element approximation of a second order elliptic problem. Finally, more recent results can be found in [9, 49, 72].

Concerning the mixed approximation of eigenvalue problems, Durán *et al.* in [40] analyzed an error estimator for the approximation of the eigensolutions of a second-order elliptic problem by using the equivalence between the mixed finite element method of Raviart-Thomas of the lowest order and the non-conforming piecewise linear approximation of Crouzeix and Raviart. Then Alonso *et al.* in [6] adapted the techniques used in [40] to derive an error estimator for the lowest order Raviart-Thomas approximation of the acoustic vibration problem. Moreover in [3, 4] this error estimator has been used together with the one presented in [5] to deal with structural-acoustic vibration problems on matching and non matching grids, respectively. A posteriori error estimators for eigenvalue problems in mixed form have been studied in [44, 45] without using the equivalence with a non-conforming approximation. Finally, the Stokes eigenvalue problem has been considered in [61].

Eventually, the convergence of adaptive methods for the finite element approximation of eigenvalue problems has been studied quite recently in [32, 38, 42, 43, 48, 62].

6.2 A Posteriori Error Estimators

In this section we recall the properties of the error estimators and we describe a simple mesh-refinement algorithm.

Let η denote the error estimator, which is usually given by the sum of local error indicators

$$\eta^2 = \sum_{K \in \mathcal{T}_h} \eta_K^2.$$

The error estimator has to satisfy the following properties:

Reliability. It should bound from above the global error e_h in a suitable norm $\| \cdot \|$:

$$\|e_h\| \leq C \eta + \text{h.o.t.},$$

where h.o.t. denotes higher order terms.

Efficiency. It should provide local lower error estimates, in order to point out which elements should be effectively refined:

$$\eta_K \leq C \|e_h\|_{V, K^*} + \text{h.o.t.},$$

where K^* is the union of K and few neighboring elements.

Low computational cost. The computation of η_K should be inexpensive in comparison with the overall computation of the discrete solution.

Here and thereafter, C denotes a generic constant, not necessarily always the same, but always independent of the mesh size.

Having an a posteriori error estimator, an adaptive mesh-refinement algorithm, which applies a usual procedure from [71], reads as follows:

1. Start with an initial coarse mesh \mathcal{T}_0 . Set $k = 0$.
2. Solve the discrete problem on \mathcal{T}_k .
3. For each element $K \in \mathcal{T}_k$ compute the local error indicator η_K .
4. Evaluate stopping criterion and decide to finish or go to next step.
5. Decide which elements have to be refined and construct the new mesh.
6. Define resulting mesh as \mathcal{T}_{k+1} , replace k by $k + 1$ and go to step 2.

Heuristic arguments show that for a linear finite element discretization of the Poisson problem the optimal mesh among all partitions with a given number of elements is the one which equilibrates the error, i.e. the error in each element is almost the same (see [13, 14, 66]).

Based on this strategy, there are two main possibilities to decide which elements have to be refined (see [71]):

1. Let K be an element in \mathcal{T}_h and let τ be an element obtained by subdividing K . It is quite reasonable to assume that the errors in K and τ behave like Ch_K^r and Ch_τ^r with unknown constants C and r . Computing error estimators η_K and η_τ , one can roughly calculate C and r and hence approximately predict the error in an element τ obtained by subdividing K .
2. For each element $K \in \mathcal{T}_h$ compute the local error indicator η_K . Then refine each element K' whose error indicator $\eta_{K'}$ satisfies

$$\eta_{K'} \geq \gamma \max\{\eta_K : K \in \mathcal{T}_h\},$$

where $\gamma \in (0, 1)$ is a prescribed threshold (very often $\gamma = 0.5$).

The first possibility clearly is more sophisticated. However, in practice the second possibility, which is cheaper, gives satisfactory results.

Another issue concerns the shape regularity of the mesh: it is mandatory to preserve it during the refinement process. For triangular meshes there exist essentially three different strategies which preserve the shape regularity:

1. *Regular refinement*: divide triangles into four by joining the midpoints of edges.
2. *Longest edge bisection*: bisect triangles by joining the midpoint of the longest edge with the vertex opposite to this edge.
3. *Marked edge bisection*: bisect triangles by joining the midpoint of a marked edge with the vertex opposite to this edge.

Finally, in order to obtain an admissible triangulation, i.e. without hanging nodes, the refinement process has to obey some additional rules (see, in particular, [15–17, 59, 67, 68]).

6.3 Standard Finite Element Approximation

The aim of the present section is to highlight the difficulties which arise in the a posteriori error analysis moving from the source problem to the eigenvalue problem.

For the sake of simplicity, we consider the Laplace problem as a model:

$$\begin{aligned} &\text{given } f \in L^2(\Omega), \text{ find } u \text{ such that} \\ &\begin{cases} -\Delta u = f & \text{in } \Omega \\ u = 0 & \text{on } \partial\Omega, \end{cases} \end{aligned} \quad (52)$$

where $\Omega \subset \mathbb{R}^d$ ($d = 2, 3$) is a polygonal or polyhedral domain.

Let us first consider the standard variational formulation of problem (52), which reads

$$\begin{aligned} &\text{given } f \in L^2(\Omega), \text{ find } u \in V \text{ such that} \\ &(\nabla u, \nabla v) = (f, v) \quad \forall v \in V, \end{aligned}$$

where as usual (\cdot, \cdot) denotes the L^2 -inner product and $V = H_0^1(\Omega)$.

Let $\{\mathcal{T}_h\}$ denote a shape-regular family (i.e., satisfying the minimum angle condition, see [35]) of triangulations of Ω . As usual we require that any two elements in \mathcal{T}_h share at most a common face, edge or a common vertex, and we denote by h the maximum diameter of the elements K in \mathcal{T}_h . Let \mathcal{E} be the set of interior edges (faces in three dimensions) of the mesh and $\mathcal{E}_K \subset \mathcal{E}$ be the subset of the edges (faces in three dimensions) of the element K .

We denote by $V_h \subset V$ a finite element subspace of V (we can take for example the space consisting of continuous piecewise linear functions vanishing on the boundary of Ω). The discrete problem reads:

$$\begin{aligned} &\text{given } f \in L^2(\Omega), \text{ find } u_h \in V_h \text{ such that} \\ &(\nabla u_h, \nabla v_h) = (f, v_h) \quad \forall v_h \in V_h. \end{aligned}$$

In the following we shall denote by $a(u, v)$ the bilinear form $(\nabla u, \nabla v)$ and by $e_h = u - u_h$ the error which belongs to the space V and satisfies the residual equation

$$a(e_h, v) = (f, v) - a(u_h, v) \quad \forall v \in V. \quad (53)$$

Moreover, the standard Galerkin orthogonality property holds

$$a(e_h, v_h) = 0 \quad \forall v_h \in V_h.$$

The first step in the error analysis is to write the residual equation (53) as a sum of local contribution and to apply integration by parts on each element. Moreover,

observing that the traces of functions in V match along the interface between two elements, we obtain the following expression

$$a(e_h, v) = \sum_{K \in \mathcal{T}_h} \left\{ (f + \Delta u_h, v)_K - \frac{1}{2} \sum_{e \in \mathcal{E}_K} \int_e \left[\left[\frac{\partial u_h}{\partial n} \right] \right]_e v \right\} \quad \forall v \in V,$$

where $(\cdot, \cdot)_K$ and $\left[\left[\cdot \right] \right]_e$ denote respectively the L^2 -inner product restricted to the element K and the jump across the edge (face in three dimensions) e , which is defined as follows

$$\left[\left[\frac{\partial u_h}{\partial n} \right] \right]_e = \nabla u_h|_{K_e^1} \cdot \mathbf{n}_{K_e^1} + \nabla u_h|_{K_e^2} \cdot \mathbf{n}_{K_e^2},$$

K_e^1 and K_e^2 being the two elements in \mathcal{T}_h sharing the edge (face in three dimensions) e and $\mathbf{n}_{K_e^1}$ and $\mathbf{n}_{K_e^2}$ the unit outward normals on ∂K_e^1 and ∂K_e^2 , respectively.

Given any $v \in V$, let $v^I \in V_h$ be such that

$$\|v - v^I\|_{0,K} \leq Ch_K |v|_{1,\tilde{K}}$$

and

$$\|v - v^I\|_{0,e} \leq Ch_e^{1/2} |v|_{1,\tilde{K}},$$

where \tilde{K} is the union of all the elements sharing a vertex with K and h_K and h_e denote the diameter of K and the diameter of edge (face in three dimensions) e , respectively. We can take, for example, the well-known Cl  ment interpolant (see [36]).

Then, thanks to the Galerkin orthogonality, we have

$$a(e_h, v) = \sum_{K \in \mathcal{T}_h} \left\{ (f + \Delta u_h, v - v^I)_K - \frac{1}{2} \sum_{e \in \mathcal{E}_K} \int_e \left[\left[\frac{\partial u_h}{\partial n} \right] \right]_e (v - v^I) \right\} \quad \forall v \in V.$$

Using the Cauchy-Schwarz inequality and the properties of v^I , we obtain

$$a(e_h, v) \leq C \|v\|_1 \left\{ \sum_{K \in \mathcal{T}_h} \left(h_K^2 \|r\|_{0,K}^2 + \frac{1}{2} \sum_{e \in \mathcal{E}_K} h_e \|R\|_{0,e}^2 \right) \right\}^{1/2},$$

where r is the interior residual

$$r|_K = f + \Delta u_h \quad \forall K \in \mathcal{T}_h$$

and R is the boundary residual

$$R|_e = \left[\left[\frac{\partial u_h}{\partial n} \right] \right]_e \quad \forall e \in \mathcal{E}_K.$$

Hence, we can estimate the energy norm, or equivalently the H^1 -norm of the error, as follows:

$$|e_h|_1 \leq C \left\{ \sum_{K \in \mathcal{T}_h} \left(h_K^2 \|r\|_{0,K}^2 + \frac{1}{2} \sum_{e \in \mathcal{E}_K} h_e \|R\|_{0,e}^2 \right) \right\}^{1/2}.$$

Apart from the constant C , all of the quantities in the right-hand side can be computed explicitly from the data of the problem and the finite element approximation. This suggests to define the local error indicator associated with the element K by

$$\eta_K^2 = h_K^2 \|r\|_{0,K}^2 + \frac{1}{2} \sum_{e \in \mathcal{E}_K} h_e \|R\|_{0,e}^2$$

and the corresponding error estimator by

$$\eta = \left(\sum_{K \in \mathcal{T}_h} \eta_K^2 \right)^{1/2}.$$

As usual in residual-type error indicators, η_K consist of the L^2 -norm of the volumetric and edge (face in three dimensions) residual, suitably weighted.

We have then proved the reliability of the error estimator for the source problem.

Theorem 7. *There exists a constant C , depending only on the regularity of the mesh, such that*

$$|e_h|_1 \leq C \eta.$$

Let us now consider the eigenvalue problem corresponding to problem (52), which reads

find $\lambda \in \mathbb{R}$ such that there exists u , with $u \neq 0$:

$$\begin{cases} -\Delta u = \lambda u & \text{in } \Omega \\ u = 0 & \text{on } \partial\Omega. \end{cases} \quad (54)$$

The classical variational formulation of (54) is given by

$$\begin{aligned} & \text{find } \lambda \in \mathbb{R} \text{ such that there exists } u \in V, \text{ with } u \neq 0 : \\ & \begin{cases} a(u, v) = \lambda(u, v) & \forall v \in V \\ \|u\|_0 = 1, \end{cases} \end{aligned}$$

and its discretization by

$$\begin{aligned} & \text{find } \lambda_h \in \mathbb{R} \text{ such that there exists } u_h \in V_h, \text{ with } u_h \neq 0 : \\ & \begin{cases} a(u_h, v_h) = \lambda_h(u_h, v_h) & \forall v_h \in V_h \\ \|u_h\|_0 = 1. \end{cases} \end{aligned}$$

Let (λ, u) be an eigensolution of the continuous problem with λ simple, and (λ_h, u_h) be the corresponding discrete eigensolution. We denote by $e_h = u - u_h$ the error in the approximation of the eigenfunction, which satisfies the following residual equation:

$$a(e_h, v) - (\lambda u - \lambda_h u_h, v) = -a(u_h, v) + \lambda_h(u_h, v) \quad \forall v \in V. \quad (55)$$

First of all we observe that the Galerkin orthogonality property does not hold anymore, indeed

$$a(e_h, v_h) = (\lambda u - \lambda_h u_h, v_h) \quad \forall v_h \in V_h.$$

Therefore, the analysis developed for the source problem cannot be extended in a straightforward fashion.

Trying to generalize the analysis developed for the source problem to the eigenvalue problem, one has to deal with terms such as

$$(\lambda u - \lambda_h u_h, e_h)$$

and, in order to prove the efficiency of the estimator, as

$$\|\lambda u - \lambda_h u_h\|_{0,K},$$

which appear in the error estimate since the Galerkin orthogonality does not hold. Duran *et al.* in [41] proved that these terms are of higher order than the error. Due to the normalization on the eigenfunction, the first term can be treated in the following way

$$(\lambda u - \lambda_h u_h, e_h) = (\lambda + \lambda_h)(1 - (u, u_h)) = \frac{\lambda + \lambda_h}{2} \|e_h\|_0^2.$$

Then, proceeding as for the source problem rewriting the residual equation (55) as a sum over the elements and applying integration by part yields

$$\begin{aligned}
 a(e_h, v) &= a(e_h, v - v^I) + a(e_h, v^I) \\
 &= \sum_{K \in \mathcal{T}_h} \left\{ (\Delta u_h + \lambda_h u_h, v - v^I)_K - \frac{1}{2} \sum_{e \in \mathcal{E}_K} \int_e \left[\left[\frac{\partial u_h}{\partial n} \right] \right]_e (v - v^I) \right\} \\
 &\quad + (\lambda u - \lambda_h u_h, v - v^I) + (\lambda u - \lambda_h u_h, v^I) \\
 &= \sum_{K \in \mathcal{T}_h} \left\{ (\Delta u_h + \lambda_h u_h, v - v^I)_K - \frac{1}{2} \sum_{e \in \mathcal{E}_K} \int_e \left[\left[\frac{\partial u_h}{\partial n} \right] \right]_e (v - v^I) \right\} \\
 &\quad + (\lambda u - \lambda_h u_h, v) \quad \forall v \in V.
 \end{aligned}$$

Taking $v = e_h$ in the above equation, we obtain

$$\|e_h\|_a^2 \leq C \left\{ \sum_{K \in \mathcal{T}_h} \left(h_K^2 \|r\|_{0,K}^2 + \frac{1}{2} \sum_{e \in \mathcal{E}_K} h_e \|R\|_{0,e}^2 \right) \right\}^{1/2} \|e_h\|_a + \frac{\lambda + \lambda_h}{2} \|e_h\|_0^2,$$

where for the eigenvalue problem the volumetric and edge (face in three dimensions) residuals are given respectively by

$$r|_K = \Delta u_h + \lambda_h u_h \quad \forall K \in \mathcal{T}_H$$

and

$$R|_e = \left[\left[\frac{\partial u_h}{\partial n} \right] \right]_e \quad \forall e \in \mathcal{E}_h.$$

Hence, the local error indicator associated with the element K is defined by

$$\eta_K^2 = h_K^2 \|r\|_{0,K}^2 + \frac{1}{2} \sum_{e \in \mathcal{E}_K} h_e \|R\|_{0,e}^2$$

and the error estimator by

$$\eta = \left(\sum_{K \in \mathcal{T}_h} \eta_K^2 \right)^{1/2}.$$

Then the following theorem, which gives an upper error estimate, holds true.

Theorem 8. *There exists a constant C , depending only on the regularity of the mesh, such that*

$$|e_h|_1 \leq C \eta + \left(\frac{\lambda + \lambda_h}{2} \right)^{1/2} \|e_h\|_0.$$

Remark 7. By the a priori error estimates (see [12, 21]), $\|e_h\|_0$ is of higher order than $|e_h|_1$ and thus the estimator provides an upper bound of the error in the energy norm up to a multiplicative constant and a higher order term.

Remark 8. Thanks to the normalization of the eigenfunctions, the following result holds true:

$$|e_h|_1^2 = \lambda + \lambda_h - 2\lambda(u, u_h) = \lambda_h - \lambda + \lambda\|e_h\|_0^2.$$

Therefore, if the error estimator is reliable, then we automatically have that it bounds from above, up to a multiplicative constant dependent on λ and higher order terms, the square root of the error in the approximation of the eigenvalues as well.

The efficiency of the error indicator has been proved using a technique introduced for the source problem firstly by Verfürth in [70]. The key idea is to use *interior* bubble functions, supported on a single element, and *edge* (face in three dimensions) bubble functions, supported on a pair of neighboring elements.

The following lemma provides a local upper estimate for the volumetric residual r .

Lemma 3. *There exists a constant C , depending only on the regularity of the mesh, such that*

$$h_K \|r\|_{0,K} \leq C (|e|_{1,K} + h_K \|\lambda u - \lambda_h u_h\|_{0,K}).$$

Proof. Let b_K denote the standard cubic bubble function on the element K . Choosing $v = r b_K$ in the residual equation (55), we get

$$a(e_h, r b_K) = (\lambda u - \lambda_h u_h, r b_K) + (r, r b_K).$$

Thanks to the property of bubble functions, it holds

$$\|r\|_{0,K}^2 \leq C \int_K r^2 b_K = C [a(e_h, r b_K) - (\lambda u - \lambda_h u_h, r b_K)]$$

and hence, since $|r b_K|_{1,K} \leq C h_K^{-1} \|r\|_{0,K}$, we get the result. \square

We now estimate from above the edge (face in three dimensions) residual R .

Lemma 4. *There exists a constant C , depending only on the regularity of K_e^1 and K_e^2 , such that*

$$h_e^{1/2} \|R\|_{0,e} \leq C (|e_h|_{1,K_e^1 \cup K_e^2} + h_e \|\lambda u - \lambda_h u_h\|_{0,K_e^1 \cup K_e^2}).$$

Proof. Let b_e denote the edge (face in three dimensions) bubble function relative to edge e . Writing the residual equation (55) as a sum of elemental contributions and integrating by part yields

$$a(e_h, v) - (\lambda u - \lambda_h u_h, v) = \sum_{K \in \mathcal{T}_h} \left(\int_K r v - \frac{1}{2} \sum_{e \in \mathcal{E}_K} \int_e R v \right).$$

Taking $v = Rb_e$ in the above equation, we get

$$\int_e R^2 b_e = (r, Rb_e) - a(e_h, Rb_e) + (\lambda u - \lambda_h u_h, Rb_e).$$

□

We conclude the proof using Lemma 3 together with the fact that

$$\|R\|_{0,e}^2 \leq C \int_e R^2 b_e \quad \text{and} \quad h_K^{-1/2} \|Rb_e\|_{0,K} + h_K^{1/2} |Rb_e|_{1,K} \leq C \|Rb_e\|_{0,e}.$$

As an immediate consequence of the previous lemmas, we get the following theorem.

Theorem 9. *Let K^* be the union of K and the neighboring elements K' sharing an edge (face in three dimensions) with K . There exists a positive constant, depending only on the regularity of the mesh, such that*

$$\eta_K \leq C (|e_h|_{1,K^*} + h_K \|\lambda u - \lambda_h u_h\|_{0,K^*}).$$

Remark 9. The term $h_K \|\lambda u - \lambda_h u_h\|_{0,K^*}$ in the previous theorem is a higher order term. Indeed, for each element $K \in \mathcal{T}_h$, it holds

$$h_K \|\lambda u - \lambda_h u_h\|_{0,K^*} \leq \lambda h_K \|u - u_h\|_{0,K^*} + |\lambda - \lambda_h| h_K \|u_h\|_{0,K^*}.$$

By the a priori error estimates (see [12, 21]) both terms in the above equation are higher order than the local error $|e_h|_{1,K^*}$.

In [41] it has also been proved that, for linear elements, the volumetric part of the error indicator is dominated, up to higher order terms, by the edge (face in three dimensions) residuals. This result was known for the source problem, see [33]. The simpler error indicator is defined as

$$\tilde{\eta}_K = \left(\frac{1}{2} \sum_{e \in \mathcal{E}_K} h_e \|R\|_{0,e}^2 \right)^{1/2}$$

and the corresponding global error estimator as

$$\tilde{\eta} = \left(\sum_{K \in \mathcal{T}_h} \tilde{\eta}_K^2 \right)^{1/2}.$$

The following theorem states the reliability and efficiency of the new error estimator.

Theorem 10. *There exists a constant C , depending only on the regularity of the mesh, such that*

$$|e_h|_1 \leq C \left[\tilde{\eta} + \left(\frac{\lambda + \lambda_h}{2} \right)^{1/2} \|e_h\|_0 + \lambda_h^{3/2} h^2 \right]$$

and

$$\tilde{\eta}_K \leq C (|e_h|_{1,K^*} + h_K \|\lambda u - \lambda_h u_h\|_{0,K^*}).$$

The additional term $\lambda_h^{3/2} h^2$ in the first estimate of the above theorem is of higher order (see [41, Remark 4.1])

6.4 Mixed Finite Element Approximation

Error estimators for mixed approximations of the Poisson equation have been introduced in [2, 31] starting from the Helmholtz decomposition of the error and using the Galerkin orthogonality which holds for the second equation of the problem.

Changing to the eigenvalue problem, difficulties similar to the ones underlined for the classical approximation and due to the lack of the Galerkin orthogonality arise.

The first a posteriori error estimators for mixed approximation of eigenvalue problems have been obtained in a very particular situation using the equivalence between the mixed method of Raviart-Thomas of the lowest order and the non-conforming Crouzeix-Raviart approximation of the classical formulation (see [40] and [6] for an application to fluid-structure interactions).

An a posteriori error analysis for mixed approximations of eigenvalue problems has been developed in [44, 45] without resorting to the equivalence with a non-conforming discretization. Moreover, an a posteriori error analysis for the finite element approximation of the Stokes eigenvalue problem has been presented in [61].

6.4.1 A Posteriori Error Analysis for Brezzi–Douglas–Marini Finite Elements

In this section we present the a posteriori error analysis developed in [44, 45] for the Brezzi–Douglas–Marini (BDM) approximation of an eigenvalue problem which arises from the displacement formulation to compute the vibration modes of an acoustic fluid contained within a rigid cavity. We define an error estimator of the residual type and prove that, under some regularity conditions on the continuous eigensolution, it is equivalent to the $H(\text{div})$ -norm of the error up to higher order terms. The constants involved in this equivalence depend on the corresponding

eigenvalue, but are independent of the mesh size. Moreover, the square root of the error in the approximation of the eigenvalue is also bounded by a constant times the estimator.

We consider an eigenvalue problem which has already been introduced in Sect. 5.3. For the ease of the reader, we present the problem again.

$$\begin{aligned} &\text{find } \lambda \in \mathbb{R} \text{ such that there exists } \mathbf{u} \neq \mathbf{0} \\ &\left\{ \begin{array}{ll} -\nabla \operatorname{div} \mathbf{u} = \lambda \mathbf{u} & \text{in } \Omega \\ \operatorname{rot} \mathbf{u} = 0 & \text{in } \Omega \\ \mathbf{u} \cdot \mathbf{n} = 0 & \text{on } \partial\Omega, \end{array} \right. \end{aligned} \quad (56)$$

where $\Omega \subset \mathbb{R}^2$ is a simply connected polygonal domain, $\partial\Omega$ its boundary, and \mathbf{n} its outward normal unit vector.

This problem has been studied by many authors concerning fluid-structure interaction (see [19, 73]). Moreover, since in two dimensions the divergence and rotational operators are isomorphic, it is equivalent to Maxwell's eigenproblem for a cavity resonator with dielectric constant ε and magnetic permeability μ constant and equal to 1 (see [25, 52]).

A variational formulation of (56) reads:

$$\begin{aligned} &\text{find } \lambda \in \mathbb{R} \text{ such that there exists } \mathbf{u} \in H_0(\operatorname{div}, \Omega), \text{ with } \mathbf{u} \neq \mathbf{0} : \\ &\left\{ \begin{array}{ll} (\operatorname{div} \mathbf{u}, \operatorname{div} \mathbf{v}) = \lambda(\mathbf{u}, \mathbf{v}) & \forall \mathbf{v} \in H_0(\operatorname{div}, \Omega) \\ (\mathbf{u}, \operatorname{rot} \mathbf{q}) = 0 & \forall \mathbf{q} \in H_0^1(\Omega), \end{array} \right. \end{aligned} \quad (57)$$

where $H_0(\operatorname{div}, \Omega) = \{\mathbf{v} \in L^2(\Omega)^2 : \operatorname{div} \mathbf{v} \in L^2(\Omega) \text{ and } \mathbf{v} \cdot \mathbf{n} = 0 \text{ on } \partial\Omega\}$ is endowed with the norm $\|\mathbf{v}\|_{\operatorname{div}}^2 = \|\mathbf{v}\|_0^2 + \|\operatorname{div} \mathbf{v}\|_0^2$. It is well known that problem (57) admits a countable set of real and positive eigenvalues, which can be ordered in an increasing divergent sequence. Moreover the eigenfunctions satisfy $\mathbf{u} \in H^s(\operatorname{div}, \Omega) = \{\mathbf{v} \in H^s(\Omega)^2 : \operatorname{div} \mathbf{v} \in H^s(\Omega)\}$, for some $s > 1/2$ depending on Ω ($s = 1$ when Ω is convex) (see [7]).

Let $\{\mathcal{T}_h\}$ be a regular family of triangulations of Ω , where as usual h denotes the maximum diameter of the elements K in \mathcal{T}_h . The Brezzi-Douglas-Marini spaces are defined for $k \geq 1$ by

$$BDM_k = \{\mathbf{v} \in H(\operatorname{div}, \Omega) : \mathbf{v}|_K \in P_k(K)^2 \forall K \in \mathcal{T}_h\},$$

where $P_k(K)$ denotes the space of polynomial of degree at most k on K (see [29]).

Setting $V_h = BDM_k \cap H_0(\operatorname{div}, \Omega)$, and denoting by Q_h the subspace of $H_0^1(\Omega)$ consisting of continuous piecewise polynomial of degree at most $k + 1$, the discrete problem is then given by:

$$\begin{aligned} &\text{find } \lambda_h \in \mathbb{R} \text{ such that there exists } \mathbf{u}_h \in V_h, \text{ with } \mathbf{u}_h \neq \mathbf{0} : \\ &\left\{ \begin{array}{ll} (\operatorname{div} \mathbf{u}_h, \operatorname{div} \mathbf{v}) = \lambda_h(\mathbf{u}_h, \mathbf{v}) & \forall \mathbf{v} \in V_h \\ (\mathbf{u}_h, \operatorname{rot} \mathbf{q}) = 0 & \forall \mathbf{q} \in Q_h. \end{array} \right. \end{aligned} \quad (58)$$

Let (λ, \mathbf{u}) be an eigensolution of (57) such that λ is a simple eigenvalue and $\|\mathbf{u}\|_0 = 1$. It follows from the abstract theory (see [12, 21]) and known a priori estimates that, for h small enough (depending on λ), there exists $(\lambda_h, \mathbf{u}_h)$ eigenpair of (58) with $\|\mathbf{u}_h\|_0 = 1$ such that

$$\|\mathbf{u} - \mathbf{u}_h\|_{\text{div}} = O(h^t) \quad (59)$$

$$\|\mathbf{u} - \mathbf{u}_h\|_0 = O(h^r) \quad (60)$$

$$|\lambda - \lambda_h| = O(h^{2t}), \quad (61)$$

where $t = \min\{s, k\}$, and $r = \min\{s, k + 1\}$.

Since the problem we are dealing with consists of two equations, it is reasonable to expect that the error estimator will be given by the sum of two terms, related one to the residual of the first equation and the other to the residual of the second equation.

Let \mathcal{E} be the set of the interior edges of the mesh and $\mathcal{E}_K \subset \mathcal{E}$ be the subset of edges of K . We denote by $\mathbf{e}_h = \mathbf{u} - \mathbf{u}_h$ the error in the approximation of the eigenfunctions.

For any $K \in \mathcal{T}_h$ we define two local error indicators by

$$\eta_{1,K}^2 = h_K^2 \|\nabla \operatorname{div} \mathbf{u}_h + \lambda_h \mathbf{u}_h\|_{0,K}^2 + \frac{1}{2} \sum_{e \in \mathcal{E}_K} h_e \|\llbracket \operatorname{div} \mathbf{u}_h \rrbracket_e\|_{0,e}^2,$$

$$\eta_{2,K}^2 = h_K^2 \|\operatorname{rot} \mathbf{u}_h\|_{0,K}^2 + \frac{1}{2} \sum_{e \in \mathcal{E}_K} h_e \|\llbracket \mathbf{u}_h \cdot \mathbf{t} \rrbracket_e\|_{0,e}^2,$$

and the corresponding error estimators by

$$\eta_1 = \left(\sum_{K \in \mathcal{T}_h} \eta_{1,K}^2 \right)^{1/2},$$

$$\eta_2 = \left(\sum_{K \in \mathcal{T}_h} \eta_{2,K}^2 \right)^{1/2}.$$

The jump of the tangential component across the edge e is defined as follows

$$\llbracket \mathbf{u}_h \cdot \mathbf{t} \rrbracket_e = \mathbf{u}_h|_{K_e^1} \cdot \mathbf{t}_{K_e^1} + \mathbf{u}_h|_{K_e^2} \cdot \mathbf{t}_{K_e^2}$$

where, for each triangle K , \mathbf{t}_K denotes the unit tangent vector to ∂K oriented counterclockwise.

The following lemmas provide the residual equations which will be the starting points of our error analysis.

Lemma 5. For $\mathbf{v} \in H_0(\operatorname{div}, \Omega) \cap H^\sigma(\operatorname{div}, \mathcal{T}_h)$, with $\sigma > 0$, there holds

$$\begin{aligned} (\operatorname{div} \mathbf{e}_h, \operatorname{div} \mathbf{v}) - (\lambda \mathbf{u} - \lambda_h \mathbf{u}_h, \mathbf{v}) &= -(\operatorname{div} \mathbf{u}_h, \operatorname{div} \mathbf{v}) + \lambda_h(\mathbf{u}_h, \mathbf{v}) \\ &= \sum_{K \in \mathcal{T}_h} \left[(\mathbf{r}_1, \mathbf{v})_K - \frac{1}{2} \sum_{e \in \mathcal{E}_K} \int_e \llbracket \operatorname{div} \mathbf{u}_h \rrbracket_e \mathbf{v} \cdot \mathbf{n} \right], \end{aligned} \quad (62)$$

where $\mathbf{r}_1|_K = \nabla \operatorname{div} \mathbf{u}_h + \lambda_h \mathbf{u}_h$ is the volumetric residual of the first equation of problem (56).

Lemma 6. For $q \in H_0^1(\Omega)$ there holds

$$(\mathbf{e}_h, \operatorname{rot} q) = \sum_{K \in \mathcal{T}_h} \left[(r_2, q)_K + \frac{1}{2} \sum_{e \in \mathcal{E}_K} \int_e q \llbracket \mathbf{u}_h \cdot \mathbf{t} \rrbracket_e \right], \quad (63)$$

where $r_2|_K = -\operatorname{rot} \mathbf{u}_h$ is the volumetric residual of the second equation of problem (56).

Proof. The results easily follow by writing the residual equations as a sum over the elements $K \in \mathcal{T}_h$ and integrating by parts over each element. \square

Remark 10. In order to write the boundary term coming from the integration by parts as a sum of integrals over the edges of K , we had to require that $\mathbf{v} \in H_0(\operatorname{div}, \Omega) \cap H^\sigma(\operatorname{div}, \mathcal{T}_h)$, for some $\sigma > 0$. In the following we shall use Lemma 5 taking $\mathbf{v} = \mathbf{e}_h - \mathbf{e}_h^I$, where $\mathbf{e}_h^I \in V_h$ denotes a suitable interpolant of \mathbf{e}_h . Hence, the regularity assumption on \mathbf{v} is not restrictive for our purposes.

Then the following propositions hold true.

Proposition 1. There exists a positive constant C , independent of h , such that

$$\|\mathbf{e}_h\|_0 \leq C \|\operatorname{div} \mathbf{e}_h\|_0 + C \eta_2. \quad (64)$$

Proof. Since $\mathbf{e}_h = \mathbf{u} - \mathbf{u}_h \in H_0(\operatorname{div}, \Omega)$, by the Helmholtz decomposition we can write

$$\mathbf{e}_h = \nabla \alpha + \operatorname{rot} \beta,$$

where $\alpha \in H^1(\Omega)/\mathbb{R}$ and $\beta \in H_0^1(\Omega)$ are the solutions of the Laplace problem with homogeneous boundary condition and datum $-\operatorname{div} \mathbf{e}_h$ and $\operatorname{rot} \mathbf{e}_h$, respectively.

Using the stability of the Laplace problem and the Galerkin orthogonality property of \mathbf{e}_h , we have that

$$\|\mathbf{e}_h\|_0^2 \leq C \|\mathbf{e}_h\|_0 \|\operatorname{div} \mathbf{e}_h\|_0 + (\mathbf{e}_h, \operatorname{rot} (\beta - \beta^I)),$$

where β^I denotes the Clément interpolant of β (see [36]).

Applying Lemma 6 with $q = \beta - \beta^I$ and taking into account the properties of Clément interpolation operator, we get

$$\|\mathbf{e}_h\|_0^2 \leq C \|\mathbf{e}_h\|_0 \|\operatorname{div} \mathbf{e}_h\|_0 + \|\beta\|_1 \sum_{K \in \mathcal{T}_h} \left[h_K \|r_2\|_{0,K} + \frac{1}{2} \sum_{e \in \mathcal{E}_K} h_e^{\frac{1}{2}} \|[\![\mathbf{u}_h \cdot \boldsymbol{\nu}]\!]\|_{0,e} \right].$$

We conclude the proof using the Helmholtz decomposition and Cauchy-Schwarz inequality. \square

Proposition 2. *There holds*

$$\|\operatorname{div} \mathbf{e}_h\|_0^2 \leq C_\lambda [\eta_1^2 + \eta_2^2 + (\lambda \mathbf{u} - \lambda_h \mathbf{u}_h, \mathbf{e}_h)], \quad (65)$$

where C_λ is a positive constant dependent on λ .

Proof. Let $\mathbf{e}_h^I \in V_h$ be a suitable interpolant of \mathbf{e}_h , then

$$\begin{aligned} \|\operatorname{div} \mathbf{e}_h\|_0^2 &= (\operatorname{div} \mathbf{e}_h, \operatorname{div}(\mathbf{e}_h - \mathbf{e}_h^I)) + (\operatorname{div} \mathbf{e}_h, \operatorname{div} \mathbf{e}_h^I) \\ &= (\lambda \mathbf{u} - \lambda_h \mathbf{u}_h, \mathbf{e}_h) - (\operatorname{div} \mathbf{u}_h, \operatorname{div}(\mathbf{e}_h - \mathbf{e}_h^I)) + \lambda_h (\mathbf{u}_h, \mathbf{e}_h - \mathbf{e}_h^I), \end{aligned}$$

where the last equality follows from the residual equation (62).

The following decomposition of $H_0(\operatorname{div}, \Omega)$ plays a key role in the proof (see [64] for the details of the proof):

Proposition 3. *For any $\mathbf{v} \in H_0(\operatorname{div}, \Omega)$ there exists $\mathbf{z} \in H_0^1(\Omega)^2$ and $\varphi \in H^1(\Omega)$ such that*

$$\mathbf{v} = \mathbf{z} + \mathbf{rot} \varphi$$

and the following estimates hold:

$$\|\mathbf{z}\|_1 \leq C \|\operatorname{div} \mathbf{v}\|_0 \text{ and } \|\varphi\|_1 \leq C \|\mathbf{v}\|_0.$$

Then we write the error as $\mathbf{e}_h = \mathbf{z} + \mathbf{rot} \varphi$ and define $\mathbf{e}_h^I = \mathbf{z}^I + \mathbf{rot} \varphi^I$, where \mathbf{z}^I and φ^I denote the Clément interpolant of \mathbf{z} and φ , respectively. Note that with this definition, $\mathbf{e}_h^I \in V_h$ and $\mathbf{e}_h - \mathbf{e}_h^I = (\mathbf{z} - \mathbf{z}^I) + \mathbf{rot}(\varphi - \varphi^I)$. It follows from Lemmas 5 and 6 that

$$\begin{aligned} & -(\operatorname{div} \mathbf{u}_h, \operatorname{div}(\mathbf{e}_h - \mathbf{e}_h^I)) + \lambda_h (\mathbf{u}_h, \mathbf{e}_h - \mathbf{e}_h^I) \\ &= -(\operatorname{div} \mathbf{u}_h, \operatorname{div}(\mathbf{z} - \mathbf{z}^I)) + \lambda_h (\mathbf{u}_h, \mathbf{z} - \mathbf{z}^I) + \lambda_h (\mathbf{u}_h, \mathbf{rot}(\varphi - \varphi^I)) \\ &\leq \sum_{K \in \mathcal{T}_h} \left[\|\mathbf{r}_1\|_{0,K} h_K h_K^{-1} \|\mathbf{z} - \mathbf{z}^I\|_{0,K} + \frac{1}{2} \sum_{e \in \mathcal{E}_K} \|[\![\operatorname{div} \mathbf{u}_h]\!]\|_{0,e} h_e^{\frac{1}{2}} h_e^{-\frac{1}{2}} \|\mathbf{z} - \mathbf{z}^I\|_{0,e} \right] \end{aligned}$$

$$+ \lambda_h \sum_{K \in \mathcal{T}_h} \left[\|r_2\|_{0,K} h_K h_K^{-1} \|\varphi - \varphi^I\|_{0,K} + \frac{1}{2} \sum_{e \in \mathcal{E}_K} \|[\![\mathbf{u}_h \cdot \mathbf{t}]\!]_e\|_{0,e} h_e^{\frac{1}{2}} h_e^{-\frac{1}{2}} \|\varphi - \varphi^I\|_{0,e} \right].$$

Using the properties of Clément interpolation operator and the estimates in Proposition 3, we have

$$\begin{aligned} \|\operatorname{div} \mathbf{e}_h\|_0^2 &\leq C \|\operatorname{div} \mathbf{e}_h\|_0 \left[\sum_{K \in \mathcal{T}_h} \left(h_K^2 \|\mathbf{r}_1\|_{0,K}^2 + \frac{1}{2} \sum_{e \in \mathcal{E}_K} h_e \|\llbracket \operatorname{div} \mathbf{u}_h \rrbracket_e\|_{0,e}^2 \right) \right]^{\frac{1}{2}} \\ &\quad + C \lambda_h \|\mathbf{e}_h\|_0 \left[\sum_{K \in \mathcal{T}_h} (h_K^2 \|r_2\|_{0,K}^2 + \frac{1}{2} \sum_{e \in \mathcal{E}_K} h_e \|\llbracket \mathbf{u}_h \cdot \mathbf{t} \rrbracket_e\|_{0,e}^2) \right]^{\frac{1}{2}} \\ &\quad + (\lambda \mathbf{u} - \lambda_h \mathbf{u}_h, \mathbf{e}_h). \end{aligned}$$

Since $\lambda_h \rightarrow \lambda$ we can bound λ_h by a constant depending on λ . We complete the proof using two times the arithmetic-geometric mean inequality $ab \leq \frac{\varepsilon}{2} a^2 + \frac{b^2}{2\varepsilon}$. \square

Remark 11. Since $\|\mathbf{u}\|_0 = \|\mathbf{u}_h\|_0 = 1$, the last term in (65) can be written as

$$(\lambda \mathbf{u} - \lambda_h \mathbf{u}_h, \mathbf{e}_h) = (\lambda + \lambda_h) [1 - (\mathbf{u}, \mathbf{u}_h)] = \frac{\lambda + \lambda_h}{2} \|\mathbf{e}_h\|_0^2 \quad (66)$$

and hence if the continuous eigensolution is smooth enough (i.e. $\mathbf{u} \in H^\sigma(\Omega, \operatorname{div})$ for some $\sigma > k$), then by the a priori estimate (60) it turns out to be of higher order than $\|\operatorname{div} \mathbf{e}_h\|_0^2$.

As a consequence of the previous results, we can state the following theorem.

Theorem 11. *Let us assume that $\mathbf{u} \in H^\sigma(\operatorname{div}, \Omega)$, for some $\sigma > k$. Then there exists a constant C_λ , depending on λ and on the regularity of the mesh, such that*

$$\|\mathbf{e}_h\|_{\operatorname{div}} \leq C_\lambda (\eta_1 + \eta_2) + \text{h.o.t.} \quad (67)$$

Remark 12. Thanks to the normalization of the eigenfunctions, the following result holds true:

$$\|\operatorname{div} \mathbf{e}_h\|_0^2 = \lambda + \lambda_h - 2\lambda(\mathbf{u}, \mathbf{u}_h) = \lambda_h - \lambda + \lambda \|\mathbf{e}_h\|_0^2.$$

Therefore, if the error estimator is reliable, then we automatically have that it bounds from above, up to a multiplicative constant dependent on λ , the square root of the error in the approximation of the eigenvalues as well.

We split the proof of the efficiency of the error indicators into two steps.

First of all we use the following lemma to prove that the error indicator $\eta_{2,K}$ is bounded above by the L^2 -norm of the error in the neighborhood of the element K .

Lemma 7. *Let $K \in \mathcal{T}_h$. Given $q_K \in L^2(K)$, $p_{e,K} \in L^2(e)$, $e \subset \partial K$, there exists a unique $\psi_K \in P_{k+3}(K)$ such that*

$$\begin{cases} (\psi_K, r)_K = (q_K, r)_K & \forall r \in P_k(K) \\ \int_e \psi_K s = \int_e p_{e,K} s & \forall s \in P_{k+1}(e) \\ \psi_K = 0 & \text{at the vertices of } K \end{cases} \quad (68)$$

and

$$\|\psi_K\|_{0,K} \leq C \left(\|q_K\|_{0,K} + \sum_{e \subset \partial K} h_e^{\frac{1}{2}} \|p_{e,K}\|_{0,e} \right), \quad (69)$$

with C constant depending only on the regularity of K .

Then the following result holds.

Proposition 4. *There exists a constant C , depending only on the regularity of the element K , such that*

$$h_K^2 \|r_2\|_{0,K}^2 \leq C \|\mathbf{e}_h\|_{0,K}^2.$$

Proof. We apply Lemma 7 with $q_K = r_2$, $p_{e,K} = 0 \ \forall e \subset \partial K$, then $\psi_K \in H_0^1(K)$. Let $\psi \in H_0^1(\Omega)$ denote the zero extension of ψ_K . Taking $q = \psi$ in the residual equation (63) we get

$$\begin{aligned} \|r_2\|_{0,K}^2 &= (r_2, \psi_K)_K = (\mathbf{e}_h, \mathbf{rot} \psi) \leq \|\mathbf{e}_h\|_{0,K} \|\mathbf{rot} \psi_K\|_{0,K} \\ &\leq C \|\mathbf{e}_h\|_{0,K} h_K^{-1} \|\psi_K\|_{0,K}, \end{aligned}$$

where the last bound follows from an inverse inequality. We complete the proof using (69). \square

For any interior edge $\bar{e} \in \mathcal{E}$ let $K_{\bar{e}}^1$ and $K_{\bar{e}}^2$ denote the two elements of \mathcal{T}_h sharing \bar{e} .

Proposition 5. *Let $\bar{e} \in \mathcal{E}$. There exists a constant C , depending only on the regularity of $K_{\bar{e}}^1$ and $K_{\bar{e}}^2$, such that*

$$\frac{1}{2} h_{\bar{e}} \|\llbracket \mathbf{u}_h \cdot \mathbf{t} \rrbracket_{\bar{e}}\|_{0,\bar{e}}^2 \leq C \|\mathbf{e}_h\|_{0,K_{\bar{e}}^1 \cup K_{\bar{e}}^2}^2.$$

Proof. For $i = 1, 2$, we apply Lemma 7 with $q_{K_{\bar{e}}^i} = 0$, $p_{\bar{e},K_{\bar{e}}^i} = \llbracket \mathbf{u}_h \cdot \mathbf{t} \rrbracket$, and $p_{e,K_{\bar{e}}^i} = 0$ if $e \neq \bar{e}$. Let $\psi \in H_0^1(K_{\bar{e}}^1 \cup K_{\bar{e}}^2) \cap H_0^1(\Omega)$ defined by

$$\psi = \begin{cases} \psi_{K_e^1} & \text{in } K_e^1 \\ \psi_{K_e^2} & \text{in } K_e^2 \\ 0 & \text{in } \Omega \setminus (K_e^1 \cup K_e^2). \end{cases}$$

Taking $q = \psi$ in (63) we get

$$\frac{1}{2} \| [\mathbf{u}_h \cdot \mathbf{t}]_{\bar{e}} \|_{0,\bar{e}}^2 = (\mathbf{e}_h, \mathbf{rot} \psi)_{K_e^1 \cup K_e^2} \leq C \| \mathbf{e}_h \|_{0, K_e^1 \cup K_e^2} h_e^{-\frac{1}{2}} \| [\mathbf{u}_h \cdot \mathbf{t}]_{\bar{e}} \|_{0,\bar{e}},$$

where the last bound follows from an inverse inequality and (69). \square

We can therefore state the following theorem.

Theorem 12. *There exists a constant C , depending only on the regularity of the mesh, such that*

$$\eta_2 \leq C \| \mathbf{e}_h \|_0.$$

Moreover, the following local estimate holds

$$\eta_{2,K} \leq C \| \mathbf{e}_h \|_{0,K^*},$$

with C constant depending only on the regularity of the elements K of K^* .

Now we prove that the error indicator $\eta_{1,K}$ is bounded above, up to higher order terms, by the L^2 -norm of the divergence of the error in the neighborhood of the element K . This, together with the previous result, yields the efficiency of the error indicator $\eta_{1,K} + \eta_{2,K}$.

We shall use the following lemma, which generalizes Lemma 7 to vector-valued functions.

Lemma 8. *Let $K \in \mathcal{T}_h$. Given $\mathbf{q}_K \in [L^2(K)]^2$, $\mathbf{p}_{e,K} \in [L^2(e)]^2$, $e \subset \partial K$, there exists a unique $\psi_K \in [P_{k+3}(K)]^2$ such that*

$$\begin{cases} (\psi_K, \mathbf{r})_K = (\mathbf{q}_K, \mathbf{r})_K & \forall \mathbf{r} \in [P_k(K)]^2 \\ \int_e \psi_K \cdot \mathbf{s} = \int_e \mathbf{p}_{e,K} \cdot \mathbf{s} & \forall \mathbf{s} \in [P_{k+1}(e)]^2 \\ \psi_K = 0 & \text{at the vertices of } K \end{cases} \quad (70)$$

$$\| \psi_K \|_{0,K} \leq C (\| \mathbf{q}_K \|_{0,K} + \sum_{e \subset \partial K} h_e^{\frac{1}{2}} \| \mathbf{p}_{e,K} \|_{0,e}), \quad (71)$$

with C constant depending only on the regularity of the element K .

Then the following propositions hold.

Proposition 6. *There exists a constant C , depending only on the regularity of K , such that*

$$h_K \| \mathbf{r}_1 \|_{0,K} \leq C (\| \operatorname{div} \mathbf{e}_h \|_{0,K} + h_K \| \lambda \mathbf{u} - \lambda_h \mathbf{u}_h \|_{0,K}).$$

Proof. We apply Lemma 8 with $\mathbf{q}_K = \mathbf{r}_1$, $\mathbf{p}_{e,K} = 0 \ \forall e \subset \partial K$, then $\psi_K \in [H_0^1(K)]^2$. Let $\psi \in [H_0^1(\Omega)]^2$ denote the zero extension of ψ_K . Then taking $\mathbf{v} = \psi$ in (62), we get

$$\begin{aligned} \|\mathbf{r}_1\|_{0,K}^2 &= (\mathbf{r}_1, \psi_K)_K = (\operatorname{div} \mathbf{e}_h, \operatorname{div} \psi_K)_K - (\lambda \mathbf{u} - \lambda_h \mathbf{u}_h, \psi_K)_K \\ &\leq \|\operatorname{div} \mathbf{e}_h\|_{0,K} \|\operatorname{div} \psi_K\|_{0,K} + \|\lambda \mathbf{u} - \lambda_h \mathbf{u}_h\|_{0,K} \|\mathbf{r}_1\|_{0,K} \\ &\leq C h_K^{-1} \|\operatorname{div} \mathbf{e}_h\|_{0,K} \|\mathbf{r}_1\|_{0,K} + \|\lambda \mathbf{u} - \lambda_h \mathbf{u}_h\|_{0,K} \|\mathbf{r}_1\|_{0,K}, \end{aligned}$$

where the last bound follows from an inverse inequality and from (71). \square

Proposition 7. *Let $\bar{e} \in \mathcal{E}$. There exists a constant C , depending only on the regularity of $K_{\bar{e}}^1$ and $K_{\bar{e}}^2$, such that*

$$\frac{1}{2} h_{\bar{e}}^{\frac{1}{2}} \|[\![\operatorname{div} \mathbf{u}_h]\!]\bar{e}\|_{0,\bar{e}} \leq C (\|\operatorname{div} \mathbf{e}_h\|_{0,K_{\bar{e}}^1 \cup K_{\bar{e}}^2} + h_{\bar{e}} \|\lambda \mathbf{u} - \lambda_h \mathbf{u}_h\|_{0,K_{\bar{e}}^1 \cup K_{\bar{e}}^2}).$$

Proof. For $i = 1, 2$, we apply Lemma 8 with $\mathbf{q}_{K_{\bar{e}}^i} = \mathbf{0}$, $\mathbf{p}_{\bar{e},K_{\bar{e}}^i} = (0, -[\![\operatorname{div} \mathbf{u}_h]\!]\bar{e})$, and $\mathbf{p}_{e,K_{\bar{e}}^i} = \mathbf{0}$ if $e \neq \bar{e}$. Let $\psi \in [H_0^1(K_{\bar{e}}^1 \cup K_{\bar{e}}^2)]^2 \cap [H_0^1(\Omega)]^2$ be defined by

$$\psi = \begin{cases} \psi_{K_{\bar{e}}^1} & \text{in } K_{\bar{e}}^1 \\ \psi_{K_{\bar{e}}^2} & \text{in } K_{\bar{e}}^2 \\ \mathbf{0} & \text{in } \Omega \setminus (K_{\bar{e}}^1 \cup K_{\bar{e}}^2). \end{cases}$$

Taking $\mathbf{v} = \psi$ in the residual equation (62) we get

$$\begin{aligned} \frac{1}{2} \|[\![\operatorname{div} \mathbf{u}_h]\!]\bar{e}\|_{0,\bar{e}}^2 &= (\operatorname{div} \mathbf{e}_h, \operatorname{div} \psi)_{K_{\bar{e}}^1 \cup K_{\bar{e}}^2} - (\lambda \mathbf{u} - \lambda_h \mathbf{u}_h, \psi)_{K_{\bar{e}}^1 \cup K_{\bar{e}}^2} \\ &\leq C (\|\operatorname{div} \mathbf{e}_h\|_{0,K_{\bar{e}}^1 \cup K_{\bar{e}}^2} h_{\bar{e}}^{-\frac{1}{2}} \|[\![\operatorname{div} \mathbf{u}_h]\!]\bar{e}\|_{0,\bar{e}} \\ &\quad + \|\lambda \mathbf{u} - \lambda_h \mathbf{u}_h\|_{0,K_{\bar{e}}^1 \cup K_{\bar{e}}^2} h_{\bar{e}}^{\frac{1}{2}} \|[\![\operatorname{div} \mathbf{u}_h]\!]\bar{e}\|_{0,\bar{e}}), \end{aligned}$$

where the last bound follows from an inverse inequality and from (71). \square

As a consequence of Propositions 6 and 7 the following theorem holds.

Theorem 13. *There exists a constant C , depending only on the regularity of the elements of K^* , such that*

$$\eta_{1,K} \leq C (\|\operatorname{div} \mathbf{e}_h\|_{0,K^*} + h_K \|\lambda \mathbf{u} - \lambda_h \mathbf{u}_h\|_{0,K^*}).$$

Remark 13. The term $h_K \|\lambda \mathbf{u} - \lambda_h \mathbf{u}_h\|_{0,K^*}$ in the previous theorem is a higher order term. Indeed, for each element $K \in \mathcal{T}_h$

$$\begin{aligned} h_K \|\lambda \mathbf{u} - \lambda_h \mathbf{u}_h\|_{0,K^*} &\leq |\lambda - \lambda_h| h_K \|\mathbf{u}_h\|_{0,K^*} + \lambda h_K \|\mathbf{e}_h\|_{0,K^*} \leq C h^{2t+1} \\ &\quad + \lambda h_K \|\mathbf{e}_h\|_{0,K^*}, \end{aligned}$$

where the last bound follows from the a priori estimate (61). Note that the right hand side is asymptotically negligible with respect to the local error $\|\operatorname{div} \mathbf{e}_h\|_{0,K^*}$.

Putting together the results of Theorems 12 and 13, we have that the error indicator $\eta_{1,K} + \eta_{2,K}$ is bounded above by the local error up to a multiplicative constant and higher order terms, namely,

$$\eta_{1,K} + \eta_{2,K} \leq C \|\mathbf{e}_h\|_{\operatorname{div},K^*} + O(h^{2t+1}) + O(h_K) \|\mathbf{e}_h\|_{0,K^*}.$$

We summarize all the result we presented in the following theorem.

Theorem 14. *There exists a constant C , depending only on the regularity of the mesh, such that*

$$\eta_{1,K} + \eta_{2,K} \leq C \|\mathbf{e}_h\|_{\operatorname{div},K^*} + \text{h.o.t.} \quad (72)$$

Moreover if $\mathbf{u} \in H^\sigma(\operatorname{div}, \Omega)$ for some $\sigma > k$, then there exist two constants $C_{1,\lambda}$ and $C_{2,\lambda}$, depending on λ and on the regularity of the mesh, such that

$$\|\mathbf{e}_h\|_{\operatorname{div}} \leq C_{1,\lambda} (\eta_1 + \eta_2) + \text{h.o.t.} \quad (73)$$

$$|\lambda - \lambda_h|^{\frac{1}{2}} \leq C_{2,\lambda} (\eta_1 + \eta_2) + \text{h.o.t.} \quad (74)$$

6.4.2 A Posteriori Error Analysis for Raviart-Thomas Finite Elements

In this section we develop an a posteriori error analysis for the Raviart-Thomas (RT) approximation of the Laplace eigenproblem with Neumann boundary condition.

It is known (see [25]) that the mixed formulation of the Laplace eigenproblem with Neumann boundary condition is equivalent to the eigenvalue problem considered in the previous section. Moreover, if we consider Raviart-Thomas or Brezzi-Douglas-Marini finite elements, then the corresponding discrete problems are equivalent as well. Nevertheless, the a posteriori error analysis developed for Brezzi-Douglas-Marini approximation does not hold for Raviart-Thomas finite elements. This is due to the fact that, contrary to BDM elements, RT elements provide an approximation of the same order in L^2 and $H(\operatorname{div})$ and thus the term $(\lambda \mathbf{u} - \lambda_h \mathbf{u}_h, \mathbf{e}_h)$, which appears in the analysis, is not a higher order term (see Remark 11).

We prove that, if a superconvergence result holds true, then the error estimator η_2 previously introduced in Sect. 6.4.1 is equivalent to the L^2 -norm of the error up to higher order terms.

In order to prove this result, we also prove that the *grad*-part of the L^2 -norm of the error is negligible. A similar result is known to hold for the source problem, provided the solution is smooth enough. Nevertheless, the proof given for the source problem cannot be extended in a straightforward fashion to the eigenvalue problem. Indeed the proof strongly relies on the Galerkin orthogonality, which holds for the source problem but not for the eigenvalue problem.

The mixed formulation of the Laplace eigenproblem with Neumann boundary condition reads:

$$\begin{aligned} & \text{find } \lambda \in \mathbb{R} \text{ such that there exist } (\boldsymbol{\sigma}, \varphi) \in H_0(\text{div}, \Omega) \times L_0^2(\Omega), \text{ with } \varphi \neq 0 : \\ & \left\{ \begin{array}{ll} (\boldsymbol{\sigma}, \boldsymbol{\tau}) + (\text{div } \boldsymbol{\tau}, \varphi) = 0 & \forall \boldsymbol{\tau} \in H_0(\text{div}, \Omega) \\ (\text{div } \boldsymbol{\sigma}, \psi) = -\lambda(\varphi, \psi) & \forall \psi \in L_0^2(\Omega) \end{array} \right. \end{aligned} \quad (75)$$

and its discretization by means of Raviart-Thomas finite elements is given by

$$\begin{aligned} & \text{find } \lambda_h \in \mathbb{R} \text{ such that there exist } (\boldsymbol{\sigma}_h, \varphi_h) \in \Sigma_h \times \Phi_h, \text{ with } \varphi_h \neq 0 : \\ & \left\{ \begin{array}{ll} (\boldsymbol{\sigma}_h, \boldsymbol{\tau}) + (\text{div } \boldsymbol{\tau}, \varphi_h) = 0 & \forall \boldsymbol{\tau} \in \Sigma_h \\ (\text{div } \boldsymbol{\sigma}_h, \psi) = -\lambda_h(\varphi_h, \psi) & \forall \psi \in \Phi_h, \end{array} \right. \end{aligned} \quad (76)$$

where

$$\Sigma_h = RT_k \cap H_0(\text{div}, \Omega),$$

and

$$\Phi_h = \{\psi \in L_0^2(\Omega) : \psi|_K \in P_k \ \forall K \in \mathcal{T}_h\}.$$

The Raviart-Thomas spaces are defined for $k \geq 0$ as follows:

$$RT_k = \{\boldsymbol{\tau} \in H(\text{div}, \Omega) : \boldsymbol{\tau}|_K \in P_k(K)^2 + P_k(K)(x, y)^t \ \forall K \in \mathcal{T}_h\}.$$

Due to regularity results (see [7]), there exists a constant $s > 1/2$ (depending on Ω), such that $(\boldsymbol{\sigma}, \varphi)$ belongs to the space $H^s(\Omega)^2 \times H^{1+s}(\Omega)$. Furthermore, the following estimate holds true:

$$\|\boldsymbol{\sigma}\|_s + \|\text{div } \boldsymbol{\sigma}\|_{1+s} \leq C \|\boldsymbol{\sigma}\|_0, \quad (77)$$

where C is a constant depending on the eigenvalue λ . In (77), s is at least one if Ω is convex, while s is at least $\pi/\omega - \varepsilon$ for any $\varepsilon > 0$ for a non convex domain, $\omega < 2\pi$ being the maximum interior angle of Ω .

Let $(\lambda, \boldsymbol{\sigma})$ be an eigensolution of (75) such that λ is a simple eigenvalue and $\|\boldsymbol{\sigma}\|_0 = 1$. From the abstract theory (see [12, 21]) and known a priori estimates it

follows that, for h small enough (depending on λ), there exists (λ_h, σ_h) eigenpair of (76) with $\|\sigma_h\|_0 = 1$ such that

$$\|\sigma - \sigma_h\|_{\text{div}} = O(h^t) \quad (78)$$

$$\|\sigma - \sigma_h\|_0 = O(h^t) \quad (79)$$

$$|\lambda - \lambda_h| = O(h^{2t}), \quad (80)$$

where $t = \min\{s, k + 1\}$.

In the following we denote by $e_h = \sigma - \sigma_h$ the error in the approximation of the eigenfunction and by P_h the L^2 -projection on Φ_h .

The main result of this section is stated in the following theorem.

Theorem 15. *If $\|P_h\varphi - \varphi_h\|_0$ is of higher order than $\|e_h\|_0$, then there exist a constant C , depending on the regularity of the mesh, such that*

$$\|e_h\|_0 \leq C\eta_2 + \text{h.o.t.},$$

where “h.o.t.” denotes higher order terms.

The error indicator η_2 in the above theorem is the one introduced in Sect. 6.4.1 and it is given by

$$\eta_{2,K}^2 = h_K^2 \|\text{rot } \sigma_h\|_{0,K}^2 + \frac{1}{2} \sum_{e \in \mathcal{E}_K} h_e \|\llbracket \sigma_h \cdot \mathbf{t} \rrbracket_e\|_{0,e}^2.$$

As for Brezzi-Douglas-Marini approximation, the a posteriori error analysis starts from the Helmholtz decomposition of the error

$$e_h = \nabla \alpha + \text{rot } \beta.$$

The *rot*-part of the L^2 -norm of the error is then bounded above by the error indicator η_2 , as it has been done in Sect. 6.4.1. But, contrary to what has been done for Brezzi-Douglas-Marini approximation, we prove that if a superconvergence property holds, then the *grad*-part of the L^2 -norm of the error $(e_h, \nabla \alpha)$ is of higher order than $\|e_h\|_0^2$. It is known that a similar result holds true for the source problem, provided the solution is smooth enough. Indeed, thanks to the Helmholtz decomposition, it holds

$$\|\sigma^s - \sigma_h^s\|_0^2 = (\sigma^s - \sigma_h^s, \nabla a) + (\sigma^s - \sigma_h^s, \text{rot } b),$$

where σ^s and σ_h^s denote the solution of the continuous and discrete source problem, respectively. Moreover, due to the Galerkin orthogonality property, we have

$$(\sigma^s - \sigma_h^s, \nabla a) = -(\text{div}(\sigma^s - \sigma_h^s), a) = -(\text{div}(\sigma^s - \sigma_h^s), a - P_h a). \quad (81)$$

Therefore, if σ^s is smooth enough, then from the standard a priori error analysis for mixed problems it follows that

$$(\sigma^s - \sigma_h^s, \nabla a) \leq C h^{k+2} \|\sigma^s - \sigma_h^s\|_0, \quad (82)$$

and hence it turns out to be of higher order than $\|\sigma^s - \sigma_h^s\|_0^2$.

We observe that the previous proof cannot be generalized in a straightforward way to the eigenvalue problem. In fact in this case, the Galerkin orthogonality does not hold and hence we are not allowed to subtract $P_h a$ in the right hand side of (81). In what follows we shall generalize equation (82) to the eigenvalue problem and we will use it to prove Theorem 15.

We start proving the following theorem.

Theorem 16. *There exist a constant C , depending on the regularity of the mesh, such that*

$$\|e_h\|_0 \leq C(\eta_2 + |\lambda - \lambda_h| + \|\varphi - P_h \varphi\|_{(H^1/\mathbb{R})^*} + \|P_h \varphi - \varphi_h\|_0) \quad (83)$$

Proof. By the Helmholtz decomposition, we write the error as

$$e_h = \nabla \alpha + \mathbf{rot} \beta,$$

where $\alpha \in H^1(\Omega)/\mathbb{R}$ and $\beta \in H_0^1(\Omega)$ are the solutions of the Laplace problem with homogeneous Neumann and Dirichlet boundary condition and datum $-\operatorname{div} e_h$ and $\mathbf{rot} e_h$, respectively. Then the L^2 -norm of the error is given by

$$\|e_h\|_0^2 = (e_h, \nabla \alpha) + (e_h, \mathbf{rot} \beta).$$

Arguing as in the proof of Proposition 1, we have that

$$(e_h, \mathbf{rot} \beta) \leq C \eta_2 \|e_h\|_0.$$

Hence, it remains to prove that

$$(e_h, \nabla \alpha) \leq C(|\lambda - \lambda_h| + \|\varphi - P_h \varphi\|_{(H^1/\mathbb{R})^*} + \|P_h \varphi - \varphi_h\|_0) \|e_h\|_0.$$

Integrating $(e_h, \nabla \alpha)$ by parts and using the second equation of problems (75) and (76), we get

$$(e_h, \nabla \alpha) = -(\operatorname{div}(\sigma - \sigma_h), \alpha) = -(\lambda \varphi - \lambda_h \varphi_h, \alpha).$$

We now estimate $(\lambda \varphi - \lambda_h \varphi_h, \alpha)$ in the following way:

$$(\lambda \varphi - \lambda_h \varphi_h, \alpha) \leq \|\lambda \varphi - \lambda_h \varphi_h\|_{(H^1/\mathbb{R})^*} \|\alpha\|_{H^1/\mathbb{R}} \leq C \|\lambda \varphi - \lambda_h \varphi_h\|_{(H^1/\mathbb{R})^*} \|e_h\|_0.$$

Finally, we bound $\|\lambda\varphi - \lambda_h\varphi_h\|_{(H^1/\mathbb{R})^*}$ as follows:

$$\|\lambda\varphi - \lambda_h\varphi_h\|_{(H^1/\mathbb{R})^*} \leq |\lambda - \lambda_h| \|\varphi\|_0 + |\lambda_h| \|\varphi - \varphi_h\|_{(H^1/\mathbb{R})^*}.$$

We conclude the proof by adding and subtracting $P_h\varphi$ in the last term of the above equation, and applying triangular inequality. \square

The following corollary, which states the reliability of the error estimator η_2 , holds true.

Corollary 6. *If $\|P_h\varphi - \varphi_h\|_0$ is of higher order than $\|\mathbf{e}_h\|_0$, then there exists a constant C , depending on the regularity of the mesh, such that*

$$\|\mathbf{e}_h\|_0 \leq C\eta_2 + \text{h.o.t..}$$

Proof. The terms $|\lambda - \lambda_h|$ and $\|\varphi - P_h\varphi\|_{(H^1/\mathbb{R})^*}$ in (83) are of higher order than $\|\mathbf{e}_h\|_0$. Indeed, thanks to the a priori error estimate (80),

$$|\lambda - \lambda_h| = O(h^{2t}),$$

while, taking into account the properties of the L^2 -projection P_h together with the a priori estimate (77), the second term is bounded in this way

$$\|\varphi - P_h\varphi\|_{(H^1/\mathbb{R})^*} = \sup_{\psi \in H^1/\mathbb{R}} \frac{(\varphi - P_h\varphi, \psi - P_h\psi)}{\|\psi\|_{H^1/\mathbb{R}}} \leq Chh^{\min\{k,s\}+1}. \quad (84)$$

\square

The superconvergence result required by Corollary 6 has been proved for the lowest order Raviart-Thomas elements in [46]. Moreover, numerical evidence of the superconvergence property for Brezzi-Douglas-Marini space of lowest order has also been shown.

In order to prove that the local error indicator $\eta_{2,K}$ is bounded above by the L^2 -norm of the error in the neighborhood of the element K , we can argue in the same way as it has been done in Sect. 6.4.1 for Brezzi-Douglas-Marini approximation. Indeed, the following propositions holds true for Raviart-Thomas finite elements as well.

Proposition 8. *There exists a constant C , depending only on the regularity of the element K , such that*

$$h_K^2 \|\text{rot } \boldsymbol{\sigma}_h\|_{0,K}^2 \leq C \|\mathbf{e}_h\|_{0,K}^2.$$

Proposition 9. *Let $\bar{e} \in \mathcal{E}$. There exists a constant C , depending only on the regularity of $K_{\bar{e}}^1$ and $K_{\bar{e}}^2$, such that*

$$\frac{1}{2} h_{\bar{e}} \|\llbracket \boldsymbol{\sigma}_h \cdot \mathbf{t} \rrbracket_e\|_{0,\bar{e}}^2 \leq C \|\mathbf{e}_h\|_{0,K_{\bar{e}}^1 \cup K_{\bar{e}}^2}^2,$$

where $K_{\bar{e}}^1$ and $K_{\bar{e}}^2$ denote the two elements in \mathcal{T}_h sharing \bar{e} .

We omit the details of the proof, which are as in Sect. 6.4.1. Collecting the results of the above propositions, we can state the following theorem.

Theorem 17. *For each element $K \in \mathcal{T}_h$ there exists a constant C , depending only on the regularity of the elements in K^* , such that*

$$\eta_{2,K} \leq C \|\mathbf{e}_h\|_{0,K^*}.$$

Moreover the following global estimate holds

$$\eta_2 \leq C \|\mathbf{e}_h\|_0,$$

with C constant depending only on the regularity of the mesh.

The following theorem summarizes the results we proved.

Theorem 18. *For each element $K \in \mathcal{T}_h$ there exists a constant C , depending only on the regularity of the elements in K^* , such that*

$$\eta_{2,K} \leq C \|\mathbf{e}_h\|_{0,K^*}.$$

Moreover if $\|P_h\varphi - \varphi\|_0$ is h.o.t., then there exist a constant C , depending on the regularity of the mesh, such that

$$\|\mathbf{e}_h\|_0 \leq C \eta_2 + \text{h.o.t.},$$

where “h.o.t.” denotes higher order terms.

6.5 Numerical Results

In this section we present the results of some preliminary numerical computation which confirm the good behavior of the error indicators introduced in Sects. 6.4.1 and 6.4.2 when used to mark the elements to be refined.

The numerical tests concern the problem of a rigid L-shaped cavity, as shown in Fig. 11. Since the domain has a re-entrant corner, eigenfunctions with singularities are expected.

Fig. 11 L-shaped domain

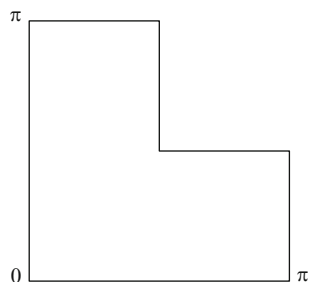
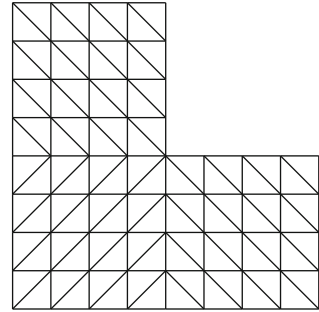


Fig. 12 Initial triangulation

We present the results obtained with meshes generated by the adaptive method described in Sect. 6.2. We use the longest edge bisection refinement and the refinement strategy 2 with $\gamma = 0.5$. The process starts with a coarse uniform triangulation \mathcal{T}_0 shown in Fig. 12.

The tests have been performed taking as approximation spaces the lowest order Brezzi-Douglas-Marini (BDM_1) and Raviart-Thomas elements (RT_0), respectively. In this particular case, the error indicators introduced in Sects. 6.4.1 and 6.4.2 reduce to

$$\eta_K = \eta_{1,K} + \eta_{2,K}$$

with

$$\eta_{1,K}^2 = h_K^2 \lambda_h^2 \|\sigma_h\|_{0,K}^2 + \frac{1}{2} \sum_{e \in \mathcal{E}_K} h_e \|\llbracket \operatorname{div} \sigma_h \rrbracket_e\|_{0,e}^2$$

and

$$\eta_{2,K}^2 = h_K^2 \|\operatorname{rot} \sigma_h\|_{0,K}^2 + \frac{1}{2} \sum_{e \in \mathcal{E}_K} h_e \|\llbracket \sigma_h \cdot \mathbf{t} \rrbracket_e\|_{0,e}^2$$

for the first order Brezzi-Douglas-Marini finite element, while

$$\eta_K^2 = \frac{1}{2} \sum_{e \in \mathcal{E}_K} h_e \|\llbracket \sigma_h \cdot \mathbf{t} \rrbracket_e\|_{0,e}^2$$

for the lowest order Raviart-Thomas elements.

The numerical computations concern the first eigensolution, which is the one which presents local singularities in the neighborhood of the re-entrant corner.

Figure 13 shows the triangulations obtained after four, six and seven steps of the refinement process for BDM approximation, whereas Fig. 14 uses the RT approximation. As can be seen, in both cases the error indicators correctly detect the elements which have to be refined, namely the ones in the neighborhood regions of the singularities.

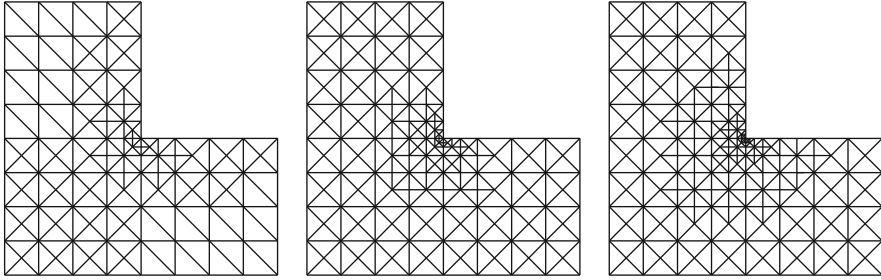


Fig. 13 Fourth, sixth, and seventh refinement steps (BDM_1)

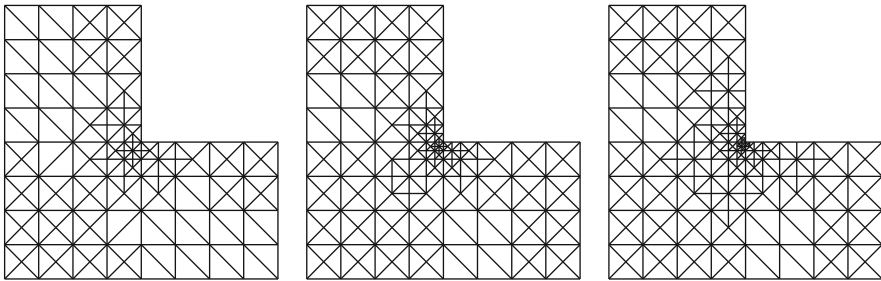


Fig. 14 Fourth, sixth, and seventh refinement steps (RT_0)

References

1. M. Ainsworth and J. T. Oden. *A posteriori error estimation in finite element analysis*. Pure and Applied Mathematics (New York). Wiley-Interscience [John Wiley & Sons], New York, 2000.
2. A. Alonso. Error estimators for a mixed method. *Numer. Math.*, 74(4):385–395, 1996.
3. A. Alonso, A. Dello Russo, C. Otero-Souto, C. Padra, and R. Rodríguez. An adaptive finite element scheme to solve fluid-structure vibration problems on non-matching grids. *Comput. Vis. Sci.*, 4(2):67–78, 2001. Second AMIF International Conference (Il Ciocco, 2000).
4. A. Alonso, A. Dello Russo, C. Padra, and R. Rodríguez. A posteriori error estimates and a local refinement strategy for a finite element method to solve structural-acoustic vibration problems. *Adv. Comput. Math.*, 15(1-4):25–59 (2002), 2001. A posteriori error estimation and adaptive computational methods.
5. A. Alonso, A. Dello Russo, and V. Vampa. A posteriori error estimates in finite element solution of structure vibration problems with applications to acoustical fluid-structure analysis. *Comput. Mech.*, 23(3):231–239, 1999.
6. A. Alonso, A. Dello Russo, and V. Vampa. A posteriori error estimates in finite element acoustic analysis. *J. Comput. Appl. Math.*, 117(2):105–119, 2000.
7. C. Amrouche, C. Bernardi, M. Dauge, and V. Girault. Vector potential in three-dimensional nonsmooth domains. *Math Methods Appl. Sci.*, 21(9):823–864, 1998.
8. P. M. Anselone. *Collectively compact operator approximation theory and applications to integral equations*. Prentice-Hall Inc., Englewood Cliffs, N. J., 1971. With an appendix by Joel Davis, Prentice-Hall Series in Automatic Computation.

9. M. G. Armentano and C. Padra. A posteriori error estimates for the Steklov eigenvalue problem. *Appl. Numer. Math.*, 58(5):593–601, 2008.
10. D. N. Arnold, R. S. Falk, and R. Winther. Finite element exterior calculus: from Hodge theory to numerical stability. *Bull. Amer. Math. Soc. (N.S.)*, 47(2):281–354, 2010.
11. I. Babuška and R. Narasimhan. The Babuška-Brezzi condition and the patch test: an example. *Comput. Methods Appl. Mech. Engrg.*, 140(1-2):183–199, 1997.
12. I. Babuška and J. Osborn. Eigenvalue problems. In *Handbook of numerical analysis, Vol. II*, Handb. Numer. Anal., II, pages 641–787. North-Holland, Amsterdam, 1991.
13. I. Babuška and W. C. Rheinboldt. A-posteriori error estimates for the finite element method. *Int. J. Numer. Meth. Eng.*, 12:1597–1615, 1978.
14. I. Babuška and W. C. Rheinboldt. Error estimates for adaptive finite element computations. *SIAM J. Numer. Anal.*, 15(4):736–754, 1978.
15. R. E. Bank. The efficient implementation of local mesh refinement algorithms. In *Adaptive computational methods for partial differential equations (College Park, Md., 1983)*, pages 74–81. SIAM, Philadelphia, PA, 1983.
16. R. E. Bank. *PLTMG: a software package for solving elliptic partial differential equations*. Software, Environments, and Tools. Society for Industrial and Applied Mathematics (SIAM), Philadelphia, PA, 1998. Users' guide 8.0.
17. R. E. Bank, A. H. Sherman, and A. Weiser. Refinement algorithms and data structures for regular local mesh refinement. In *Scientific computing (Montreal, Que., 1982)*, IMACS Trans. Sci. Comput., I, pages 3–17. IMACS, New Brunswick, NJ, 1983.
18. K.-J. Bathe, C. Nitikitpaiboon, and X. Wang. A mixed displacement-based finite element formulation for acoustic fluid-structure interaction. *Comput. & Structures*, 56(2-3):225–237, 1995.
19. A. Bermúdez, R. Durán, M. A. Muschietti, R. Rodríguez, and J. Solomin. Finite element vibration analysis of fluid-solid systems without spurious modes. *SIAM J. Numer. Anal.*, 32(4):1280–1295, 1995.
20. A. Bermúdez and D. G. Pedreira. Mathematical analysis of a finite element method without spurious solutions for computation of dielectric waveguides. *Numer. Math.*, 61(1):39–57, 1992.
21. D. Boffi. Finite element approximation of eigenvalue problems. *Acta Numer.*, 19:1–120, 2010.
22. D. Boffi, F. Brezzi, and L. Gastaldi. On the convergence of eigenvalues for mixed formulations. *Ann. Scuola Norm. Sup. Pisa Cl. Sci. (4)*, 25(1-2):131–154 (1998), 1997. Dedicated to Ennio De Giorgi.
23. D. Boffi, F. Brezzi, and L. Gastaldi. On the problem of spurious eigenvalues in the approximation of linear elliptic problems in mixed form. *Math. Comp.*, 69(229):121–140, 2000.
24. D. Boffi, C. Chinosi, and L. Gastaldi. Approximation of the grad div operator in nonconvex domains. *CMES Comput. Model. Eng. Sci.*, 1(2):31–43, 2000.
25. D. Boffi, P. Fernandes, L. Gastaldi, and I. Perugia. Computational models of electromagnetic resonators: analysis of edge element approximation. *SIAM J. Numer. Anal.*, 36(4):1264–1290 (electronic), 1999.
26. D. Boffi and C. Lovadina. Remarks on augmented Lagrangian formulations for mixed finite element schemes. *Boll. Un. Mat. Ital. A (7)*, 11(1):41–55, 1997.
27. A. Bossavit. Solving Maxwell equations in a closed cavity and the question of spurious modes. *IEEE Trans. on Magnetics*, 26:702–705, 1990.
28. J. H. Bramble, J. E. Pasciak, and A. V. Knyazev. A subspace preconditioning algorithm for eigenvector/eigenvalue computation. *Adv. Comput. Math.*, 6(2):159–189 (1997), 1996.
29. F. Brezzi and M. Fortin. *Mixed and hybrid finite element methods*, volume 15 of *Springer Series in Computational Mathematics*. Springer-Verlag, New York, 1991.
30. C. Canuto, M. Y. Hussaini, A. Quarteroni, and T. A. Zang. *Spectral methods*. Scientific Computation. Springer-Verlag, Berlin, 2006. Fundamentals in single domains.
31. C. Carstensen. A posteriori error estimate for the mixed finite element method. *Math. Comp.*, 66(218):465–476, 1997.
32. C. Carstensen and J. Gedicke. An oscillation-free adaptive FEM for symmetric eigenvalue problems. Technical report, DFG Research Center MATHEON, Berlin, 2008.

33. C. Carstensen and R. Verfürth. Edge residuals dominate a posteriori error estimates for low order finite element methods. *SIAM J. Numer. Anal.*, 36(5):1571–1587, 1999.
34. H. Chen and R. Taylor. Vibration analysis of fluid-solid systems using a finite element displacement formulation. *Int. J. Numer. Methods Eng.*, 29:683–698, 1990.
35. P. G. Ciarlet. *The finite element method for elliptic problems*. North-Holland Publishing Co., Amsterdam, 1978. Studies in Mathematics and its Applications, Vol. 4.
36. P. Clément. Approximation by finite element functions using local regularization. *Rev. Française Automat. Informat. Recherche Opérationnelle Sér. Rouge Anal. Numér.*, 9(R-2):77–84, 1975.
37. M. Costabel and M. Dauge. Singularities of electromagnetic fields in polyhedral domains. *Arch. Ration. Mech. Anal.*, 151(3):221–276, 2000.
38. X. Dai, J. Xu, and A. Zhou. Convergence and optimal complexity of adaptive finite element eigenvalue computations. *Numer. Math.*, 110(3):313–355, 2008.
39. M. Dauge. Benchmark computations for Maxwell equations for the approximation of highly singular solutions. <http://perso.univ-rennes1.fr/monique.dauge/benchmax.html>.
40. R. Durán, L. Gastaldi, and C. Padra. A posteriori error estimators for mixed approximations of eigenvalue problems. *Math. Models Methods Appl. Sci.*, 9(8):1165–1178, 1999.
41. R. Durán, C. Padra, and R. Rodríguez. A posteriori error estimates for the finite element approximation of eigenvalue problems. *Math. Models Methods Appl. Sci.*, 13(8):1219–1229, 2003.
42. E. M. Garau and P. Morin. Convergence and quasi-optimality of adaptive FEM for Steklov eigenvalue problems. *Cuad. Mat. Mec.*, page 30, 2009.
43. E. M. Garau, P. Morin, and C. Zuppa. Convergence of adaptive finite element methods for eigenvalue problems. *Math. Models Methods Appl. Sci.*, 19(5):721–747, 2009.
44. F. Gardini. A posteriori error estimates for an eigenvalue problem arising from fluid-structure interaction. *Istit. Lombardo Accad. Sci. Lett. Rend. A*, 138:17–34 (2005), 2004.
45. F. Gardini. *A posteriori error estimates for eigenvalue problems in mixed form*. PhD thesis, Università degli Studi di Pavia, 2005.
46. F. Gardini. Mixed approximation of eigenvalue problems: a superconvergence result. *M2AN Math. Model. Numer. Anal.*, 43(5):853–865, 2009.
47. L. Gastaldi. Mixed finite element methods in fluid structure systems. *Numer. Math.*, 74(2):153–176, 1996.
48. S. Giani and I. G. Graham. A convergent adaptive method for elliptic eigenvalue problems. *SIAM J. Numer. Anal.*, 47(2):1067–1091, 2009.
49. L. Grubišić and J. S. Owall. On estimators for eigenvalue/eigenvector approximations. *Math. Comp.*, 78(266):739–770, 2009.
50. F. Hecht. *FreeFem++, Third Edition, Version 3.12*, 2011. <http://www.freefem.org/ff++/>.
51. V. Heuveline and R. Rannacher. A posteriori error control for finite approximations of elliptic eigenvalue problems. *Adv. Comput. Math.*, 15(1-4):107–138 (2002), 2001.
52. R. Hiptmair. Finite elements in computational electromagnetism. *Acta Numerica*, 11:237–339, 2002.
53. T. Kato. *Perturbation theory for linear operators*. Springer-Verlag, New York, 1976.
54. F. Kikuchi. Mixed and penalty formulations for finite element analysis of an eigenvalue problem in electromagnetism. *Comput. Methods Appl. Mech. Engrg.*, 64:509–521, 1987.
55. A. V. Knyazev. Sharp a priori error estimates of the rayleigh-ritz method without assumptions of fixed sign or compactness. *Math. Notes*, 38:998–1002, 1986.
56. A. V. Knyazev. New estimates for Ritz vectors. *Math. Comp.*, 66(219):985–995, 1997.
57. A. V. Knyazev and J. E. Osborn. New a priori FEM error estimates for eigenvalues. *SIAM J. Numer. Anal.*, 43(6):2647–2667 (electronic), 2006.
58. W. G. Kolata. Approximation in variationally posed eigenvalue problems. *Numer. Math.*, 29(2):159–171, 1978.
59. I. Kossaczky. A recursive approach to local mesh refinement in two and three dimensions. *J. Comput. Appl. Math.*, 55(3):275–288, 1994.

60. M. G. Larson. A posteriori and a priori error analysis for finite element approximations of self-adjoint elliptic eigenvalue problems. *SIAM J. Numer. Anal.*, 38(2):608–625 (electronic), 2000.
61. C. Lovadina, M. Lyly, and R. Stenberg. A posteriori estimates for the Stokes eigenvalue problem. *Numer. Methods Partial Differential Equations*, 25(1):244–257, 2009.
62. D. Mao, L. Shen, and A. Zhou. Adaptive finite element algorithms for eigenvalue problems based on local averaging type a posteriori error estimates. *Adv. Comput. Math.*, 25(1-3):135–160, 2006.
63. P. Monk. *Finite element methods for Maxwell's equations*. Numerical Mathematics and Scientific Computation. Oxford University Press, New York, 2003.
64. J. E. Pasciak and J. Zhao. Overlapping Schwarz methods in $H(\text{curl})$ on polyhedral domains. *J. Numer. Math.*, 10(3):221–234, 2002.
65. P.-A. Raviart and J.-M. Thomas. A mixed finite element method for second order elliptic problems. In I. Galligani and E. Magenes, editors, *Mathematical Aspects of the Finite Element Method*, volume 606 of *Lecture Notes in Math.*, pages 292–315, New York, 1977. Springer-Verlag.
66. W. C. Rheinboldt. On a theory of mesh-refinement processes. *SIAM J. Numer. Anal.*, 17(6):766–778, 1980.
67. M.-C. Rivara. Algorithms for refining triangular grids suitable for adaptive and multigrid techniques. *Internat. J. Numer. Methods Engrg.*, 20(4):745–756, 1984.
68. M.-C. Rivara. Design and data structure of fully adaptive, multigrid, finite-element software. *ACM Trans. Math. Software*, 10(3):242–264, 1984.
69. G. Valle. Problemi agli autovalori per equazioni alle derivate parziali: autovalori multipli. Tesi di laurea, Università degli Studi di Pavia, 2011.
70. R. Verfürth. A posteriori error estimates for nonlinear problems. *Math. Comp.*, 62(206):445–475, 1994.
71. R. Verfürth. *A Review of a posteriori error estimation and adaptive mesh-refinement techniques*. Wiley and Teubner, 1996.
72. T. F. Walsh, G. M. Reese, and U. L. Hetmaniuk. Explicit a posteriori error estimates for eigenvalue analysis of heterogeneous elastic structures. *Comput. Methods Appl. Mech. Engrg.*, 196(37-40):3614–3623, 2007.
73. X. Wang and K.-J. Bathe. On mixed elements for acoustic fluid-structure interactions. *Math. Models Methods Appl. Sci.*, 7(3):329–343, 1997.
74. J. Webb. Edge elements and what they can do for you. *IEEE Trans. on Magnetics*, 29:1460–1465, 1993.

Frontiers in Numerical Analysis - Durham 2010

Blowey, J.; Jensen, M. (Eds.)

2012, XII, 292 p., Hardcover

ISBN: 978-3-642-23913-7